

The Differentiation of Patient-derived Prostate Organoids and the Influence of Vitamin D

BY

TARA McCRAY

B.S., University of North Carolina at Greensboro 2013

THESIS

Submitted as partial fulfillment of the requirements
for the degree of Doctor of Philosophy in Pathology
in the Graduate College of the
University of Illinois at Chicago, 2020

Chicago, Illinois

Defense Committee:

Larisa Nonn, Advisor

Michael Walsh, Chair

Maarten Bosland

Gail Prins, Urology

Joanna Burdette, Pharmacy

DEDICATION

This work is dedicated to cancer patients, especially the prostate cancer patient tissue donors from University of Illinois at Chicago Hospital. Without their invaluable contribution, this research could not have been achieved.

ACKNOWLEDGEMENTS

I would like to acknowledge my committee members, Drs. Gail Prins, Maarten Bosland, Michael Walsh and Joanna Burdette, for all of their efforts in my training. My committee has supported me at meetings and at department seminars, offering constructive and contemplative guidance on my project over the last 4 years. I would like to especially thank my mentor, Dr. Larisa Nonn, for giving me so much freedom and independence on this project. She fostered a lab space that nourishes creativity and collaboration amongst its members. She drove me to try advanced techniques and analyses, pushed me out of my comfort zone to give talks and provided me with professional development opportunities, without which my next career steps would be impossible. I could not have asked for a more mindful and considerate mentor, and regard myself as infinitely lucky to have trained under her.

I would also like to acknowledge my lab mates, the GEMS program and the entire Pathology department. Mia Johnson and Dr. Diamond helped me endure the first year of coursework. Lab members Zachary Richards, Morgan Zenner, Bethany Baumann, Jason Garcia, Chuck Blajszczak, Yves Helou, Julian Pacheco, Mike Schlicht, and students in the department Lenny Hong, Larischa de Wet, and Ryan Brown all offered technical troubleshooting and emotional motivation. Cooperative endeavors and a friendly department are the *sine qua non* of team science.

Last, I would like to acknowledge my friends, family, and the other students of the GEMS program: Majd, James and Elena, Stefanie, Josh, Isha, Ryan, Adam, Sarah, Octavia, and Georgina who have helped me feel at home in Chicago since the first week I moved here. Our collective struggles got me through the tribulations of this degree. My family, most specifically my mom and my Aunt Jan, offered their unconditional love and encouragement over the years. Finally, my boyfriend Sean has held me up through this whole process, helping me battle all the self-doubt, imposter syndrome, and anxiety that comes with graduate school. I could not have made it through without him, or them.

TNM

CONTRIBUTION OF AUTHORS

Chapter II is from work previously published in *iScience*, *JoVE* and *AJCEU*:

- McCray T, Moline D, Baumann B, Vander Griend DJ, Nonn L. (2019). "Single-Cell RNA-Seq Analysis Identifies a Putative Epithelial Stem Cell Population in Human Primary Prostate Cells in Monolayer and Organoid Culture Conditions", *Am J Clin Exp Urol.*, June 15 2019, 7(3):123-138
- Richards Z*, McCray T*, Marsili J, Zenner ML, Manlucu JT, Garcia J, Kajdacsy-Balla A, Murray M, Voisine C, Murphy AB, Abdulkadir SA, Prins GS, Nonn L. (2019). "Prostate stroma increases the viability and maintains the branching phenotype of human prostate organoids", *iScience*, February 22 2019, 12:304-317
- McCray T, Richards Z, Marsili J, Prins GS, Nonn L. (2019) "Handling and Assessment of Human Primary Prostate Organoid Culture", *J. Vis. Exp.*, Jan 17 2019, (143)

Chapter III is from submitted work to *Cell Reports* regarding the role of vitamin D in organoid differentiation.

- McCray T, Pacheco J, Valyi-Nagy K., Nonn L (submitted, 2020). "Patient-derived Prostate Organoids Reveal Vitamin D as a Vital Regulator of Epithelial Differentiation"

UIC Biorepository (Dr. Klara Valyi-Nagy, Alex Susma), urologists (Drs. Michael Abern, Daniel Moreira, and Simone Crivallero), facilitated tissue acquisition for primary cell cultures. Core facilities assisted with imaging and sequencing: UIC Fluorescence Imaging Core (Dr. Ke Ma), UIUC DNA Services (Dr. Alvaro Hernandez, Chris Wright, Jenny Zadeh, and Jessica Holmes). In **Chapter II**, Joseph Marsili and Zachary Richards assisted with generating organoids, developing the image analysis pipeline and data interpretation, Daniel Moline assisted in cell capture and library prep, qPCR and data interpretation. In **Chapter III**, Julian Pacheco assisted with organoid growth and size assessment.

TABLE OF CONTENTS

CHAPTER I: INTRODUCTION	1
A. Prostate Biology, Disease, and Modeling	1
i. Prostate function, cell types, and epithelial differentiation.....	1
ii. Prostate disease and prostate cancer.....	6
iii. The biology of prostate cancer	7
iv. Modeling prostate development and disease in vitro and in vivo.....	8
B. Goals of the thesis.....	11
CHAPTER II: CHARACTERIZING THE CELL TYPES AND DIFFERENTIATION OF PROSTATE EPITHELIAL ORGANOIDS	12
A. Introduction.....	12
i. Organoid background.....	12
ii. Single cell RNA sequencing.....	13
iii. Goals of chapter.....	15
B. Materials and methods.....	16
i. Patient biospecimens	16
ii. Primary cell culture.....	19
iii. Organoid culture	19
iv. Single cell RNA sequencing and analysis.....	19
v. Pathway analysis.....	22
vi. RNA extraction, amplification, and gene expression analysis.....	22
vii. Histology.....	23
viii. Imaging.....	24
ix. Edu assay.....	24
x. Quantification and statistical analysis.....	24
xi. Data availability.....	25

TABLE OF CONTENTS

C. Results.....	26
i. Developing the primary prostate cell organoid Matrigel model.....	26
ii. Organoid culture exhibits more heterogeneous epithelial differentiation states than monolayer culture.....	29
iii. In vitro models cultivate stem and progenitor cells from patient tissue.....	34
iv. Elucidation of organoid differentiation trajectory.....	36
D. Discussion.....	41
i. Summary.....	41
ii. In vitro stem and progenitor cells.....	42
iii. Implications for the Integrin ^{High} cluster in the differentiation of organoids.....	42
iv. Integrin signaling in the prostate and prostate cancer.....	44
v. Limitations and pitfalls.....	45
vi. Conclusions.....	46

CHAPTER III: THE EFFECT OF VITAMIN D ON PROSTATE ORGANOID

DIFFERENTIATION.....	47
A. Introduction.....	47
i. Vitamin D metabolism and activity.....	47
ii. Vitamin D deficiency is associated with prostate cancer aggression.....	49
iii. Vitamin D as a regulator of differentiation.....	50
iv. Hypothesis and goals of chapter.....	51
B. Materials and methods.....	51
i. Patient biospecimens.....	51
ii. Cell lines.....	51
iii. Primary cell culture and treatments.....	52

TABLE OF CONTENTS

iv.	Primary organoid culture.....	52
v.	Brightfield image acquisition, processing, and analysis.....	52
vi.	Single cell RNA sequencing and analysis.....	53
vii.	Pathway analysis.....	54
viii.	Flow cytometry.....	54
ix.	RNA extraction, amplification, and gene expression analysis.....	55
x.	Protein isolation and western blotting.....	55
xi.	Histology.....	56
xii.	ELISA.....	56
xiii.	Lentiviral transduction.....	57
xiv.	Quantification and statistical analysis.....	57
xv.	Data availability.....	57
C.	Results.....	58
i.	Vitamin D supplementation enlarges prostate organoids and alters their epithelial composition.....	58
ii.	Vitamin D supports normal organoid growth and drives differentiation.....	60
iii.	Vitamin D modulates the Wnt pathway in organoids.....	62
iv.	Vitamin D inhibits Wnt family member DKK3.....	70
v.	DKK3 inhibition by vitamin D is required to alter organoid growth.....	72
vi.	DKK3 and DKK1 are expressed by lineage-committed cells.....	74
D.	Discussion.....	76
i.	Summary.....	76
ii.	The Wnt pathway in prostate epithelium.....	76
iii.	Vitamin D activity in Wnt pathway.....	78
iv.	Wnt pathway in prostate cancer.....	79

TABLE OF CONTENTS

v. DKK3.....	80
vi. Limitations and future directions.....	81
CHAPTER IV: CONCLUSIONS.....	82
A. Contribution to literature.....	82
B. Implications and considerations for patient health and prostate cancer.....	82
i. Expression level of vitamin D pathway proteins.....	83
ii. Patient body weight.....	84
iii. Dosage and differentiation status of tissue.....	84
iv. Proliferation capacity of tissue.....	85
C. Future directions.....	86
D. Summary.....	87
CITED LITERATURE	88
APPENDICES	104
A. Patient tissue IRB for generation primary cell cultures and tissue staining.....	104
B. <i>iScience</i> permission of inclusion.....	105
C. <i>AJCEU</i> permission of inclusion.....	106
D. <i>JoVE</i> permission of inclusion.....	107
E. iThenticate document.....	108
VITA	109

LIST OF TABLES

	Page
TABLE I Gene expression profiles for prostate epithelial cells	5
TABLE II Commonly used benign and cancer prostate epithelial cell lines	10
TABLE III Patient characteristics.....	17
TABLE IV Primers used for RT-qPCR.....	18
TABLE V Quality metrics for scRNAseq input, sequencing and analysis.....	21

LIST OF FIGURES

	Page
Figure 1. Prostate epithelial cells and hierarchy.....	2
Figure 2. Diagram of single cell RNA seq workflow.....	14
Figure 3. Developing the PrE organoid model system.....	28
Figure 4. ScRNAseq of monolayer and organoid PrE cells derived from a single patient.....	31
Figure 5. Immunostaining validates expression of stem, basal, luminal and polarity markers.....	33
Figure 6. Integration of monolayer, organoid, and patient tissue scRNAseq data shows conserved stem cell population in model systems.....	35
Figure 7. ScRNAseq of early (day 8) and late (day 14) stage organoids derived from a single patient.....	37
Figure 8. Enriched pathways in each scRNAseq cluster.....	38
Figure 9. Pseudotime analysis of early and late stage organoids reveals differentiation trajectory.....	40
Figure 10. Vitamin D signaling pathway.....	48
Figure 11. Figure 11. Vitamin D supplementation enlarges prostate organoids and alters their epithelial composition.....	59
Figure 12. Organoid populations shift with vitamin D.....	61
Figure 13. Vitamin D regulates lineage-committed cells.....	63
Figure 14. Predicted upstream regulators with vitamin D in each organoid cluster.....	65
Figure 15. Diseases & Functions enrichment analysis with vitamin D in each organoid cluster.....	66
Figure 16. Vitamin D modulates the Wnt pathway.....	68
Figure 17. Diagram of the canonical Wnt signaling pathway.....	69
Figure 18. Vitamin D inhibits Wnt family member DKK3.....	71
Figure 19. DKK3 inhibition by vitamin D is required to alter organoid growth.....	73
Figure 20 DKK3 and DKK1 are expressed by lineage-committed cells.....	75
Figure 21. Diagram summarizing the effects of 1,25D on prostate epithelial organoids and the implications for human health.....	77

LIST OF ABBREVIATIONS

1,25D	1,25-dihydroxyvitamin D
25D	25-hydroxyvitamin D
2D	Two dimensional, monolayer culture
3D	Three-dimensional, organoid culture
AA	African American
AR	Androgen Receptor
BMP	Bone Morphogenic Protein
CK5	Cytokeratin 5, protein
CK8/18	Cytokeratin 8/18, protein
CK13	Cytokeratin 13, protein
BPH	Benign Prostatic Hyperplasia
CYP24A1	Cytochrome P450 Family 24 Subfamily A Member 1, vitamin D inactivator
CYP27B1	Cytochrome P450 Family 27 Subfamily B Member 1, vitamin D activator
DBP	Vitamin D Binding Protein
DEG	Differentially Expressed Gene
DKK3	Dickkopf WNT Signaling Pathway Inhibitor 3, gene and protein
EA	European American
ECM	Extracellular matrix
ELISA	Enzyme-linked Immunosorbent Assay
FACS	Fluorescence activated cell sorting
FBS	Fetal Bovine Serum
FGF	Fibroblast Growth Factor
ITG	Integrin, α - or β -
KRT5	Cytokeratin 5, gene
KRT8	Cytokeratin 8, gene
KRT13	Cytokeratin 13, gene
PCa	Prostate Cancer
PrE	Primary Epithelial Cells
PrS	Primary Stromal Cells
PSA	Prostate Specific Antigen
RQ	Relative quantity
RXR	Retinoid X Receptor
scRNAseq	Single Cell RNA Sequencing
SD	Standard Deviation
UGS	Urogenital sinus
UMI	Unique Molecular Identifier
UMAP	Uniform Manifold Approximation and Projection
VDR	Vitamin D Receptor
VDRE	Vitamin D Response Element

SUMMARY

Prostate cancer is a leading cause of death in men, involving de-differentiation and outgrowth of malignant epithelial cells. To understand the underlying biology of the gland, organoids are a useful tool that model the epithelial differentiation and structure of prostate tissue. This thesis characterizes the prostate organoid model by single cell RNA sequencing and determines the cell populations observed throughout differentiation. Once fully described, organoids were grown in the presence of vitamin D, a steroid hormone that is associated with prostate health. It was hypothesized that vitamin D would promote epithelial differentiation in the prostate and this was tested using the organoid model of differentiation. Vitamin D regulation over Wnt signaling and DKK3 expression were identified as mechanisms. This thesis offers a catalog of the cell types cultivated in organoids, and the influence of vitamin D in the organoids as a means to promote differentiation.

CHAPTER I: INTRODUCTION

A. Prostate biology, disease, and modeling

i. Prostate function, cell types, and epithelial differentiation

The prostate is a male endocrine gland that produces a majority of the seminal fluid and harbors disease in a significant proportion of elderly men (Prins and Lindgren, 2015). Its primary function is to generate anions (such as citrate) and enzymes (such as proteases and acid phosphatases) to promote the successful transport of sperm in the female reproductive tract (Prins and Lindgren, 2015). The kallikrein-related protease gene family is highly expressed in the prostate: *KLK3*, *pro-KLK3*, *KLK4*, *KLK5*, *KLK14* and *KLK15*; and their resulting proteins aid in semen liquefaction and sperm motility (Kalinska et al., 2016). *KLK3* codes for prostate specific antigen (PSA), which is used as a serum biomarker for prostate disease. Prostate cells also secrete alkaline substances and buffering anions to protect sperm in the seminal fluid from the acidic vaginal environment (Banjoko and Adeseolu, 2013; Prins and Lindgren, 2015).

The prostate gland is composed of branching epithelial ducts which are surrounded by fibromuscular stroma, as shown in **Figure 1A**. The epithelial constituent consists of secretory luminal cells lining the lumen, basal cells bordering the basement membrane, and rare neuroendocrine cells (Prins and Lindgren, 2015). Luminal cells are terminally differentiated and perform the secretory function of the gland. They are distinguished by high cytokeratin 8/18 (CK8/18) and androgen receptor (AR) expression. Basal cells exhibit high cytokeratin 5 (CK5), cytokeratin 14 (CK14), and p63 (Wang et al., 2001). The scarce population of neuroendocrine cells in the epithelium are discerned by expression of chromogranin A (Henry et al., 2018). Commonly used markers for epithelial cells are listed on **TABLE I**. The stromal component consists of multiple cell types, including smooth muscle cells, myofibroblasts, fibroblasts, and endothelial cells. The smooth muscle performs the contractile function of the gland and highly express α -smooth muscle actin, while fibroblasts support epithelial cells via secretion of growth factors and are marked by high vimentin. Myofibroblasts are an intermediate, transdifferentiated

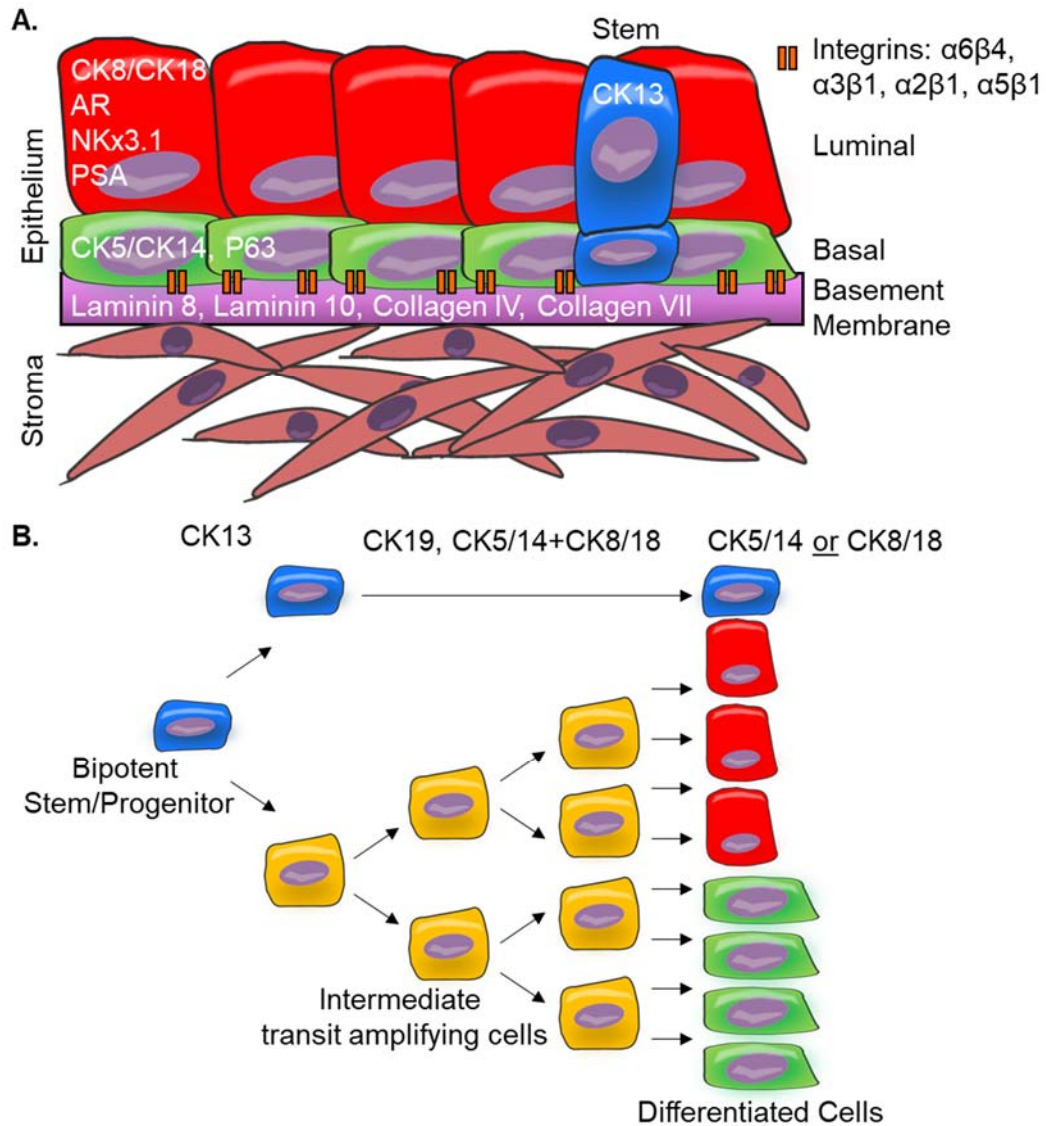


Figure 1. Prostate cells and hierarchy. (A) Diagram of cell types found in the prostate and **(B)** diagram of epithelial cell hierarchy during organoid formation. Adapted from (Frank and Miranti, 2013; Suyin et al., 2013; Toivanen and Shen, 2017; Uzgare et al., 2004)

stromal cell that expresses both smooth muscle and fibroblastic markers (Henry et al., 2018; Kwon et al., 2019; Prins and Lindgren, 2015). Other cells types such as endothelial cells, immune cells and fat cells are also present, but are not the focus of this thesis (Henry et al., 2018).

Prostate gland development and epithelial differentiation is a hormonally-regulated process that is controlled by transcription factors, epithelial-stromal cross talk and is tightly regulated by spatial gradients of morphogens (Prins and Lindgren, 2015; Prins and Putz, 2008; Toivanen and Shen, 2017). Prostate organogenesis is broken into multiple stages: determination, budding, branching morphogenesis, and differentiation. During determination, circulating androgens from the testes commit primitive tissue to the prostatic fate. Once determined, early epithelial cells of the urogenital sinus (UGS) invade and bud into the immature stroma, which is followed by outgrowth and branching morphogenesis of the epithelial ducts. At this stage, the epithelial cells may co express basal and luminal markers, and some intermediate markers such as cytokeratin 19 (CK19) (Wang et al., 2001). Once rudimentary ducts are formed, they undergo a process of anoikis (Toivanen and Shen, 2017), to hollow into lumens, and cellular differentiation, to form the organized basal and luminal layers with distinct CK5/14 and CK8/18 expression (Wang et al., 2001). Due limitations in availability of developing human tissue, insights into prostate organogenesis have been achieved through rodent models. Major features are consistent across species, although there are differences in timing (Toivanen and Shen, 2017). Patient-derived epithelial organoids, which are discussed in detail later in this chapter, can be used to model development and differentiation to validate findings between rodent and humans.

The stages of prostate development are directed by steroid hormones (androgens, retinoic acids, estrogens, etc) and secreted signaling ligands (Wnts, fibroblast growth factors (FGFs), bone morphogenic proteins (BMPs), etc) (Prins and Lindgren, 2015). Stromal androgens drive FGF7 and FGF10 expression to promote epithelial growth and branching (Toivanen and Shen, 2017). Androgen in epithelial cells bind to the androgen receptor (AR) which interacts with transcription factors Nkx3.1, FoxA1 or Hoxb13 to regulate specification and differentiation. Sonic

hedgehog (Shh) and BMP signaling between the stromal and epithelial cells coordinate branching morphogenesis (Prins and Putz, 2008; Toivanen and Shen, 2017). Retinoic acid has been shown to interact with Shh and BMP signaling to promote bud formation in mouse UGS culture (Vezina et al., 2008). Estrogen receptor α knockout mice show impaired FGF signaling and branching morphogenesis, implicating an important role for estrogen (Chen et al., 2009). The hormone vitamin D likely plays a part in development or differentiation, which is the focus of the second half of this thesis.

The epithelial layer of the prostate is maintained through resident stem and progenitor cells (Blackwood et al., 2011; Gaisa et al., 2011; Ousset et al., 2012). Epithelial turnover involves a quiescent bipotent stem cell to undergo asymmetric division, with one progeny maintaining stemness and the other being lineage committed, as shown in **Figure 1B**. The lineage committed progenitor is capable of rapid division and expansion into intermediate cells that express both basal and luminal markers, followed by differentiation into the luminal or basal phenotype. Mouse studies involving lineage tracing, tissue recombination and castration have shown the presence of stem/progenitors in both basal and luminal compartments (Frank and Miranti, 2013). This was also confirmed in human, through lineage tracing of prostate tissue and organoid modeling (Gaisa et al., 2011; Karthaus et al., 2014). Markers used to identify prostate epithelial cells at different stages of the hierarchy are shown on **TABLE I**.

TABLE I. Gene expression profiles for prostate epithelial cells

	Pan-Epi	Luminal	Basal	Intermed	Stem
(Henry et al., 2018)	CD326, CD324, TACSTD2 ITGA6	DPP4, KRT8,SMB, KRT18,GP2,KLK3, MSMB ACPP, KLK4, PLA2G2A, MT1E, KLK2, SOCS2, TSPAN8	PDPN, KRT5, TP63, CD104, CD271, RGCC KRT14, DST, NOTCH4, LTBP2, DKK1, KRT15	KRT19 KRT18 KRT14	SCGB1A1,PSCA KRT13,LCN2, LYPD3, SCGB3A1, SERPINB1,PIGR, WFDC2,FCGBP, APOBEC3A, CSTB
(Zhang et al., 2016)	TACSTD2	AR, KLK3, ALOX15B, ACPP, TOX3,FOLH1, OSTA, DPP4, CKK, PLA2G2A, MB,CWH43, SYT7, TRPV6, ELOVL2, CPNE4, ANO7, POTEM, MUC2, LMAN1L, C2, DNAJC12, ASRGL1, DLL4, DOCK11, GPR98, INHB8,TBXAS1, SERHL2, NPTX2, GFPT2, PTPRN2, CSGALNACT1, ST8SIA1, VNN3, TRPM8,RAMP1PD E8B, SPDEF, LTB, HLA-DMB, LOC286002, FGF13, DCDC2, KRT20, FBP1, SLC2A12, TSPAN8	TP63, KRT5, TNC, KRT14,ITGA6,IL33 KRT6A, BNC1 KRT34, FAT3, SYNE1, COL17A1, FGFR3,DKK3 CSMD2, JAM3, PDPN,CDH13, FJX1, MUM1L1, MMP3, DLK2, FLRT2, VSNL1, GIMAP8, FHL1, NRG,IGFBP7, ERG,HMGA2, IL1A, NOTCH3, THBS2,TAGLNS MSRB3, NGFR NIPAL4,KIRREL ANXABL2,PARC COL4A6,FOXI1 KCNMA1,KCNQs, JAG2,WNT7A, LTBP2,SH2D5, MRC2,C16orf74, SERPINB13, CNTAP3B, ARHGAP25, AEBP1, DLC1, SERPINF1		
(Hu et al., 2017)					KRT13, IGF2,NES CCL2,CARM1 LDH1A2, NANOG, ALDH8A1,LIFRCA PSCA FOXA1, SOX2,PRAC1 C15, PCAT1,VEGFC
(Moad et al., 2017)					SCNN1A, PPL, CENPF,DDIT4, KLK11, DLK1,
(Wang et al., 2001)		KRT8 KRT18	KRT19,GSTpi KRT5, TP63, KRT14	KRT19	
(Schmelz et al., 2005)		TPJ1 KLK3	KRT5	KRT19	KRT6A

ii. Prostate disease and prostate cancer

Prostate tissue has a high incidence of disease, affecting most elderly men with some form of ailment (Prins and Lindgren, 2015). Common conditions include prostatitis, benign prostatic hyperplasia (BPH), and prostate cancer (PCa) (Aaron et al., 2016). Prostatitis is inflammation of the prostate, approximately half of men will suffer from prostatitis at some point in their lives (Khan et al., 2017). It is generally caused from acute or chronic bacterial infection (*E. coli*, *N. gonorrhoea*, *Chlamydia*, *Salmonella*, etc.), and in some cases the etiology cannot be determined, or inflammation is asymptomatic and detected from elevated PSA (Khan et al., 2017). BPH involves hyperplasia of the transition zone, resulting in an enlarged prostate, affecting most men by the time they reach 90 years old (Aaron et al., 2016). Prostate cancer arises in the glandular epithelium of the peripheral zone and predominantly consists of adenocarcinoma (Wang et al., 2018). When excluding skin cancer, PCa is the highest diagnosed malignancy in men and the second highest cause of death in men for 2020, behind lung cancer (Siegel et al., 2020). Roughly 30% of men over 50 who die from a non-prostatic illness could also harbor prostate cancer at autopsy (Scardino, 1989). Age is a risk factor for PCa: risk is elevated in European Americans after age 50 and in African Americans after age 40 (Rawla, 2019). After the age of 65, incidence increases to ~60% in men worldwide (Rawla, 2019). The estimated number of PCa cases for 2020 is 191,930, accounting for 21% of newly diagnosed cases, and 33,330 cancer deaths at 10% of total deaths (Siegel et al., 2020).

PCa typically initiates with prostatic intraepithelial neoplasia (PIN) lesions, in which there is a loss of basal cells from the epithelium (Gandhi et al., 2018). High-grade PIN can develop into adenocarcinoma, but this does not always occur. Lesions are detected by digital rectal exam and blood screening for prostate specific antigen (PSA), which is normally produced by the prostate but will leak into the blood stream after injury (Descotes, 2019). PCa prognosis involves determination of PSA levels, histologic assessment of Gleason score from biopsy, and staging through magnetic resonance imaging (MRI) (Descotes, 2019). When disease is deemed non-

indolent (due to high PSA levels and Gleason score), surgical resection and radiation therapy are performed (Arora and Barbieri, 2018). PCa may progress and metastasize and the next line of treatment involves androgen blockade, termed androgen-deprivation therapy, to shut down the essential hormone signaling pathway normally required for prostate cell growth (Arora and Barbieri, 2018). Particularly aggressive adenocarcinoma may cease to respond to androgen deprivation therapy, becoming castration resistant (Arora and Barbieri, 2018). This occurs through several mechanisms including expression of AR variants, constitutively active AR, AR gene amplifications for efficient use of trace androgen, etc (Arora and Barbieri, 2018; Gandhi et al., 2018). Some PCa may develop into a lethal subtype that resembles neuroendocrine cells (Arora and Barbieri, 2018). Ongoing studies aim to determine profiles of PCa that can distinguish between indolent disease and those which will progress to aggressive and resistant subtypes. With these profiles, treatments that avoid hormone signaling, such as immunotherapy, will directly target metastatic sites that may contain the androgen independent cell types that drive disease progression (Anselmo da Costa et al., 2019; Gandhi et al., 2018).

iii. The biology of prostate cancer

Prostate disease involves re-awakening of developmental programs (Aaron et al., 2016). In BPH, stromal cells activate inductive cues that normally function during prostate morphogenesis and epithelial invasion, resulting in new epithelial gland formation in the adult transition zone (Aaron et al., 2016). Prostate cancer also involves a dysregulation of developmental pathways resulting in unchecked growth of luminal cells (Frank and Miranti, 2013; Wang et al., 2018). PCa drivers include genetic mutations related to cell division and DNA repair pathways (*PTEN*, *MYC*, *ERG*, *ATM*, *TP53*, *BRCA1/2*, etc.) along with genes important during prostate development (*HOXB13*, *NKx3.1*, *FOXA1*, *AR*) (Frank and Miranti, 2013; Wang et al., 2018). The NKx3.1 transcription factor is commonly deleted as an initiating event in PCa (Frank and Miranti, 2013), and is an early marker of prostate epithelium during specification. FoxA1 and

Hoxb13 are other essential transcription factors during specification that interact with AR, and are mutated in PCa (Arora and Barbieri, 2018; Frank and Miranti, 2013). Stromal-epithelial interactions through Shh and BMP signaling drive branching morphogenesis, and are also disrupted in disease (Hyuga et al., 2019; Prins and Putz, 2008). The Shh pathway is generally low in adult tissue and only activated during regeneration, but increased expression in PCa is correlated with higher Gleason score (Hyuga et al., 2019). Stromal FGF7 and 10 interaction with epithelial FGFR2 regulates branching morphogenesis, castration-resistant PCa involves a loss of FGFR2 and gain of FGFR1 (Carstens et al., 1997; Wang et al., 2019). These examples illustrate how essential developmental and differentiative programs can be perturbed in malignancy and drive disease progression. In order to understand and treat prostate cancer, it is necessary to study and model these basic biological processes in the lab.

iv. Modeling prostate development and disease in vitro and in vivo

To study prostatic development and disease, labs utilize rodents, cell lines, primary cells and xenografts. Rodents are a useful tool to study prostate biology: access to rodent prostate at different developmental time points is much easier to acquire than human tissue, castration experiments can be readily performed to study hormonal regulation, and genetic models have been developed for drivers of prostate disease to study progression (Grabowska et al., 2014). These models are not without drawbacks: mouse and human vary drastically in the physiology of the lobes and content of basal and luminal cells, where humans have a 1:1 ratio of basal to luminal and mouse have a 1:7 ratio (Prins and Lindgren, 2015). Additionally, animal experiments require specialized facilities and can be costly.

In vitro culture models for human prostate address some of these concerns and have produced valuable insights. Commonly used prostate benign and cancer cell lines are listed on **TABLE II**. However, there are a limited number of lines available and all benign lines are immortalized with human papilloma virus or telomerase alterations (Sobel and Sadar, 2005a, b).

Cancer lines are primarily isolated from late stage metastatic disease, so modeling early and intermediate disease presents a significant obstacle to understanding initiating events in the human and unifying data with clinically relevant findings (Sobel and Sadar, 2005a, b). Patient-derived primary epithelial cell culture (PrE) is an alternative strategy, which preserves patient heterogeneity (Niranjan et al., 2013; Peehl, 2002; Peehl, 2003; Peehl and Stamey, 1986; Peehl et al., 1988; Wise, 2002). PrE culture is an advantageous tool for studying “normal” cells, as they are non-immortalized and untransformed. However, PrE are limited in the number of passages available, as they have not been immortalized for indefinite growth. PrE culture is also restricted to selectively expand epithelial cells that display a transit-amplifying phenotype and lack the luminal differentiation of prostate epithelium observed in vivo (Bühler P, 2010; Ivan V. Litvinov, 2006; Peehl, 2004; Uzgare et al., 2004).

Organoids are three-dimensional (3D) structures grown in extracellular matrix that recapitulate many facets of prostate epithelial tissue morphology, including structure and cell polarity (Clevers, 2016; Drost et al., 2016; Karthaus et al., 2014). Compared to their traditional two-dimensional (2D) monolayer PrE counterparts, organoids can grow from a single stem or progenitor cell in the presence of charcoal-stripped FBS and androgen to differentiate into both basal and luminal epithelial populations (Chua et al., 2014; Drost et al., 2016; Karthaus et al., 2014). They have been grown using cells originating from a variety of organ types: salivary gland, stomach, intestine, liver, prostate, lung, brain, etc (Fatehullah et al., 2016). As organoids are becoming a more widely used system for biological questions, it is important to advance our understanding of their composition, differentiation, and ability to mimic tissue.

TABLE II. Commonly used benign and cancer prostate epithelial cells*

CELL TYPE	NAME	IMMORTALIZED/ TRANSFORMED	DERIVED FROM []	AR EXPRESSION
BENIGN CELL LINES	RWPE1 (Bello et al., 1997)	HPV	Cystoprostatectomy, histologically normal prostate	No**
	957E (Yasunaga et al., 2001)	hTERT	44 year old, primary PCa tumor of familial adenocarcinoma, (Gleason 3+3), phenotype appears benign	No
CANCER CELL LINES	22Rv1	Transformed Xenograft	Xenograft of a primary prostatic carcinoma from patient with osseous metastases (Gleason sum 9)	Responsive
	DU 145	Transformed	63 year old, bone metastasis, patient had androgen-independent PCa adenocarcinoma	No
	LNCaP	Transformed	Metastasis, lymph node	Androgen sensitive***
	MDA-PCa 2b	Transformed	Metastasis, bone	Yes
	VCaP	Transformed	Metastasis.	Yes
	PC3	Transformed	Metastasis, lumbar	No
	LAPC4	Transformed	Xenograft from lymph node metastasis	Yes
PRIMARY CELL	RWPE2 (Bello et al., 1997)	HPV, infection with v-K-ras tumorigenic	Cystoprostatectomy, histologically normal prostate	Yes/No**
	2D Benign	No		No
	2D Cancer	No	Primary lesion	No
	Organoid	No		Yes

*Adapted from publications (Bello et al., 1997; Bennett et al., 2014; Hepburn et al., 2020; Russell and Kingsley, 2003; Sobel and Sadar, 2005a, b; Yasunaga et al., 2001), and the ATCC cell line webpage (<https://www.atcc.org/>)

**Reported to respond to androgen derivatives

***Some sublines are androgen insensitive

B. Goals of thesis

Organoids are a valuable tool to study organogenesis and disease. They provide an inexpensive alternative to animal models, and patient-derived organoids could be used in the future as a strategy for personalized medicine (Clevers, 2016; Kretzschmar and Clevers, 2016; Marina and Bissell, 2017). It is currently known that monolayer PrE cells propagate a rare stem cell, transit-amplifying and intermediate cell types; organoids cultivate those epithelial cells along with basal and luminal differentiated cells. A direct comparison of the in vitro systems has not been performed, and contrasting these cultures to tissue needs to be conducted to determine the effectiveness of each model. Additionally, the differentiation trajectory of the organoids is not well understood, and could vary greatly in the in vitro setting without direction from stromal cells. This thesis aims to address some of these questions in **Chapter II**, and to characterize the prostate epithelial organoid model as fully as possible. Next, in **Chapter III**, the organoid model will be used to test the hypothesis that vitamin D promotes differentiation of prostate and determine the effect of vitamin D on each of the epithelial sub-populations identified by scRNAseq.

CHAPTER II: CHARACTERIZING THE CELL TYPES AND DIFFERENTIATION OF PROSTATE EPITHELIAL ORGANOIDS

A. Introduction

i. Organoid Background

The human prostate consists of stratified epithelial secretory glands surrounded by a fibromuscular stroma. The epithelial glands are composed of a basal layer, a secretory luminal layer, and a rare neuroendocrine population (Long et al., 2005; Toivanen and Shen, 2017). To study epithelial cells, primary prostate epithelial cells (PrE) are traditionally grown as a monolayer in two-dimensional culture. It has been recently demonstrated that expansion of primary cells into three-dimensional prostatic organoids better mimics prostate epithelial glands by recapitulating epithelial differentiation and cell polarity (Clevers, 2016; Kretzschmar and Clevers, 2016). These protocols have two major limitations that will be addressed in this chapter: availability of tissue and primary cells, and use of elaborate conditioned media.

For generation of prostate organoids, protocols use fluorescence activated cell sorting (FACS) of dissociated tissue to isolate cells with stem, luminal or basal characteristics for a homogenous parental seeding culture (Drost et al., 2016; Karthaus et al., 2014; Yamamoto et al., 2012). These protocols require large amounts of tissue in order to isolate a sufficient number cells for flow cytometry, and require the use of Rho-Kinase1 inhibitor to avoid apoptosis during digestion and FACS. For labs that do not have access to whole prostate, it would be useful to develop a model that can grow organoids from passage 1 primary cells expanded from small portions of tissue punches.

Defined organoid culture medium has been published by Hans Clevers group that uses a specific set of factors to generate heterogeneous cell populations (B27, nicotinamide, N-acetyl-L-cysteine, EGF, A83-01, Noggin, R-spondin 1, Chiron, FGF10, Rho-Kinase1 inhibitor and SB202190). Some version of this list of factors has been shown to generate organoids for multiple human and rodent tissue types including intestine, prostate, liver, kidney, stomach, and even

reptilian tissue such as snake venom glands (Barker et al., 2010; Drost et al., 2016; Hu et al., 2018; Post et al., 2020; Sato et al., 2009; Schutgens et al., 2019). It's possible that, after publication from a high-profile lab, this list has become the standard defined-media to use for general epithelial organoid culture of any tissue type. Many of these factors are likely found in traditional FBS or charcoal stripped FBS, which are an abundant source of protein (Tu et al., 2018) and would be a much cheaper alternative for less-illustrious lab settings. A prostate organoid protocol with charcoal stripped FBS would likely supply the necessary growth factors and could be supplemented with DHT to allow for differentiation of AR+ luminal cells. A more general, less-defined culture media is utilized in this thesis as a more cost-efficient alternative to the Clevers' group defined-media.

ii. Single Cell RNA Sequencing

Basic profiles of the cell types within prostate in vitro models are known, but for a deeper understanding, single cell RNA-seq (scRNAseq) can be utilized to profile the transcriptomes of individual cells (**Figure 2**). ScRNAseq is a method that can identify cryptic sub-populations within a heterogeneous sample, such as organoids, using an unbiased analysis of individual expression profiles of thousands of individual cells simultaneously. This approach involves the isolation of single cells into microfluidic droplets that contain oligonucleotide-covered "barcoded" gel beads (**Figure 2A**). Each barcode contains two sequences: one barcode sequence that is specific to the bead and a second sequence that is unique to each barcode, the "unique molecular identifier" (UMI) (**Figure 2A**). Cells are lysed within the droplet, and the oligonucleotide sequences capture and barcode the transcripts from each individual cell (**Figure 2B**). Each RNA transcript will then contain a barcode for the bead it was captured by, and a UMI that identifies it as a distinct from the other transcripts in the cell. Transcripts are converted to cDNA, sequenced, and aligned to a genome. Next computational analysis is used to create a gene expression matrix, which is the

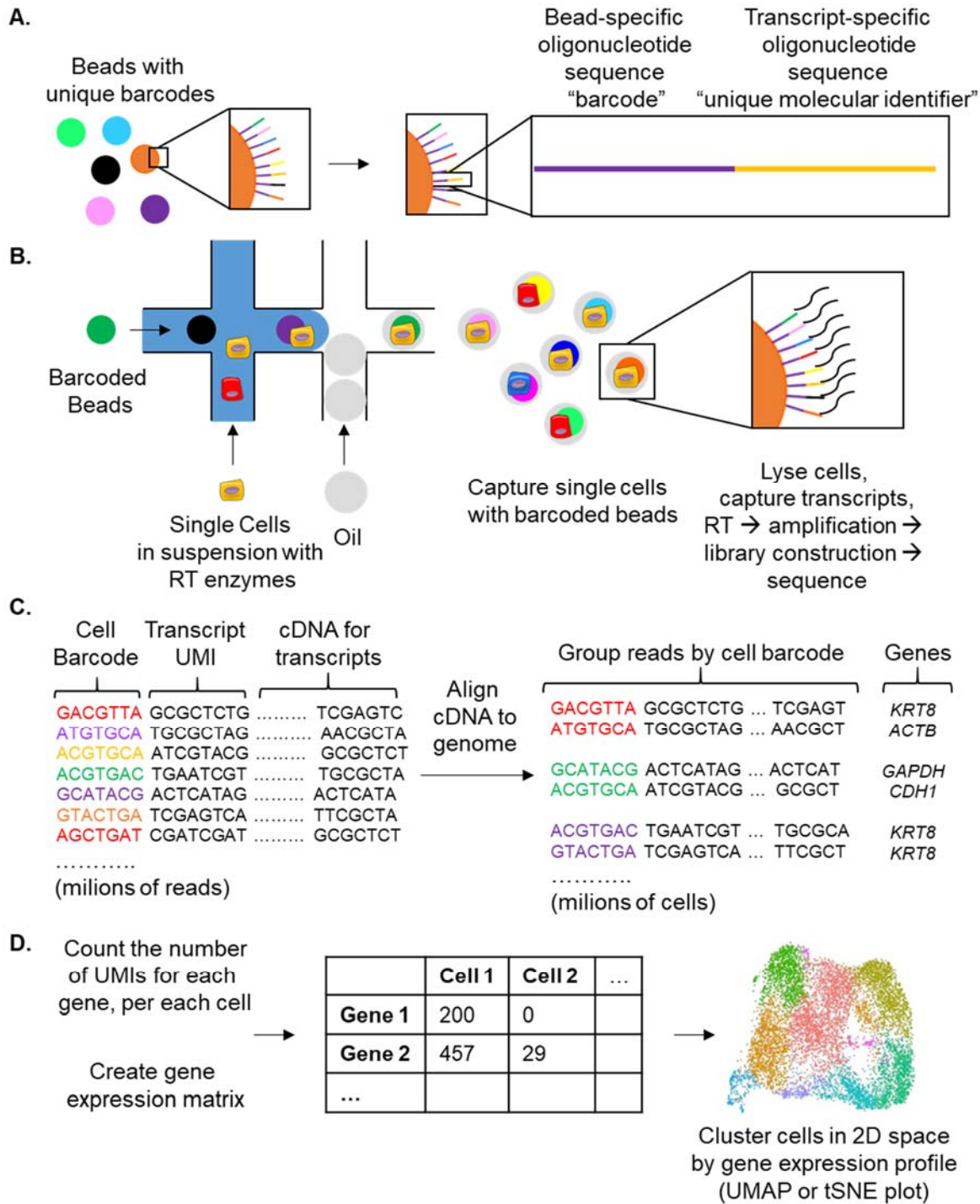


Figure 2. Diagram of single cell RNA seq workflow. (A) ScRNAseq barcoded beads **(B)** Capture of individual cells within droplets that contain beads, and barcoding of transcripts **(C)** Assignment of reads to cell **(D)** Gene expression matrix generation, adapted from Macosko (Macosko et al., 2015).

individual transcriptome library for each cell (**Figure 2 C & D**). The gene expression matrix identifies how many transcripts (number of UMIs) were detected for each gene in each cell. Using the gene expression profiles, the cells are clustered into distinct cell populations using dimensional reduction analysis (Hoffman et al., 2018; Macosko et al., 2015; Satija et al., 2015). Highly variable gene expression profiles are identified by principal component analysis, and the principal components are reduced to produce a 2D plot of the data (tSNE plot, UMAP plot). Each dot in these plots represents a cell, and each color represents a cell type. Cells with similar gene expression are found within the same cluster, and cells with very different gene expression profiles are located in separate clusters that are farther apart on the plot. In sum, this technique identifies gene expression profiles for individual cells, creating an in-depth atlas of cell populations found within a sample.

iii. Goals of chapter

This chapter establishes a primary prostate epithelial organoid model based off previously published protocols (Chua et al., 2014; Drost et al., 2016), but generates cells from small prostate tissue punches and does not utilize fluorescence activated cell sorting (FACS), Rho-Kinase1 inhibitor or defined media. To study the model, single-cell RNA-sequencing was performed on monolayer 2D PrE cells and 3D PrE organoid culture grown from the same patient. Cell populations between in vitro models were compared to each other and to those observed in patient tissue in vivo. Next, early- (day 8) and late-stage (day 14) organoids were compared to determine the differentiation trajectory. Cell populations were validated in additional patient samples by RT-qPCR and immunofluorescence microscopy. This work contributes to the field's knowledge of organoid culture, demonstrating which cell types are cultivated in vitro, and epithelial populations observed during in vitro differentiation.

B. Materials and Methods

i. Patient biospecimens

Human primary prostate cells were isolated and established from fresh radical prostatectomy tissues. Radical prostatectomy patients consented prior to surgery and prostate tissue samples from benign regions of the peripheral zone were collected according to UIC Internal Review Board-approved protocol # 2004-0679 (documentation of IRB is included in the appendix). Adjacent sections were collected for histologic inspection by a board-certified pathologist to verify the region as benign. Remaining tissue was digested in collagenase/trypsin to produce a single cell suspension. Cells were plated and grown in Prostate Cell Growth Media (Lonza, Basel, Switzerland) to select for outgrowth of epithelial cells. When ~70% confluent, cells were trypsinized to single cells, counted and cryopreserved into multiple aliquots. Epithelial purity was authenticated with RT-qPCR, confirming the expression of epithelial markers *KRT5*, *KRT8*, *KRT18* and *TP63*, and the lack of stromal marker *TIMP3*. Patient information is listed on **TABLE III**, RT-qPCR primers are listed on **TABLE IV**.

TABLE III. Patient characteristics

Patient^a	Age at radical prostatectomy	Pathology	Significance of organoid area with 1,25D^b
EA1	59	benign	0.2681
EA2	?	benign	0.0313
EA3	57	benign	0.0011
EA4	60	benign	<0.0001
AA1	71	benign	<0.0001
AA2	68	benign	0.0142
AA3	72	benign	0.1581
AA4	58	benign	0.0251
AA5	60	benign	0.0019
AA6	50	benign	0.0007
AA8	58	benign	0.0536
AA9^c			(not used for organoid experiment)
Other1	58	benign	0.4616

^aEA = European American, AA = African American, Other = non-European or African descent, self-declared by patient.

^bNon-parametric one-tailed Mann Whitney test, shown in Chapter III

^cPatient's cells were used for experiments shown in Chapter III

TABLE IV. Primers used for RT-qPCR

Target Gene	Primer sequence (5'-3')
<i>RPL13A</i>	F - GGAGCAAGGAAAGGGTCTTAG R - GGTTGCTCTTCCTATTGGTCATA
<i>KRT13</i>	F - AGGTGAAGATCCGTGACTGG R - GATGACCCGGTTGTTTTCAA
<i>AR</i>	F - CCAGGGACCATGTTTTGCC R - CGAAGACGACAAGATGGACAA
<i>KRT8</i>	F - GCTGGTGGAGGACTTCAAGA R - TCGTTCTCCATCTCTGTACGC
<i>KRT18</i>	F - CACAGTCTGCTGAGGTTGGA R - CAAGCTGGCCTTCAGATTTTC
<i>KRT5</i>	F - ATCGCCACTTACCGCAAGC R - CCATATCCAGAGGAAACACTGC
<i>VDR</i>	F- GACCTGTGGCAACCAAGACT R- GAACTTGATGAGGGGCTCAA
<i>CYP24A1</i>	F- CATTITAGCAGTCAGCTCCCG R- GGCAACAGTTCTGGGTGAAT
<i>DKK1</i>	F- ATGCGTCACGCTATGTGCT R - CCCATCCAAGGTGCTATGAT
<i>DKK3</i>	F- TCACATCTGTGGGAGACGAA R- CTGGCAGGTGTACTGGAAGC
<i>HPRT1</i>	F- TGCTGACCTGCTGGATTACA R- CTGCATTGTTTTGCCAGTGT
<i>ITGB6</i>	F- GCTTCGGATCTTTTGTGGAA R- TGTC AATGGCAA AATGTGCT
<i>ITGA3</i>	F - CTCCATCGGCAGACAGAGC R - CACCAGTCCGGTTGGTGTAG

ii. Primary cell culture

For standard monolayer culture, prostate epithelial (PrE) cells were thawed from primary passage into a collagen-coated dish and maintained in PrEGM (Lonza, Basel, Switzerland). Media was refreshed every 2-3 days. Monolayer cells were collected at ~70% confluent for endpoints.

iii. Organoid culture

Organoids were grown as previously described by our group (McCray et al., 2019b; Richards et al., 2019). Briefly, epithelial cells were thawed and grown at passage 1 on collagen-coated dishes to ~70% confluency. Single PrE cells were collected and plated sparsely (100 - 5,000 cells per well, depending on patient-specific growth ability) into 100 μ L 10-33% growth factor reduced phenol red-free Matrigel (Corning Inc., Corning NY). To prevent cells from adhering to the bottom and growing as a monolayer, cells were plated over a 50% Matrigel base layer in a 96-well plate or in a low-attachment 96-well plate without a base layer. Organoids were maintained in keratinocyte serum-free media (Gibco, Thermo Fisher Scientific, Waltham, MA) with bovine pituitary extract, and epidermal growth factor, supplemented with 5% charcoal-stripped fetal bovine serum and 10 nM dihydrotestosterone (DHT). Organoids were grown for 8 - 21 days as detailed in the figure legends, media was refreshed every 1–3 days.

iv. Single cell RNA sequencing and analysis

Patient-matched epithelial cells were grown in monolayer and organoid culture as described above. Monolayer cells were collected by TrypLE (Gibco, Thermo Fisher Scientific, Waltham, MA) dissociation. Organoids were harvested from Matrigel by Dispase (STEMCELL Technologies, Vancouver, Canada) dissociation followed by a second dissociation to single cells using TrypLE. Cell number and viability were determined by a Trypan Blue exclusion assay quantified on a Cellometer Automated Cell Counter (Nexcelom, Lawrence MA). All samples consisted of >80% viable cells prior to proceeding with the 10X Genomics (Pleasanton, CA) protocol for 3' Transcript Capture and Single Cell Library Prep. Approximately 5×10^3 total cells

were captured in gel beads for RT, cleanup, cDNA amplification, fragmenting, end repair & A-tail prep, and sample index tagging per manufacturer's instructions. The Chromium Single Cell 3' Library and Gel Bead Kit v2 was used for monolayer and organoid comparisons, the Chromium Single Cell 3' Library and Gel Bead Kit v3 kit was used for day 8 and day 14 organoid trajectory determination, as indicated in **TABLE V**. V2 libraries were sequenced on three lanes of the HiSeq 4000 (Illumina, San Diego CA), and v3 libraries were sequenced on one lane of the NovaSeq 6000 (Illumina, San Diego CA) at the University of Illinois at Urbana Champaign (UIUC) DNA services. Sequencing depth was ~ 50,000 reads per cell. Leftover cells not used for scRNA-Seq were collected into TRIzol Reagent (Thermo Fisher, Waltham MA) and reserved for RT-qPCR validation of the sequencing. Initial read alignment and quality control was performed using Cell Ranger 3.0.0 (10x Genomics, CA) for v2 libraries and Cell Ranger 3.2.1 for v3 libraries. Samples were aligned to Ensembl genome GRCh38 by UIUC DNA Services.

The Cell Ranger output was loaded into Seurat v3.0 for clustering of v2 libraries, and v3.1.0 was used for v3 libraries (Hoffman et al., 2018). Cells with high mitochondrial features (>8% of total mapped reads) were struck from the analysis to remove the influence of dead cells. Cells with unusually high or low numbers of mapped reads were removed from the dataset to exclude doublets or poorly-captured cells (Hoffman et al., 2018; Macosko et al., 2015; Satija et al., 2015). Individual genes related to the cell cycle or with uniquely low unique molecular identifier (UMI) counts within the context of the dataset had their variance regressed out to minimize their influence on variance-based clustering. Highly variable features were used for principal component analysis and reduction for tSNE and UMAP clustering. The number of principal components reduced and resulting modularity values for tSNE and UMAP plots are listed on **TABLE V**.

Canonical correlative analysis was performed in Seurat to integrate the separate datasets and allow for direct comparison of populations between samples (Hoffman et al., 2018). Two integrated datasets are included in this thesis. One is the monolayer, organoid and publicly

TABLE V. Quality metrics for scRNAseq input, sequencing and analysis

SAMPLE	2D	3D	V8	D8	V14	D14
% VIABILITY	85.60	81	93.3	93.6	93.4	85.1
10X KIT CHEMISTRY	v2		v3			
AIMED RECOVERY	5,000	5,000	5,000	5,000	5,000	5,000
ACHIEVED CELL RECOVERY	5,194	7,422	6655	3956	4561	4740
SEQUENCER	MiSeq		NovaSeq			
MEAN READS PER CELL	31,629	41,116	55963	84033	81071	70313
MEAN GENES PER CELL	3,569	3,783	4637	5567	5058	4673
% READS MAPPED CONFIDENTLY TO GENOME	87.10	86.90	92.2	91.8	93.5	93
SEURAT VERSION	Prerelease v3.0		V3.1			
PLOTTING METHOD	tSNE		UMAP			
# PRINCIPAL COMPONENTS	27	40	30			

All subsequent tSNE and UMAP plots were generated using a resolution obtained a modularity with >0.8 resolution to avoid over-clustering and bias

available human prostate tissue data set (D17_FACS_filtered GSE_117403, (Henry et al., 2018b)) shown later in **Figure 6**. The next is the day 8 and day 14 organoids shown later in **Figure 7**. Cluster markers were determined by differentially expressed genes (DEGs) in each cluster compared to all remaining cells, determined by Seurat non-parametric Wilcoxon rank sum test default settings (Butler et al., 2018). Clusters were assigned epithelial identities based on expression of known epithelial markers, as previously described (McCray et al., 2019a), markers listed on **TABLE I**. UMAP and tSNE plots, heat maps, and dot plots were generated in Seurat.

For pseudotime analysis of differentiation trajectory, CellRanger outputs for day 8 and day 14 organoids were loaded into Monocle 3 and combined. The trajectory was constructed following the Trapnell lab's workflow (Cao et al., 2019; Qiu et al., 2017; Trapnell et al., 2014). Briefly, data were loaded and normalized, samples were combined, batch effects were removed, cells with high mitochondrial gene expression were removed, and trajectories were constructed. The beginning node was selected based off of *KRT13* expression. Normalized expression of genes of interest (*MKI67*, *KRT6A*, *ITGB6*) was specifically queried in pseudotime to visualize cell location on UMAP plot.

v. Pathway analysis

Lists of cluster markers that were generated in Seurat were analyzed with IPA (QIAGEN Inc., Hilden Germany, <https://www.qiagenbioinformatics.com/products/ingenuitypathway-analysis>) (Kramer et al., 2014). Gene lists were input into the core analysis function to determine canonical pathways, Diseases & Functions, and Upstream Regulators, using the Ingenuity Knowledge Base reference set. Only genes with adjusted $p < 0.05$ were used and a cutoff of 1.3 for $-\log(P\text{-value})$ was used for significance for each analysis.

vi. RNA Extraction, amplification, and gene expression analysis

PrE monolayer and organoid cell cultures (**TABLE III**) were grown as described above. Cells were stored in TRIzol Reagent before RNA isolation. Samples were homogenized by

chloroform and RNA collected by alcohol precipitation and rehydration. RNA quantity and quality was determined by OD 260/280 and 260/230 on the NanoDrop Spectrophotometer (Thermo Fisher Scientific, Waltham MA). cDNA was synthesized with the High-Capacity cDNA Reverse Transcription Kit (Applied Biosystems, Beverly Hills CA) and qPCR run on LightCycler (Roche Applied Science, Penzberg, Germany). RQ was calculated from $\Delta\Delta CT$ to the reference gene *RPL13A* (Livak and Schmittgen, 2001). Primers are listed on **TABLE IV**.

vii. Histology

Formalin fixed paraffin embedded (FFPE) immunostaining of organoids was performed as previously described by our group (McCray et al., 2019b). Briefly, organoids were dissociated in Dispase, resuspended in HistoGel™ (Thermo Fisher Scientific, Waltham MA), solidified at 4°C, fixed in 4% paraformaldehyde for 1 hour, transferred to 70% ethanol, and paraffin-embedded. 5 μm sections were collected onto slides for staining. For immunocytochemistry (ICC) staining, organoids were whole-mounted on chamber slides as previously described by our group (McCray et al., 2019b) and monolayer cells were seeded on a chamber slide. Organoids and cells were fixed in 4% paraformaldehyde. ICC samples were permeabilized with Triton-X 100 (Sigma Aldrich, St. Louis MO). All samples were incubated with primary antibody for 1-2 nights at 4° C. Primary antibodies included monoclonal rabbit anti-Cytokeratin 13 (ab92551, Abcam), monoclonal mouse anti-E-cadherin (ab76055), polyclonal guinea pig anti-Keratin 8/18 (03-GP11, American Research Products, Inc.), monoclonal anti-p63a antibody (D2K8X, Cell Signaling Technology, MA), monoclonal rabbit anti-androgen receptor (D6F11, Cell Signaling Technology, MA), monoclonal mouse anti-integrin $\alpha 2/\beta 1$ (ab20483, Abcam, UK), and polyclonal rabbit anti-keratin 5 (905501, BioLegend, CA). ICC samples were incubated with Alexa Fluor conjugated secondaries for 1 h at room temp or overnight at 4°C. AR was detected using the rabbit specific HRP/DAB (ABC) detection IHC kit (ab64261, Abcam, Cambridge UK) following the manufacturer's instructions and counterstained with hematoxylin. ICC was counterstained with Alexa Fluor 647-phalloidin (Thermo Fisher Scientific, Massachusetts) and DAPI, when appropriate.

viii. Imaging

Brightfield images of organoids were captured using the Evos FL Auto 2 imaging System (Thermo Fisher Scientific, Waltham, MA). Fluorescent images were captured using the Evos FL Auto 2 imaging System (Thermo Fisher Scientific, Waltham, MA) or the Zeiss LSM 710 confocal microscope (ZEISS, Oberkochen Germany),

ix. Edu assay

Proliferating cells were visualized using Click-iT EdU AlexaFluor 647 Imaging Kit (Thermo Fisher Scientific, Waltham MA) as previously described (McCray et al., 2019b; Richards et al., 2019). Fully formed day 12 organoids were pulsed with EdU overnight to incorporate into dividing cells. The next day EdU was washed off and cells were given a night to recover prior to staining. On day 14, organoids were collected and fixed using the whole mount protocol described above. To visualize EdU, the Click-iT EdU protocol was followed according to manufacturer specifications. After EdU detection was complete, organoids were stained for KRT13, KRT8 and counterstained with DAPI as described above.

x. Quantification and statistical analysis

Statistical analyses were performed with GraphPad Prism version 8 (GraphPad Software Inc., CA), Microsoft Excel (Microsoft Windows, WA), Seurat R Package (Butler et al., 2018), and IPA software (QIAGEN Bioinformatics, DK); details can be found in figure legends. A non-parametric, one-sided unpaired, Mann Whitney t-test was used to compare organoid area. We considered $p < 0.1$ as statistically significant. For RT-qPCR, standard deviation of replicates is depicted by error bars, calculated with Microsoft Excel, and t-test and ANOVA comparisons were made in GraphPad Prism. Differential expression analysis was performed with Seurat, using a non-parametric Wilcoxon rank sum test, and adjusted Bonferroni corrected $p < 0.05$ was considered significant. A cutoff of 1.3 for the $-\log(P\text{-value})$ for pathway analysis in IPA was used.

xi. Data availability

The single cell RNA-seq data discussed in this publication have been deposited in NCBI's Gene Expression Omnibus (GEO). Monolayer and organoid v2 scRNAseq data are accessible through GEO Series accession number GSE130318. Day 8 and day 14 organoids are accessible through GEO Series accession number GSE142489. The publicly available patient tissue data is accessible through GEO Series accession number GSE117403 (D17_FACS_filtered) (Henry et al., 2018).

D. Results

i. Developing the primary prostate cell organoid Matrigel model

Organoids are described as 3D structures originating from a single stem cell (Kretzschmar and Clevers, 2016). To establish if the culture conditions for the 2D prostate PrE cells would support this 3D clonal outgrowth, cells from patient AA1 were separated into two aliquots and transduced with a red fluorescent protein (RFP) or green fluorescent protein (GFP) tracer. Once stably expressing the appropriate marker, cells were mixed together and plated as single cells in Matrigel as described in the Methods. Individual cells were tracked over time to observe organoid outgrowth. Resulting organoids showed distinct RFP or GFP expression and did not mix, confirming that a sole stem or progenitor cell generates the structure and that organoids are not cell aggregates (**Figure 3A**).

Matrigel is the commonly used matrix for organoid culture, but has limitations because of its undefined protein components, inter-lot variability, and its production from mouse Engelbreth-Holm-Swarm tumors (Hughes et al., 2010). Tumors produce large amounts of basement membrane (Orkin et al., 1977), so Matrigel is largely comprised of the basement membrane proteins laminin, collagen IV and enactin. However, mass spectrometry studies report over 1,500 unidentified proteins in Matrigel, some of which being intracellular proteins that could influence protein expression in culture (Hughes et al., 2010). To minimize these concerns, a Growth Factor Reduced Matrigel is available, but comparison of Growth Factor Reduced and Standard Matrigel reveals similar levels of non-basement membrane components (Hughes et al., 2010). Regarding inter-lot variability, different Matrigel lots have showed only ~53 batch-to-batch overlap in protein content (Hughes et al., 2010). In an attempt to address these issues, two alternate matrixes were attempted alongside Matrigel: uGel and bQ13. Cell-Mate 3D uGel (BRTI Life Sciences, MN) contains the polysaccharide ECM component hyaluronic acid and the biopolymer chitosan. bQ13 is a self-assembling peptide that forms nanofibers and has been shown to promote the culture of LNCaP PCa cells into 3D spheroids that produce PSA at comparable levels to Matrigel culture

(Hainline et al., 2018). When AA3 PrE cells were plated in Matrigel or the alternatives, organoids exclusively formed in Matrigel culture and cells appeared unable to divide in uGel and bQ13 (**Figure 3B**). It is likely that these supplementary scaffolds lack the undefined protein components found in Matrigel, and that those factors are necessary in the establishment of organoid culture. To avoid inter-lot variability, Matrigel was purchased in bulk for uniform use across experiments.

Growth of organoids under different experimental conditions may result in changes in shape and size, so bright-field imaging is widely used to study observed morphological phenotypes. However, recording and quantifying area or shape is a challenge for two reasons: 1) selection bias during imaging and 2) application of a two-dimensional parameter, such as area, to a three-dimensional sample. One strategy of image capture is to record a random field and measure a predetermined number of organoids in that field, however not all organoids in the selected field may be in-focus which can skew data. In this thesis, a pipeline was developed that could capture the 3D structure of organoids across multiple z-planes in an entire sample (McCray et al., 2019b). Organoids plated in a 96-well plate can be imaged in quadrants, at each z-plane that contains an organoid, and images can be stacked to obtain an Extended Depth of Focus (EDF) image that shows the in-focus portion of each z-plane. In doing so, the entire organoid population is sampled and in-focus for measurement of area or circularity to characterize morphology. This pipeline is illustrated in **Figure 3C** and was used to characterize organoids in the subsequent experiments.

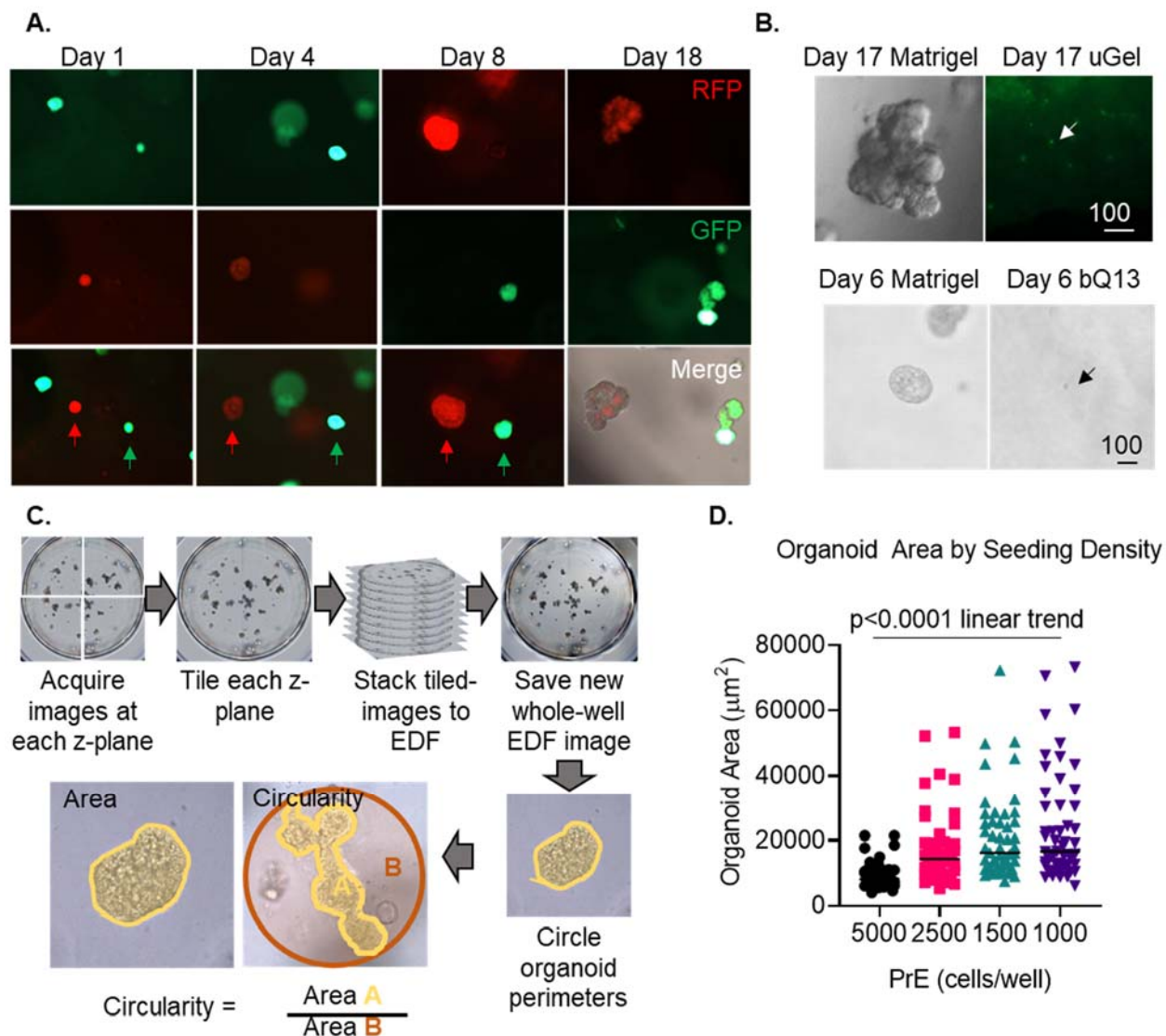


Figure 3. Developing the PrE organoid model system. (A) Organoids are derived from a single cell, RFP and GFP labeled PrE were seeded together in matrigel and resulting organoids showed exclusive reporter protein expression. **(B)** Comparison of AA3 organoids seeded in matrigel or in alternative scaffolds (uGel, bQ13). Viability dye (green) was used to visualize cell in uGel (top right). **(C)** Diagram of organoid imaging quantification pipeline. **(D)** Organoid seeding density alters size of organoids, organoids seeded more sparsely have larger area.

Organoid culture protocols often seed exceedingly high numbers of cells, up to 20k cells per 40 μ L Matrigel droplet (Drost et al., 2016). Using the 96-well plate format, cells are suspended in 100 μ L of Matrigel, which would require 50k cells per well if the Drost et al. seeding suggestions were adhered to. Primary cells are valuable and often limited in number, so sparse plating concentrations were tested in an effort to minimize the number of cells required per experiment. Organoids were plated at 5k, 2.5k, 1.5k and 1k cells per well and measured for area to determine the effect of seeding density on growth (**Figure 3D**). Organoid size was negatively correlated with seeding density, indicating an inhibitory effect of neighboring PrE cells on growth. Increased cell density increases competition for growth factors in media, degrades the Matrigel matrix more quickly and can result in cell clumping. For these reasons, sparse seeding conditions were used going forward and seeding number was determined for each patient based of cell-specific ability to proliferate.

ii. Organoid culture exhibits more heterogeneous epithelial differentiation states than monolayer culture

Patient-derived PrE cells can be grown in monolayer or organoid culture conditions as in vitro models of prostate cell biology and as useful tools for mechanistic studies. Here we compared the cell populations within these patient-derived models using scRNAseq analysis on monolayer epithelial cells and organoids derived from the same patient (**Figure 4A**). Seurat was used for clustering and analysis of the individual datasets (Satija et al., 2015), identifying four clusters in the organoids and only three within the monolayer cells. The cell type identity of each cluster was determined by cross-referencing cluster expression with previously reported gene expression profiles of epithelial cells (**TABLE I**). Highly expressed genes in each cluster are shown by heat map, and common epithelial markers are shown by dot plot (**Figure 4B**). Dividing populations were identified by having high *MKI67*, *CENPF*, *CCNB1* and histone gene expression, and were denoted luminal or basal based on co-expression of cell division markers with *KRT8/18*

or *DKK1/PDPN*, respectively (Henry et al., 2018). The “Integrin^{High}” population was named for its high expression of binding partners of integrins: laminin (*LAMA3*, *LAMC2*), vimentin (*VIM*), and fibronectin (*FN1*) (Humphries et al., 2006). The stem cells were marked by high expression of numerous putative prostate epithelial stem markers, including *KRT13*, *SERPINB1*, *LY6D*, *PSCA*, *KLK11* and *CSTB* (Henry et al., 2018; Hu et al., 2017; Moad et al., 2017).

The major differences between the culture conditions were the dividing populations and the Integrin^{High} populations. In monoculture there was one single dividing population that coexpressed basal and luminal markers, likely the transit-amplifying population that has been previously described (Bühler P, 2010; Uzgare et al., 2004). In organoids, there were two dividing populations with more distinct basal or luminal expression, indicating that the cells were differentiating in the 3D environment. The Integrin^{High} population was predicted to be a polarized cell type, as integrins are important regulators of cell-cell adhesion and polarity (Lee and Streuli, 2014). Luminal cells are the secretory, polarized cells in the prostate, and should be enriched in organoid culture compared to monoculture. That appears to be the case here, where the Integrin^{High} population is greatly enriched in 3D and co-expresses the luminal marker *KRT8*.

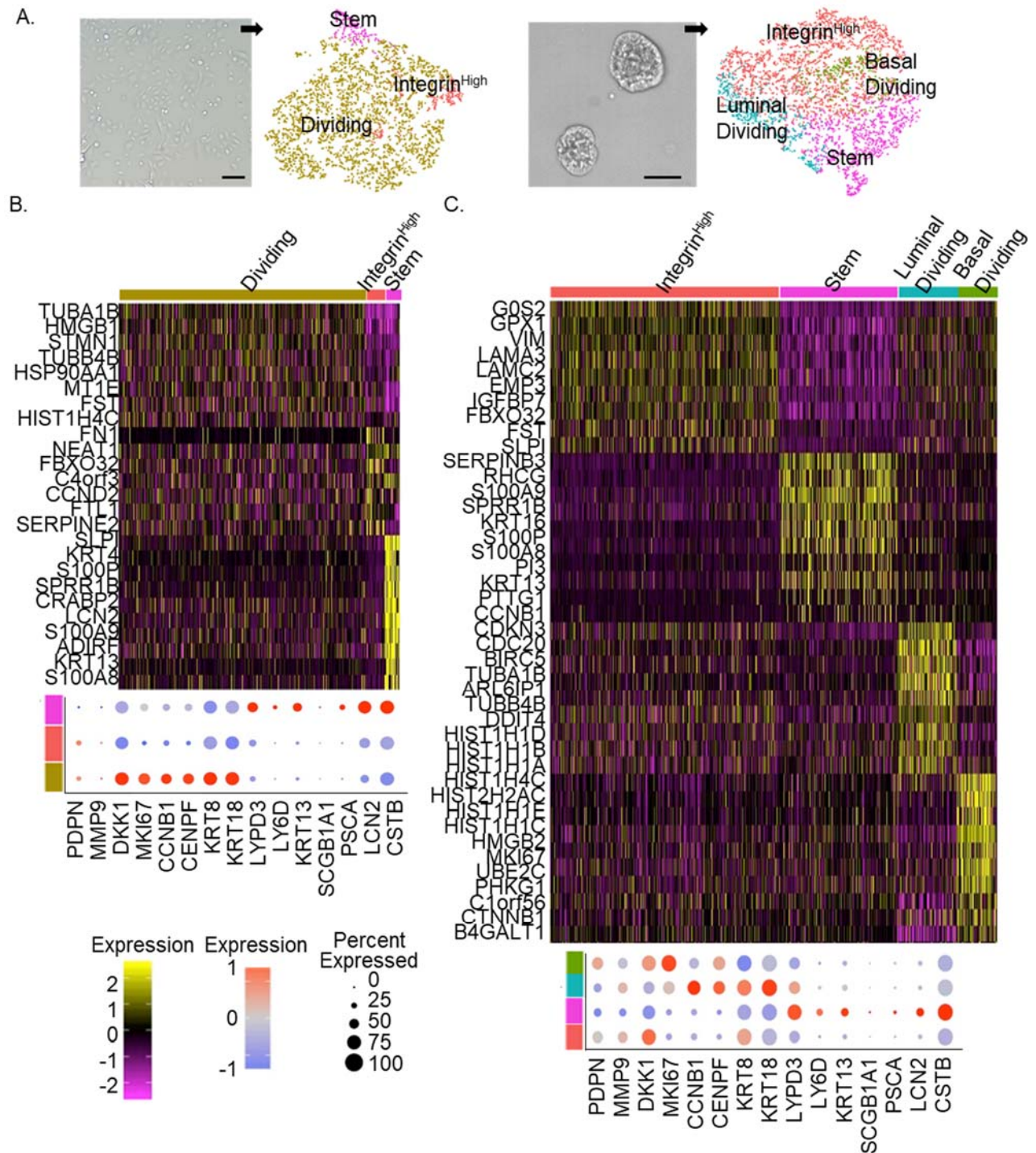


Figure 4. Single cell RNA sequencing of monolayer and organoid PrE cells derived from a single patient. (A) Monolayer (left) and day 8 organoids (right) were grown from AA8 patient tissue and collected for scRNAseq. Resulting t-SNE plots for samples are shown (adjacent). Scale bar = 100 μ m, modularity (M) > 0.80. **(B-C)** Heatmaps (top) for genes unique to each cluster and dot plots (bottom) for epithelial markers for monolayer **(B)** and organoid **(C)**.

To validate protein expression and observe the epithelial populations, immunostaining was performed. Stem marker CK13 was expressed in discrete regions of patient tissue and monolayer and organoid cells derived from that tissue (**Figure 5A**). CK13 expression was maintained in one or a limited number of cells over the course of culture (**Figure 5A**). Basal markers CK5 and p63 and luminal markers CK8 and AR were also confirmed (**Figure 5B**). There were intermediate phenotypes that showed dual positive expression of CK8/p63 and CK8/CK5 (**Figure 5B & C**). There were CK8+ cells lacked basal markers and AR+ cells, indicating luminal differentiation (**Figure 5B**, white and black arrows). Integrin $\alpha 2$ and $\beta 1$ subunits were observed at the periphery of the organoid, likely interfacing with the rich source of collagen and laminin in the Matrigel matrix. CK8 and integrin were colocalized, as was seen in the scRNAseq data, suggesting a polarized luminal cell phenotype (**Figure 5D**). Multiple organoid morphologies were present in culture (**Figure 5A, C & D**), where branching and acinar structures were observed.

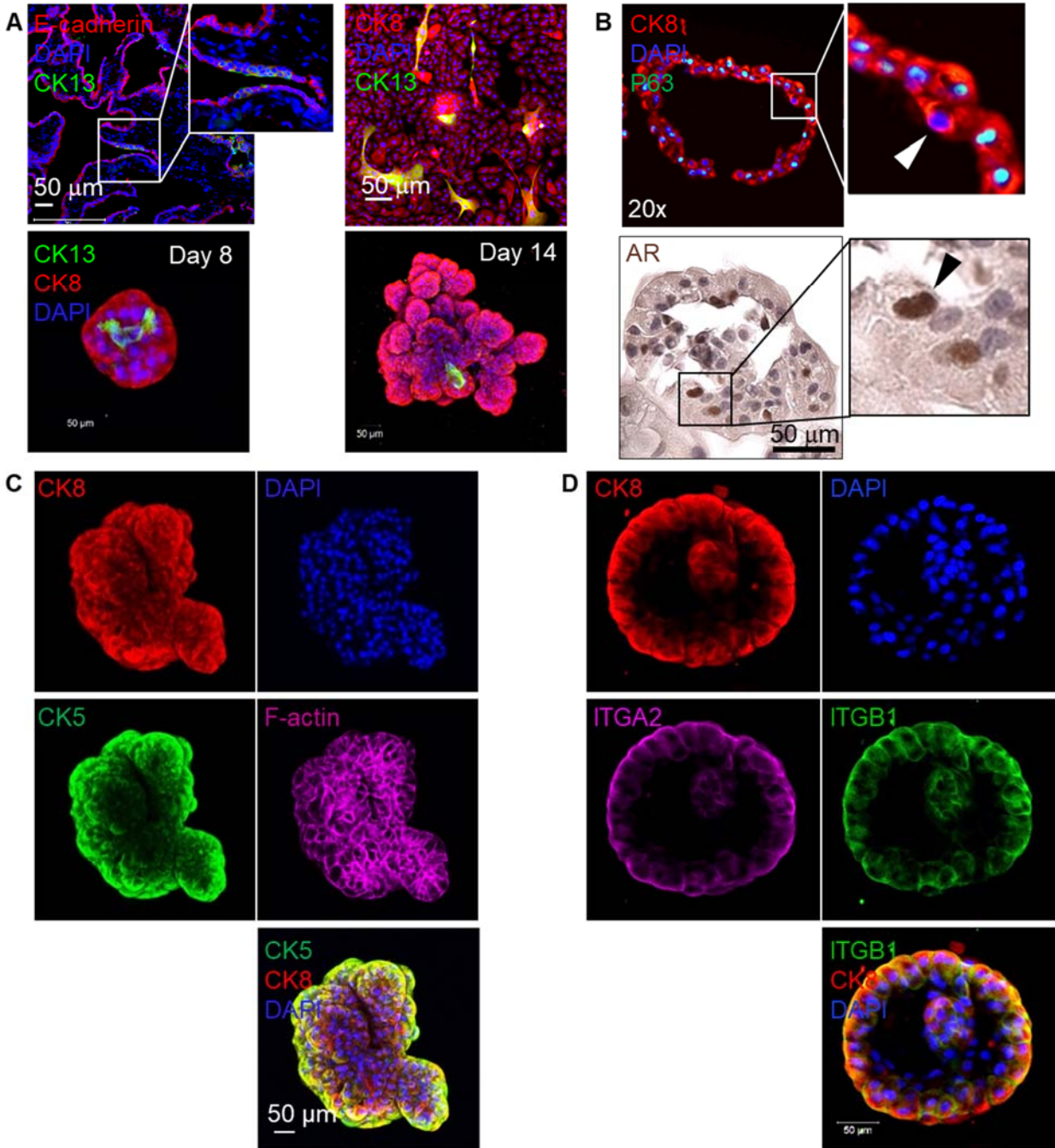


Figure 5. Immunostaining validates expression of stem, basal, luminal and polarity markers. (A) Expression of CK13 (green), CK8 (red) or E-cadherin (red) in patient tissue (top left), monolayer cells (top right), and day 8 (bottom left) and day 14 (bottom right) organoids. **(B)** Immunostaining of FFPE organoids for AR (brown, bottom) and CK8 (red, top) with P63 (green, top). **(C)** Expression of CK8 (red) and CK5 (green) in a whole mounted organoid counterstained for F-actin (pink) and DAPI (blue). **(D)** Expression of CK8 (red), integrin $\alpha 2$ (pink) and integrin $\beta 1$ (green) in a whole mounted organoid counterstained with DAPI. Scale bars = 50 μ m.

iii. In vitro models cultivate stem and progenitor cells from patient tissue

To explore how the cell populations within 2D and 3D in vitro models compare to fresh tissue, the monolayer and organoid data were integrated with a publicly available human prostate scRNAseq data set (GSE117403) (Henry et al., 2018). Integration and alignment created a single, batch-corrected dataset where highly variable features for each sample were preserved and common cell populations across the datasets were overlaid (**Figure 6A**) (Butler et al., 2018). Cell types in the newly aligned data set were named by expression of known stromal and epithelial markers, indicated on the dot plot (**Figure 6B**). Distribution of cells in each cluster for each sample are shown by bar graph (**Figure 6A**). As expected, the in vitro models were highly proliferative compared to tissue, and mostly clustered together. There was a noticeable lack of cells from the organoid sample with the luminal cluster when juxtaposed to tissue, but this could be accounted for by the overwhelming differences in cell division within the CK8/AR+ organoid luminal cells compared to terminally differentiated tissue luminal cells. Any basal or luminal separation that was observed in the unaligned, single organoid dataset would be masked by their proliferative nature when compared to tissue. Of note, the “club/hillock” *KRT13*+ stem cell population (Henry et al., 2018; Hu et al., 2017) was conserved between the in vitro cultures and tissue.

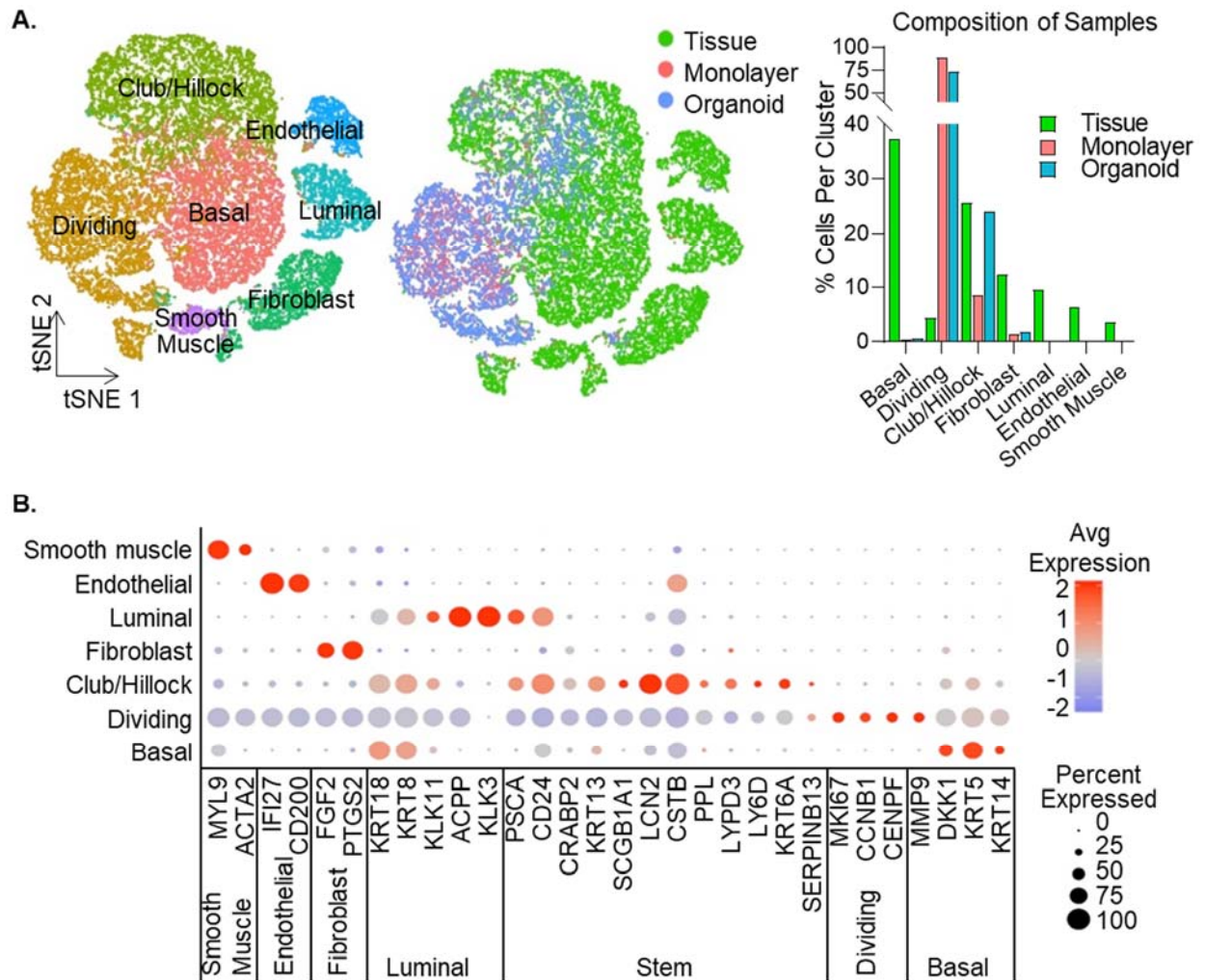


Figure 6. Integration of monolayer, organoid, and patient tissue scRNAseq data shows conserved stem cell population in model systems. (A) t-SNE plot of clusters (left) and samples (middle) for integrated dataset of monolayer, organoid and patient tissue and the composition of each sample showing the distribution of cells found in each cluster (left), the number of cells per cluster was divided by the sample input. **(B)** Dot plot depicting gene expression for epithelial and stromal markers in the integrated dataset.

iv. Elucidation of organoid differentiation trajectory

To further inspect cell populations in the organoids and characterize differentiation, AA2 organoids were collected for scRNAseq at an early time point (day 8) and a more-differentiated time point (day 14). Alignment was performed to visualize both samples on a single plot and overlay similar cell types in each condition (**Figure 7A, left & middle**). Early and late stage organoids contained scRNAseq clusters previously described (McCray et al., 2019a) and found in patient prostate tissue scRNAseq (Henry et al., 2018): a resident *KRT13*⁺ stem population (Henry et al., 2018; Hu et al., 2017), a large portion of dividing cells that express basal or luminal markers (Uzgare et al., 2004), and an Integrin^{High} population of polarized cells with high integrin expression, likely at the organoid–Matrigel interface (**Figure 7B**). By integrating the two organoid datasets, there was a great number of cells in the analysis, allowing for higher resolution clustering. This further separated the stem population into a *KRT13*⁺ and a *KRT6A*⁺ subset, and separated out a third dividing population, a basal population, and an intermediate population. Highly expressed genes unique to each cluster were input into Ingenuity Pathway Analysis (IPA) software to analyze canonical pathways (Kramer et al., 2014) (**Figure 8**). Stem cells had high enrichment for Wnt and VDR, similar to what is reported in gut and skin cells (Bikle, 2004; Peregrina et al., 2015). HIPPO signaling was enriched in the Integrin^{High} population, where it would likely regulate contact inhibition in polarized cell types (Genevet and Tapon, 2011)(**Figure 8**, red arrows). Steroid hormone pathways were enriched in the clusters, including androgen, estrogen, and aldosterone signaling. Z-score was undetermined for these steroid pathways due to an offsetting of both positively and negatively expressed genes (white score), so future validation experiments will need to be performed to determine directionality.

Distribution of epithelial clusters found in each sample at each time point revealed shifts in organoid composition during differentiation (**Figure 7A**, right). Early-stage day 8 organoids

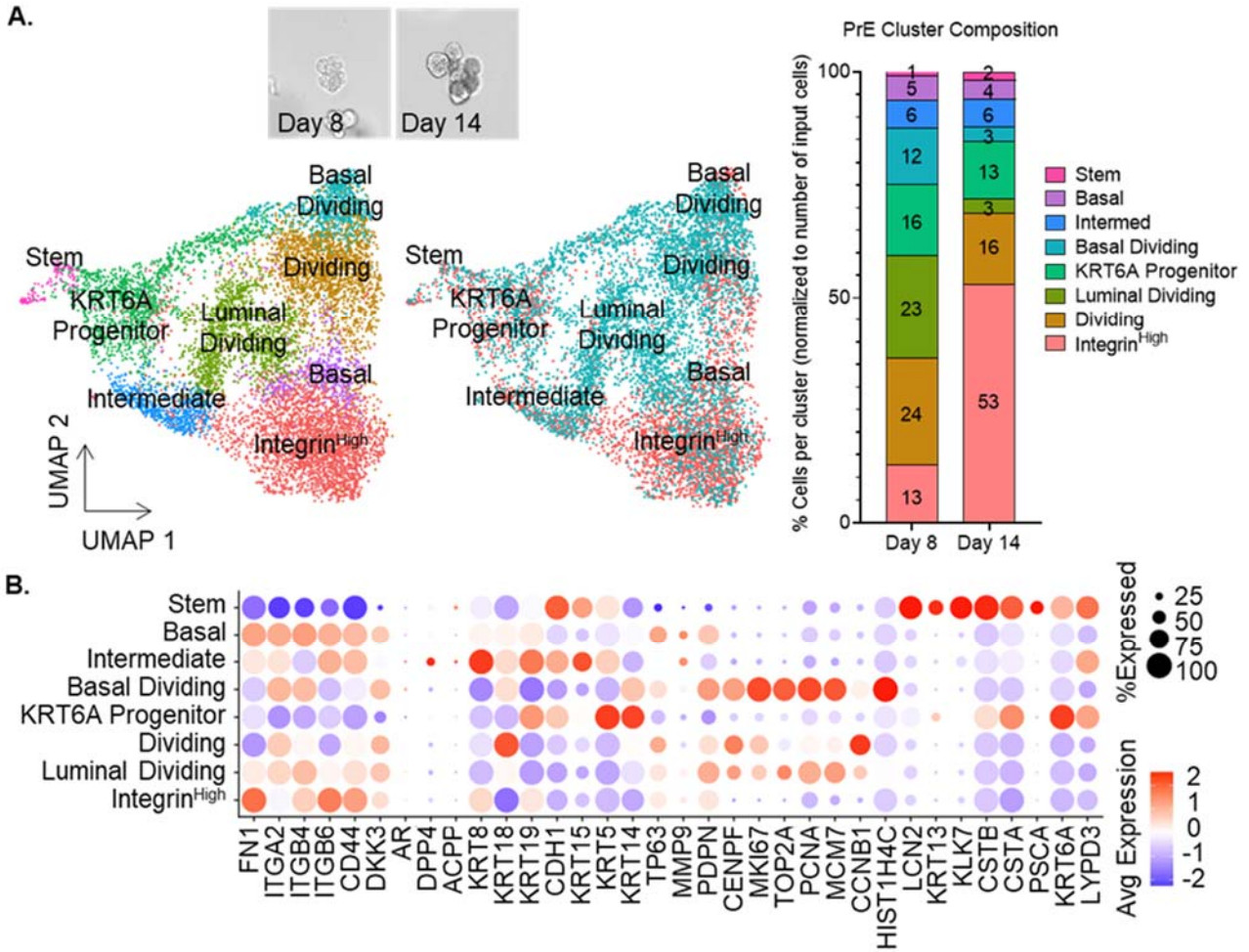


Figure 7. ScRNAseq of early (day 8) and late (day 14) stage organoids derived from a single patient. (A) AA2 organoids grown to day 8 and day 14 (top) were collected for scRNAseq and datasets were integrated, the resulting UMAP for clusters and sample distribution is shown (bottom). The composition of each sample showing the distribution of cells found in each cluster is shown (right), the number of cells per cluster was divided by the sample input. **(B)** Dot plot for epithelial markers in each cluster.

Enriched Canonical Pathways Cluster Markers

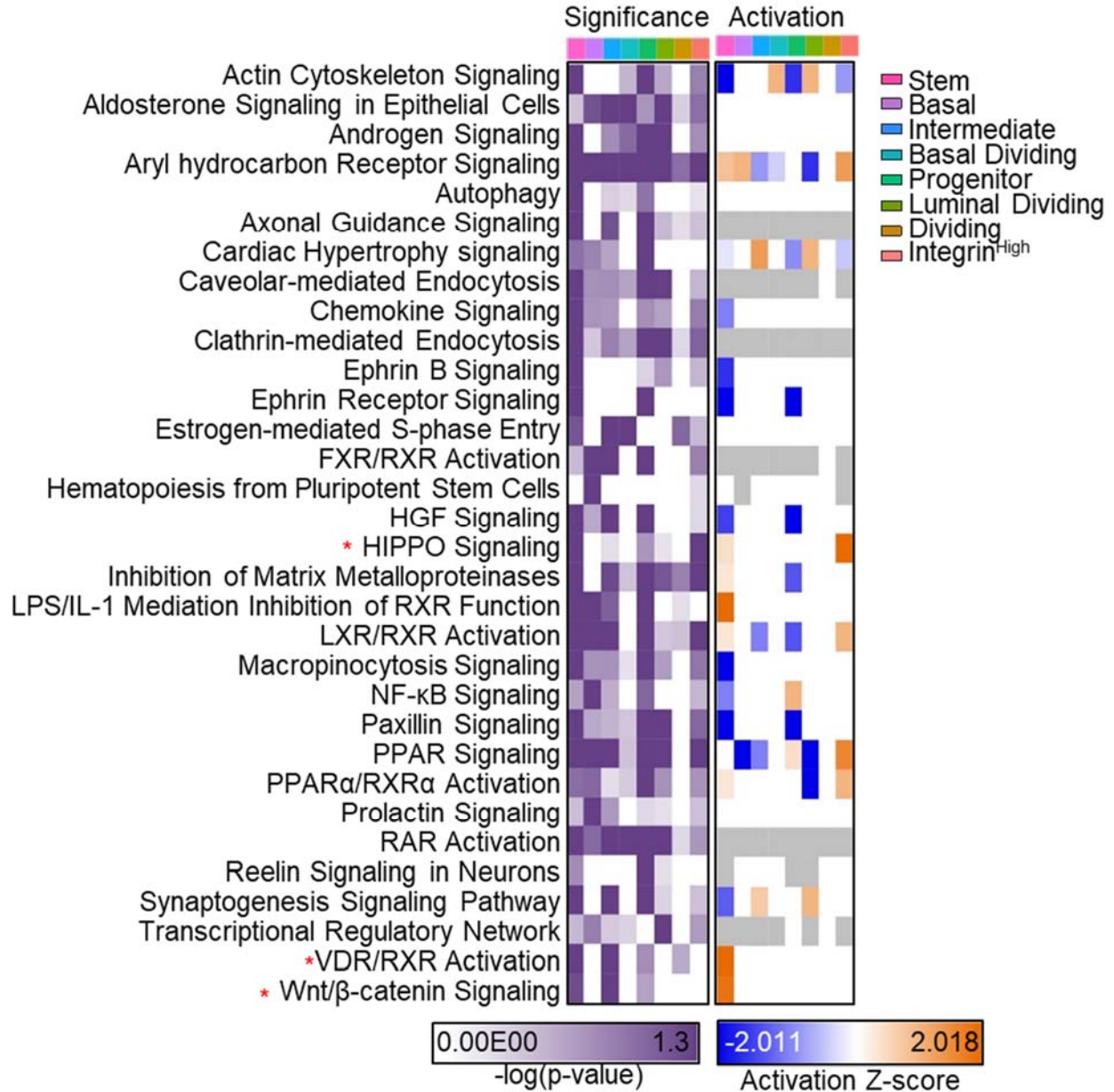


Figure 8. Enriched pathways in each scRNAseq cluster. Cluster markers were identified by Seurat as genes having uniquely high or low expression in each cluster, compared to all other cells in the dataset. Cluster markers were input into IPA canonical pathway analysis. Significantly enriched pathways related to “Nuclear Hormone Signaling” and “Organismal Growth & Development” are shown. P-value cutoff was $<\log_{10}(1.3)$. Scale represents $-\log(p\text{-value})$ for enrichment of each pathway (left) and activation z-score for enrichment of each pathway (right).

consisted primarily of dividing cell types, indicative of rapid expansion in culture. After differentiation at day 14, there was enrichment in the polarized cells compared to day 8, marked by high expression of integrins (ITGs) and their binding partner fibronectin (FN1).

To observe expression across organoid differentiation trajectories, day 8 and day 14 scRNAseq datasets were plotted together in pseudotime using Monocle 3 (**Figure 9A**) (Cao et al., 2019; Qiu et al., 2017; Trapnell et al., 2014). Pseudotime trajectories depict how much transcriptional progress a cell has undergone along the course of a cellular transcriptional program, such as differentiation. The length of the trajectory signifies different cellular states and each dot on the plot shows a cell along the trajectory. Here, *KRT13* was expressed at the beginning of pseudotime and cells from both time points were present at this stage, representing resident stem cell in organoid culture (Hu et al., 2017)(**Figure 9A**). Looking at the number of differentially expressed genes (DEGs) in cells at day 14 compared to day 8, there were the fewest DEGs in the stem cell, which should have the most stable transcriptional program (**Figure 9B**). Day 8 cells clustered in the middle of pseudotime, halfway through the differentiation trajectory, where *MKI67* was highly expressed. Day 14 cells clustered at the end of pseudotime where integrin expression was high and a fork was seen, possibly where basal and luminal lineages start to diverge.

Pseudotime analysis showed that *KRT13*-expressing cells and *MKI67*-expressing cells were mutually exclusive. To validate this, fully-formed organoids were pulsed with EdU overnight to mark actively dividing cells, followed by fixation and staining for CK13 (**Figure 9C**). As expected, CK13+ cells were EdU-negative, indicating that they proliferate slowly and fit the quiescent stem-cell phenotype. The next cell in the hierarchy would be the *KRT6A* progenitor (**Figure 9A**, top right) (Schmelz et al., 2005), which expressed modest *KRT13*+. These were observed by immunostaining for CK8 and CK13 revealed instances of dual positive cells and instances of multiple clustered *KRT13*+ cells that may represent different stages of stem/progenitor hierarchy (**Figure 9D**). To confirm the increase in Integrin^{High} cells overtime,

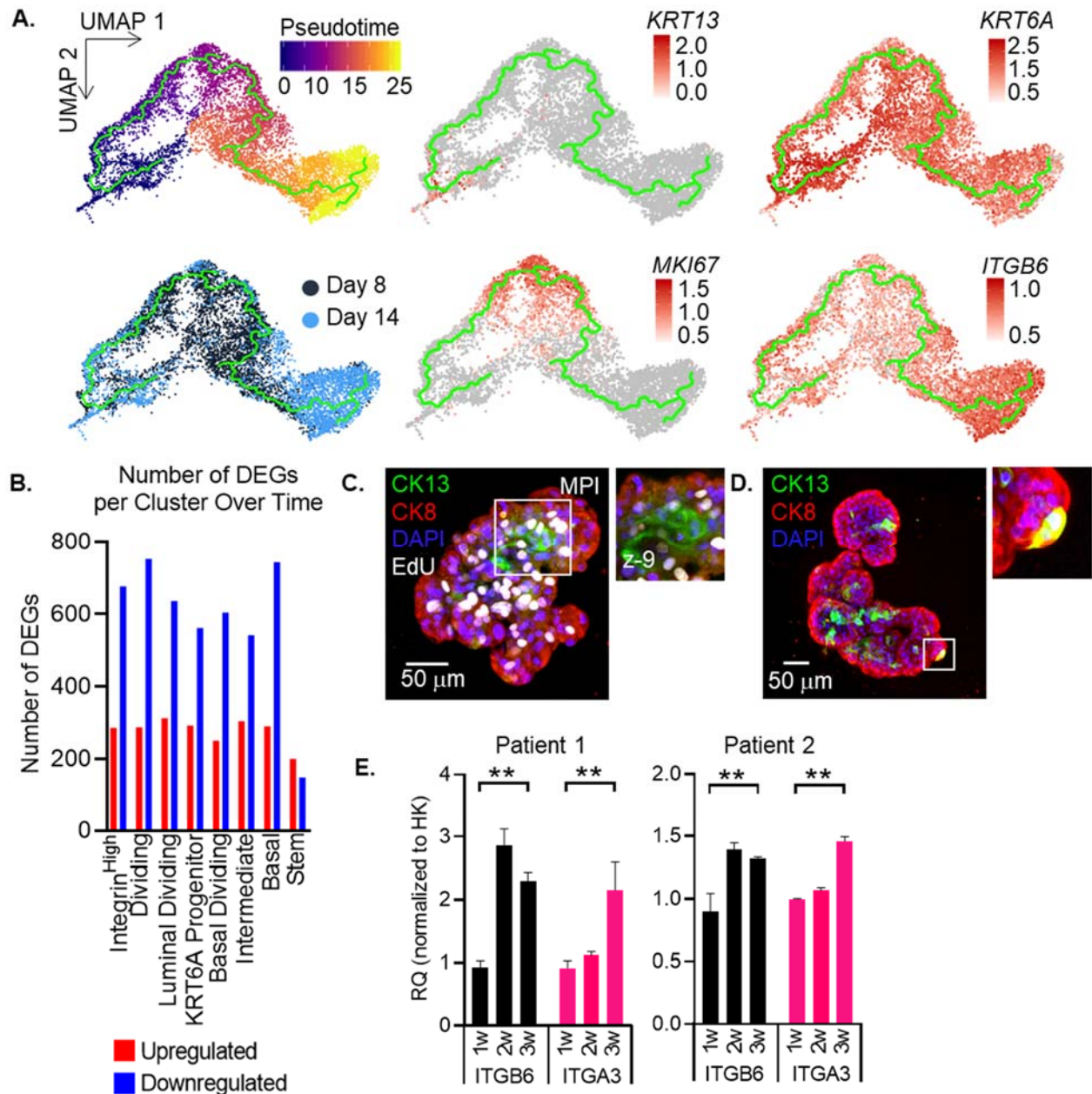


Figure 9. Pseudotime analysis of early and late stage organoids reveals differentiation trajectory. (A) Pseudotime of integrated scRNAseq data for day-8 and day-14 vehicle samples (top left). Sample distribution across pseudotime for day-8 (dark blue) and day-14 (light blue) cells (bottom left). Expression of KRT13 (top middle), KRT6A (top right), MKI67 (bottom middle), and ITGB6 (bottom right) across pseudotime. (B) The number of DEGs for each cluster over time, downregulated = blue, upregulated = red. (C) Edu (white) incorporation in organoids after 2-day pulse, stained for CK13 (green) and CK8 (red). (D) Organoid stained with CK13 (green) and CK8 (red) showing dual positive cell. (E) RT-qPCR for integrin expression in organoid samples for two patients over 3 time points. Relative quantitation shown normalized to HPRT1. Error bars represent standard deviation of replicates. ** represents $p < 0.01$ compared to 1w for 2-way ANOVA with uncorrected Fisher's comparison by row.

expression of two integrins, *ITGB6* and *ITGA3*, was tested in organoid samples over 1-3 weeks. Integrin expression positively correlated with increased time in culture by RT-qPCR and validates with the pseudotime findings.

D. Discussion

i. Summary

To experimentally investigate prostate function and disease, researchers utilize cell lines, primary cells and organoid culture for in vitro modeling. While it is known that monolayer cultures contain rare populations of stem and progenitor cells, most 2D culture consists of transit-amplifying phenotypes (Bühler P, 2010; Ivan V. Litvinov, 2006; Peehl, 2004; Uzgare et al., 2004). Prostate epithelial organoids grow out from a single cell and differentiate into basal and luminal cell types while maintaining a resident stem/progenitor cell that originated the organoid (Bhattacharyya et al., 2017; Chua et al., 2014; Drost et al., 2016; Karthaus et al., 2014). These basic profiles of in vitro epithelial cells are known, but recent utilization of scRNAseq analysis has identified novel populations of prostate epithelial cells from human prostate tissues (Henry et al., 2018), and this type of analysis has not been performed on human primary prostate organoid models. Here there were 3 monolayer and 4 organoid populations reported, confirming greater heterogeneity in organoids. To characterize differentiation, day 8 and day 14 samples were integrated and directly compared on a single plot, allowing for higher resolution clustering. This revealed 7 populations in the organoids: a KRT13⁺ stem cell, a KRT6A progenitor, dividing cells with basal and luminal markers, and a newly reported Integrin^{High} cluster. Content of these populations in the organoids shifted over time, from highly proliferative to highly regulative of cell-cell adhesion.

ii. In vitro stem and progenitor cells

Our analyses found cells at varying levels of differentiation along the epithelial hierarchy, starting with *KRT13*. *KRT13* has been previously described to mark regenerative cells in tissue and undifferentiated prostasphere culture (Henry et al., 2018; Hu et al., 2017; Schmelz et al., 2005). The populations also showed expression of *LY6D*, *LYPD3*, *CSTA*, *CSTB* and *PSCA*. Knockdown of *KRT13* in undifferentiated prostasphere culture leads to diminished sphere formation and self-renewal, validating its stem identity (Hu et al., 2017). *PSCA* and *KRT13* were described by Henry *et al.* to mark two clusters of epithelial cells termed “club” and “hillock”, based on of their similarity to immunomodulatory and progenitor-like cells found in the mouse lung, respectively (Henry et al., 2018). In contrast to the tissue-isolated cells, which had distinct populations that were either *PSCA*⁺ (club) or *KRT13*⁺ (hillock), here the in vitro cells had a single *PSCA*^{High}/*KRT13*^{High} cluster. Recently, FACS-sorted mouse prostate epithelial cells analyzed using Fluidigm qPCR showed *LY6D* expression in a population of organoid-forming cells within both the luminal and basal compartments (Barros-Silva et al., 2018). The *LY6D*⁺ cells formed solid, acinar or translucent organoids, similar to the organoid morphologies that are observed in culture (**Figure 5**). *LY6D* and *KRT13* were co-expressed 3D cells and had similar expression profiles to the reported *DLK1*⁺ cells (Moad et al., 2017). Human *DLK1*⁺ prostate basal cells have also been shown to form solid spheroids, spheroids with lumens and spheroids with tubules. Taking these reports together, there is substantial support for *KRT13* as a stem marker in tissue and in organoid culture, and the genes coexpressed by this cluster (*LY6D*, *PSCA*, *DLK1*) can be added to the growing troupe of markers suitable for isolating these cells

iii. Implications for the Integrin^{High} cluster in the differentiation of organoids

Integrin receptors bind to components of the extracellular matrix and their signaling is involved in proliferation, survival, adhesion and migration (Goel et al., 2009). Integrins mediate cross-talk between the ECM and the cellular cytoskeleton to control the cell's sense of space for

growth, requirements for detachment and migration, directionality for polarization, etc (Giancotti and Ruoslahti, 1999). Here, the Matrigel matrix is a bonanza of integrin binding partners, such as laminin and collagen. In vivo, many of these factors would likely be supplied via stromal interactions at the basement membrane (**Figure 1**). Monolayer PrE culture requires a thin coating of collagen on a dish for growth, but other ECM factors are limited (Peehl, 2002). This could explain the low number of Integrin^{High} cells observed in the 2D scRNAseq data compared to 3D. The “Integrin^{High}” population was observed at the organoid-periphery and expressed basement-membrane proteins and integrin binding partners such as vimentin (*VIM*) and fibronectin (*FN1*) (Humphries et al., 2006). These genes are also upregulated during epithelial-to-mesenchymal transition (EMT) (Odero-Marah et al., 2018). It is possible that this is not an EMT phenotype, but is the product of an in vitro culture that lacks a truly physiological basement membrane and interaction with stromal cells.

Interaction with the 3D matrix in vitro has been shown to direct polarity, disruption and transfer of gut enteroids to a matrix-free, low-attachment environment resulting in reversal of polarity into an apical-out organoid (Co et al., 2019). The upregulation of integrin expression in organoid differentiation is consistent with observations that have been reported in other 3D tissue systems. In Madin-Darby canine kidney cell 3D culture, antibody blockade of β 1-integrin function interrupts cell polarity (Yu et al., 2005). These findings translate to kidney tissue, where blocking integrin α 2 and α 6 subunits in whole-organ culture (Zent et al., 2001) or integrin β 1 deletion in developing uterine buds (Zhang et al., 2009b) inhibits branching morphogenesis of the kidney. Primary mammary epithelial cells from *ITGB1* knockout mice do not form acini in vitro, with irregular lumens and cell polarity, and knockout of *ITGB1* in mammary glands impairs lactogenesis (Naylor et al., 2005). While integrins have been shown to be necessary for differentiation (Naylor et al., 2005), they are not sufficient, as mammary cells require the agent prolactin along with integrin:laminin interaction to produce milk protein (Streuli et al., 1995). In sum, these studies support the importance of integrin expression in polarity and function of luminal

cells. While it is unclear from this thesis which specific integrin subunits are involved in prostate epithelial organoid differentiation, and whether inside-out or outside-in integrin signaling is occurring, these findings add to a literature that describes the significance of integrin interactions in cell polarity and development of 3D morphology.

iv. Integrin signaling in the prostate and prostate cancer

There is scant literature describing the role of integrin signaling in healthy prostate tissue, although the localization of integrin expression has been shown (**Figure 1**) and integrins are used as markers for cell-type separation by flow cytometry (Henry et al., 2018). Many studies exploring the role of integrin signaling in prostate tissue focus on its function in disease progression (Hall et al., 2008; Moran-Jones et al., 2012; Varzavand et al., 2016; Zhang et al., 2009a). There are few studies of integrin signaling during prostate development and normal differentiation. In other tissues, integrin signaling regulates anoikis and luminal differentiation and has been studied as a regulator of branching morphogenesis and cell polarity (Naylor et al., 2005; Romagnoli et al., 2019; Yu et al., 2005; Zent et al., 2001; Zhang et al., 2009b). Given that the prostate is also made up of hollow epithelial glands with polarized, secretory cells, it is likely that integrin signaling has a similar function in this context. There is some evidence of this in the minimal literature available. For example, blocking integrin $\alpha 6$ or $\beta 1$ in 3D RWPE1 prostate cells culture reduces acinar formation (Bello-DeOcampo et al., 2001). There is also a noted requirement for laminin in the 3D culture gel, where only laminin or matrigel scaffolds are successful, fibronectin and collagen gels do not support formation of spheres (Bello-DeOcampo et al., 2001). Blocking integrin $\beta 1$ in mice post-pubertally does not result in morphological differences in the prostate epithelium, indicating that $\beta 1$ is not required for the maintenance of mature tissue (Moran-Jones et al., 2012). However, combining knockout with castration and reintroduction of androgen to stimulate growth results in increased basal cell proliferation, suggesting that loss of integrin $\beta 1$ results in fewer differentiated luminal cells (Moran-Jones et al., 2012).

While developmental and normal adult-stage integrin function is minimally published in the prostate, there is an abundance of studies exploring integrin signaling PCa (Goel et al., 2009; Suyin et al., 2013). Multiple integrin subunits are aberrantly expressed in PCa: $\alpha 2$, $\alpha 3$, $\alpha 4$, $\alpha 5$, $\alpha 6$, $\alpha 7$, $\beta 1$, $\beta 3$, $\beta 4$, $\beta 6$ (Goel et al., 2009). Generally, α subunits are downregulated and β subunits are over expressed, although their signaling is complex and varies by disease stage (Goel et al., 2009). As regulators of cell adhesion and ECM interaction, integrin expression is lost in primary tumors to promote intravasation ($\alpha 2$, $\alpha 6$) and expression is enhanced at metastatic sites to promote interaction with collagen in the bone ($\alpha 2$, $\alpha 6$, $\beta 1$, $\beta 3$, $\beta 6$) (Hall et al., 2008). Because integrins regulate so many essential cell pathways involving adhesion, proliferation and survival, there are ongoing studies that aim to target integrin signaling for PCa therapy (Philippe, 2016).

The preservation of integrin expression in the organoid model indicates that this system could be used to study integrin signaling in cancer. For example, integrin subunits $\alpha 3$ and $\beta 6$ both showed increased gene expression over the course of organoid differentiation and are dysregulated in disease (Goel et al., 2009). In the literature, integrin $\alpha 3$ is described as a proliferative regulator in mammosphere culture, whose loss results in a *LY6D* stem/progenitor phenotype (Romagnoli et al., 2019). In the prostate, integrin $\alpha 3\beta 1$ has been shown to promote the Hippo pathway and act as a tumor suppressor in PCa (Varzavand et al., 2016). Future studies could explore the role of integrin $\alpha 3$ in differentiation using PrE organoid and tumoroid cultures.

v. **Limitations and pitfalls**

Examination of population shifts through scRNAseq analysis is a helpful tool to explore trends across conditions, but it is limited. It is not possible to apply statistics to this method of analysis so a secondary form of validation should always be applied, such as RT-qPCR and protein staining. Integrin expression was shown to be upregulated over time by RT-qPCR. Future studies will utilize flow cytometry as an approach to observe an increase in the Integrin^{High} cluster over the course of differentiation in a quantitative manner.

There was a surprising lack of expression of the luminal cell markers *AR* and *KLK3* in the organoids by scRNAseq, but this should be interpreted with caution. A limitation of all single cell sequencing technologies is that it captures only 10-20% of transcripts per cell (the 10x Chromium Single Cell 3' v2 Kit used here has a capture rate of 14-15%), thus absence of the gene in the analysis is not conclusive evidence that it is not expressed. We did detect AR protein expression in cells of day 14 organoids and observed CK8+/p63- cells (**Figure 4B**), indicating luminal differentiation.

vi. **Conclusions**

Overall, this chapter described a method of growing organoids without flow cytometry or costly defined factors and observed alterations in seeding density resulted in dramatic changes in organoid growth. Through scRNAseq it was observed that both monolayer and organoid culture are capable of cultivating a rare population of stem cells that are marked by high expression of *KRT13*, *LY6D*, *LYPD3*, and *PSCA* that are similar to those found in the basal and luminal compartments of mouse and human prostate “hillock” regions. Organoid culture expands these cells via asymmetric division into highly dividing, proliferative lineage-committed cells that differentiate through a program of polarization via cell-cell adhesion and integrin networks. This catalog of scRNAseq in vitro populations provides an in-depth atlas of the cell types present in both monolayer and organoid models. It can serve as a valuable resource to the field, allowing for a deeper understanding of which cells are present in benign prostate model systems and how they change between in vitro and in vivo conditions.

CHAPTER III: THE EFFECT OF VITAMIN D ON PROSTATE ORGANOID DIFFERENTIATION

A. Introduction

i. Vitamin D metabolism and activity

Vitamin D is a vital steroid that is metabolized to the active hormone (1,25D) to control systemic calcium homeostasis and bone mineralization and locally regulate cell fate decisions at target tissues, such as the prostate (Feldman et al., 2014) (**Figure 10 A & B**). The vitamin D signaling pathway initiates in the skin when UV light triggers the isomerization of 7-dehydrocholesterol to synthesize cholecalciferol (vitamin D₃). Some vitamin D₃ is also absorbed in the intestine after consumption of fortified foods. Once obtained, vitamin D₃ circulates in the bloodstream bound to the vitamin D-binding protein (DBP) and proceeds to the liver and kidney for subsequent hydroxylation steps to yield 25-hydroxycholecalciferol (25D) and the active, secosteroid calcitriol [1,25-dihydroxyvitamin D (1,25D)] (Feldman et al., 2014). Of note, conversion of 25D to 1,25D can also occur locally in prostate tissue (Peehl et al., 2004). At target cells, 1,25D binds to the vitamin D receptor (VDR) which complexes with the retinoid X receptor (RXR) to act as a classical steroid hormone receptor and influence gene expression at vitamin D response elements on DNA (Racz and Barsony, 1999). Vitamin D is thought to regulate at least 3% of the genome (Bouillon et al., 2008) and ChIP sequencing for VDR bound DNA reveals binding at more than 3,000 protein coding genes, and over 1,000 nonprotein coding sites (such as long noncoding RNAs and miRNAs) (Fleet et al., 2019). Two canonical 1,25D-regulated genes include the 1,25D inhibitor *CYP24A1*, and the 1,25D-activator *CYP27B1*, which are upregulated and downregulated, respectively, for tight control of the signaling pathway (**Figure 10C**) (Feldman et al., 2014). This negative feedback loop is essential to supervise vitamin D activity, as it is modulates expression of crucial cellular pathways: apoptosis, proliferation, differentiation, angiogenesis, inflammation, and hedgehog signaling (**Figure 10B**) (Feldman et al., 2014; Merchan et al., 2017).

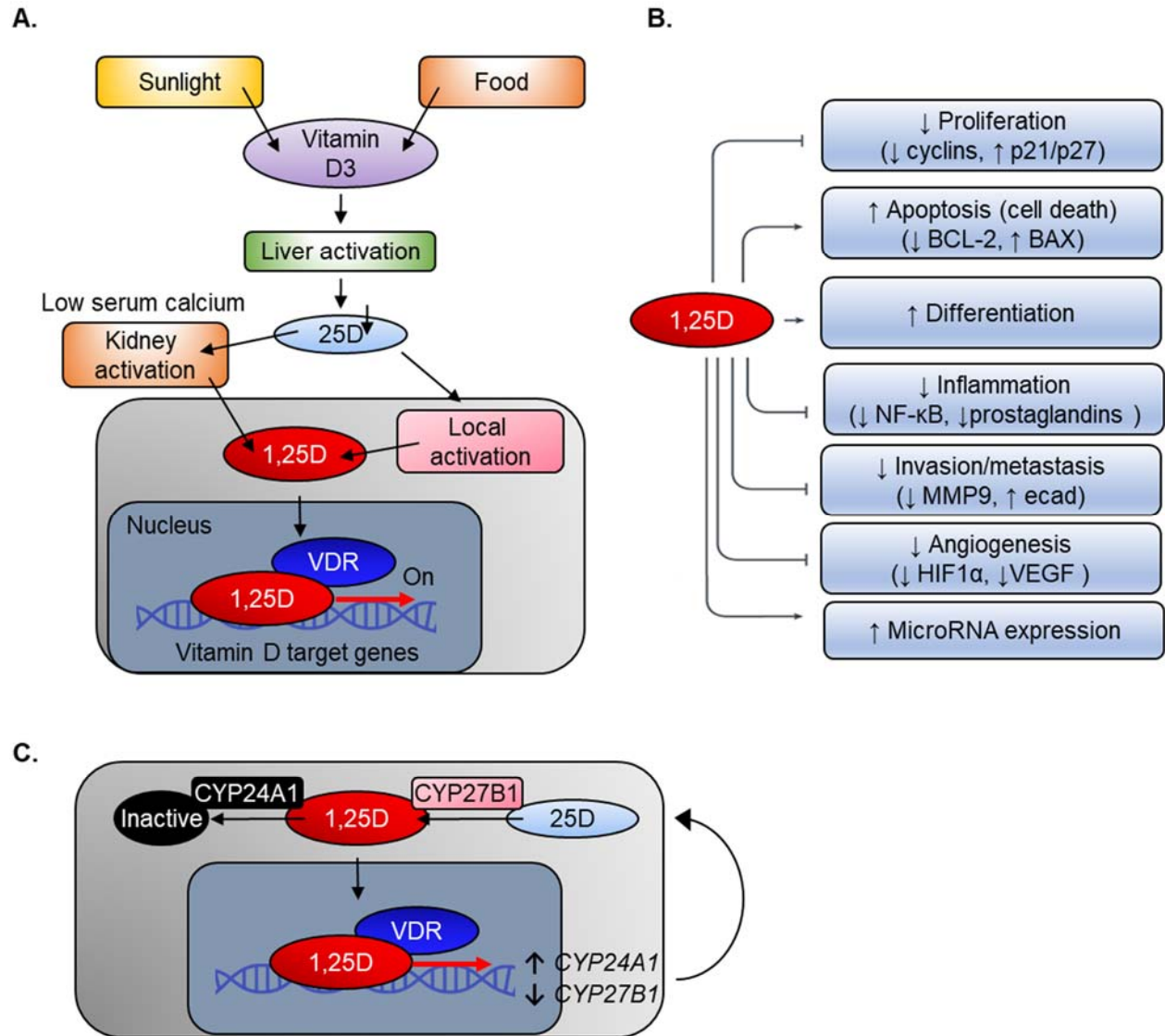


Figure 10. Vitamin D signaling pathway. (A) Vitamin D synthesis and activation. **(B)** The effect of locally-active 1,25D on cellular signaling. **(C)** Vitamin D feedback mechanism of activation (CYP27B1) and inactivation (CYP24A1). Adapted from Feldman (Feldman et al., 2014).

ii. Vitamin D deficiency is associated with prostate cancer aggression

The prostate is a hormonally responsive endocrine gland with robust expression of vitamin D receptor (VDR) and the enzymes for local production of 1,25D from the circulating pro-hormone, 25-hydroxyvitamin D (Peehl et al., 2004). In patients, vitamin D deficiency is associated with aggressive prostate cancer (Fang et al., 2011; Giovannucci et al., 2006; Murphy et al., 2014; Studzinski and Moore, 1995). This relationship is especially prevalent in patients who are frequently deficient due to protection from sunlight, such as African Americans, (Murphy et al., 2014) or lack of sun exposure (Gilbert et al., 2009), such as the elderly (Elshazly et al., 2017). The correlation is illustrated by distance from equator increasing risk of prostate cancer mortality (Hanchette and Schwartz, 1992), and diagnosis during summer improves PCa prognosis (Robsahm et al., 2004). To test if supplementation can offset the interaction between deficiency and PCa aggression, clinical trials have been performed to increase vitamin D intake in patients. Supplementation of vitamin D at 4000 IU/day decreased the number of cores positive for PCa at repeat biopsy (Marshall et al., 2012) and 2000 IU/day decreased PSA recurrence after initial treatment (Woo et al., 2005).

Hormone dysregulation plays a role in prostate cancer (PCa) initiation and progression, where local disease responds to hormone deprivation therapy but advanced disease becomes independent of androgen for growth (Karantanos et al., 2013). Similarly, well-differentiated prostate tumors have high VDR expression, whereas high Gleason grade, poorly-differentiated tumors have low VDR expression (Hendrickson et al., 2011). The relationship between vitamin D dysregulation and aggressive disease is supported by rodent models, where prostatic VDR deletion within the TgAPT mouse model of prostate carcinogenesis results in increased adenocarcinoma foci number and area (Fleet et al., 2019).

iii. Vitamin D as a regulator of differentiation

Given that the prostate gland relies heavily on hormone signaling for differentiation, and that disruption of vitamin D action in cancer is associated with decreased differentiation and aggressive tumors, there is evidence of 1,25D regulation of prostate epithelial differentiation, but the underlying mechanism is not well defined. Vitamin D's role in differentiation has been shown in many non-prostatic tissues. VDR expression occurs early in the developing rodent brain to regulate apoptosis and mitosis for brain cell differentiation (Kesby et al., 2011) and vitamin D deficiency in utero leads to defects in lung structure in mouse models (Chen et al.). Vitamin D is required for keratinocytes to form the calcium gradient that drives differentiation (MacLaughlin et al., 1990), it regulates intestinal stem cells within the crypt to control villus length (Peregrina et al., 2015; Spielvogel et al., 1972) and has roles in cardiomyocytes (Hlaing et al., 2014), odontoblasts (Mucuk et al., 2017), placenta (Hutabarat et al., 2018), and macrophages (Abe et al., 1981; James et al., 1997). While some of these studies explored 1,25D action in benign cells, the majority of reports focus on vitamin D inhibition of cancer cell growth and tumor progression (Banks and Holick, 2015; Holick et al., 2007; Larriba et al., 2013; Larriba et al., 2011; Muralidhar et al., 2019; Tavera-Mendoza et al., 2017; Yang et al., 2017) and there is limited knowledge about vitamin D and differentiation of benign prostate epithelium. Some data has been described: PC3 and LNCaP prostate cancer cells treated with a vitamin D analog show increased e-cadherin expression (Campbell et al., 1997), and rats supplemented with 1,25D show increased extracellular vesicle formation in regenerating prostate tissue (Gocek and Studzinski, 2009). These two studies indicate improved differentiation, but the mechanism has not been determined.

iv. Hypothesis and goals of chapter

Hormones are known to be important in differentiation in the prostate, but the capacity for vitamin D to do so has not been elucidated. Other steroid hormones such as androgen and retinoic acid regulate terminal differentiation of prostate luminal epithelial cells (Prins and Lindgren, 2015; Wright et al., 1996) and prostate bud formation during development (Bryant et al., 2014), respectively. In light of the in vitro data, the association between vitamin D and risk of aggressive PCa, and the high prevalence of vitamin D deficiency worldwide (Murphy et al., 2014), it is hypothesized here that vitamin D promotes epithelial differentiation in the prostate. This thesis aims to identify the process by which 1,25D drives or maintains differentiation of benign prostate epithelial cells to guard against carcinogenesis. Patient-derived organoids were used to model prostate epithelial differentiation (Richards et al., 2019) in a method adapted from the Clevers group (Chua et al., 2014; Drost et al., 2016) that was recently characterized by our lab using single-cell RNA sequencing (scRNAseq) (McCray et al., 2019a) and described in **Chapter II**. Here in **Chapter III**, we describe pro-differentiating effects of 1,25D on organoids and robust regulation of Wnt signaling and family members in the presence of physiologically relevant hormone levels.

B. Materials and methods

i. Patient biospecimens

Patient biospecimens were collected from fresh radical prostatectomy tissue as described in the previous chapter.

ii. Cell lines

RWPE1 cells were purchased from ATCC in 2014, cryopreserved in low-passaged aliquots, re-authenticated in 2016, and used only at <20 passages. LAPC4 were generously donated from Dr. Charles Sawyers and grown in RPMI 1640 (Gibco, MD) with 10% fetal bovine serum on poly-lysine-coated flasks. 957E/hTERT cells were generously donated from Dr. Don Vander Griend. RWPE1 and 957E cells were grown in uncoated cell culture dishes in Keratinocyte

Serum Free Media (Corning, NY). PC3 were purchased from ATCC, re-authenticated in 2013, and grown in RPMI 1640 (Gibco, MD) with 10% fetal bovine serum. All cells were cultured at 37°C with 5% CO₂.

iii. Primary cell culture and treatments

Monolayer and organoid primary cells and monolayer cell lines were maintained in media as described in Chapter II. Cells were treated with vehicle or 10 nM or 50 nM 1,25D (ultra-high purity 1 α ,25-Dihydroxycholecalciferol, Calcitriol, BML-DM200-0050, Enzo Life Sciences Inc, MI) over the course of culture, as indicated in figure legends. For Wnt induction, cells were treated with vehicle or 9 μ M Chiron for ~5 h before collection. For rDKK3 (1118-DK-050, R & D Systems, MN), cells were given 50 ng/mL over the course of culture, as indicated in figure legends.

iv. Primary organoid culture

Organoids were plated and maintained as described in Chapter II. On day 2-3 after plating, media was supplemented with vehicle (<0.01% EtOH) or 1,25D, and cells were grown for 7–28 days in culture, as indicated in figure legends.

v. Brightfield image acquisition, processing, and analysis

Images of organoid cultures were acquired and analyzed as previously described by our group (**Figure 3C**) (McCray et al., 2019b; Richards et al., 2019). Briefly, images were captured at 4x magnification using the Evos FL Auto 2 Imaging System (Thermo Fisher Scientific, MA), and up to 50 z-planes were collected per quadrant of a 96-well plate. Images of each quadrant were stitched together at each z-position, and z-stacks were compressed to a single enhanced depth-of-field image using Celleste Image Analysis software (Thermo Fisher Scientific, MA). Images were also collected at 10x and 20x of individual organoids for better resolution. Organoid count and area metrics were generated by manual identification of each organoid using Celleste Image Analysis software. At least three wells per patient were analyzed for technical replicates, each patient had 1-5 biological replicates performed, as permitted by sample availability. Area was

normalized to vehicle control, and a non-parametric, one-sided unpaired, Mann Whitney t-test was used to compare between treatments.

vi. Single cell RNA sequencing and analysis

Organoids were collected by Dispase and TrypLE as described above, and scRNAseq was performed as previously described (McCray et al., 2019a). Samples were >85% viable cells, and ~5,000 cells per sample were captured with the 10x Chromium chip (10x Genomics, CA). Libraries were prepared per manufacturer's instructions using the 3' Transcript Capture and Single Cell Library Prep v3 chemistry (10x Genomics, CA). Libraries were quantified and titrated by MiSeq (Illumina, CA) into an even pool and sequenced across one 2x150nt lane of the NovaSeq 6000 (Illumina, CA) at a depth of ~50,000 reads per cell. Library titration and sequencing was performed by University of Illinois at Urbana-Champaign (UIUC) DNA services. scRNAseq samples were processed and aligned to Ensembl genome GRCh38 using the Cell Ranger 3.2.1 pipeline (10x Genomics, CA) by UIUC DNA Services.

The CellRanger output was loaded into Seurat 3.1.0 clustering, following integration and differential gene expression workflows described in Chapter II. (Butler et al., 2018; Satija et al., 2015). Poor-quality cells with high mitochondrial gene expression and unusually high or low reads were subset out of the dataset to remove dying cells and doublets. Individual samples were normalized, cell cycle and mitochondrial features were scored, and data was scaled. Next, samples were integrated to find similar cells across samples, and cell cycle and mitochondrial features were regressed. Highly variable features were used for principal component analysis and reduction for UMAP clustering. We reduced 30 principal components at a resolution of 0.4 to obtain a UMAP plot with a modularity of 0.8249. Clusters were assigned epithelial identities based on expression of known epithelial markers. Cluster markers were decided by differentially expression genes (DEGs) in each cluster compared to all remaining cells, determined by Seurat default non-parametric Wilcoxon rank sum test (Butler et al., 2018). Similarly, DEGs with 1,25D

treatment compared to vehicle controls were determined for each cluster at both time points in the same fashion. Genes with adjusted $p < 0.05$ after Bonferroni correction were considered significant.

vii. Pathway analysis

The lists of cluster markers and DEGs with 1,25D treatment generated in Seurat were analyzed with IPA (QIAGEN, <https://www.qiagenbioinformatics.com/products/ingenuitypathway-analysis>). Gene lists were input into the core analysis function to determine canonical pathways, Diseases & Functions, and Upstream Regulators. Only genes with adjusted $p < 0.05$ were used. Once each core analysis was finished, a comparative analysis was performed for each pathway, function or Upstream Regulator across each cluster at each time point. For each analysis, a cutoff of 1.3 for $-\log(\text{P-value})$ was used for significance.

viii. Flow cytometry

Day-14 organoids from AA1 were dissociated with Dispase and TrypLE Express Enzyme (Gibco, MA) to generate single-cell suspensions and were fixed with ethanol. Cells were incubated with Alex Fluor 647-conjugated monoclonal rat anti-CD49f (BioLegend, CA) and PE-conjugated monoclonal mouse anti-CD26 (BioLegend, CA) antibodies and were sorted with LSRFortessa (BD Biosciences, CA). FlowJo software (FlowJo LLC, OR) was used to create scatterplot overlays of samples.

For live cell sorting for RT-qPCR array, day-17 organoids were dissociated as described above and incubated with Alex Fluor 647-conjugated monoclonal rat anti-CD49f (BioLegend, CA) and FITC-conjugated monoclonal mouse anti-CD26 (BioLegend, CA) antibodies. Cells were live-sorted with the MoFlo sorter (Beckman-Coulter, CA) directly into TRIzol (Thermo Fisher Scientific, MA) for RNA isolation. Images were generating using MoFlo companion software at the time of sort.

ix. RNA extraction, amplification, and gene expression analysis

For PCR profiling array, organoid RNA was isolated using TRIzol extraction. RNA quantity and quality was determined by NanoDrop Spectrophotometer (Thermo Fisher Scientific, MA). cDNA was generated with QIAGEN RT² First Strand Kit (QIAGEN, Germany), and gene expression was assessed using RT² Profiler PCR Array Human WNT Signaling Pathway Plus (PAHS-043YC-2, QIAGEN Germany). Arrays were run on QuantStudio6 (Thermo Fisher Scientific, MA) and normalized independently using five reference genes according to the manufacturer's protocol. The $\Delta\Delta\text{CT}$ method was used for comparative analysis (Livak and Schmittgen, 2001). For individual RT-qPCR, RNA was isolated with TRIzol and reverse-transcribed using a High Capacity cDNA Reverse Transcription Kit (Thermo Fisher Scientific, MA), with SYBR green qPCR performed on the QuantStudio6 machine. Primers are listed on **TABLE III**.

x. Protein isolation and western blotting

Organoids were collected from Matrigel, lysed in cell lysis buffer (9803, Cell Signaling, MA) with protease/phosphatase inhibitor (5872, Cell Signaling, MA), and sonicated. Bradford assay was used to detect protein concentration. Protein was denatured before separation on 1.5 mm 4%–12% NuPAGE Bis-Acrylamide gels with NuPAGE MOPS SDS running buffer and NuPage antioxidant (Thermo Fisher Scientific, MA). Gels were primed for 10 min at 100 V and run for 1 h at 125 V. Proteins were transferred from gels to 42- μm -pore Millipore PVDF membranes (Sigma-Aldrich, MO) for 1 h at 30 V. Protein membranes were blocked using Odyssey Blocking Buffer (LI-COR Biosciences, NE). Primary antibodies were diluted in Odyssey Blocking Buffer and incubated with blots overnight at 4°C. Primary antibodies used were monoclonal rabbit anti-DKK3 (ab186409, Abcam, UK), and monoclonal anti-GAPDH antibody clone 6C5 (MAB374, Millipore Sigma, MA). Secondary antibodies IRDye 800CW anti-mouse IgG (926-32210, LI-COR Biosciences, NE) and IRDye 680RD anti-rabbit IgG (926-68071, LI-COR Biosciences, NE) were

diluted in Odyssey Blocking Buffer and incubated with blots for 1 h at room temperature. Blots were imaged using the LI-COR Odyssey Imaging system.

xi. Histology

Immunostaining was performed as previously described by our group (McCray et al., 2019b). Organoids were collected from Matrigel by Dispase (STEMCELL Technologies, MA), resuspended in HistoGel (Thermo Fisher Scientific, MA), fixed in 4% paraformaldehyde, and paraffin-embedded. Whole-mounted organoids were transferred by pipette to a chamber slide, fixed in 4% paraformaldehyde, and permeabilized. GFP signal in transduced cells was quenched with 50 mM NH₄Cl if 488-channel was used for immunostaining. Sections (5- μ m) of embedded organoids or whole-mounted organoids were incubated overnight at 4°C with rabbit monoclonal anti-p63a antibody (D2K8X, Cell Signaling Technology, MA), polyclonal guinea pig anti-cytokeratin 8/18 (03-GP11, American Research Products Inc, MA), monoclonal rabbit anti-cytokeratin 13 (ab92551, Abcam, UK), monoclonal rabbit anti-androgen receptor (D6F11, Cell Signaling Technology, MA), monoclonal mouse anti-integrin α 2/ β 1 (ab20483, Abcam, UK), polyclonal rabbit anti-keratin 5 (905501, BioLegend, CA), or monoclonal rabbit anti-DKK3 (ab186409, Abcam, UK). Samples were incubated with Alexa Fluor conjugated secondaries for 1 h at room temp or overnight at 4°C. Samples were counterstained with Alexa Fluor 647-phalloidin and DAPI, when appropriate. For whole-mount staining of cytokeratin 13 and DKK3, incubation with unconjugated monoclonal rabbit anti-DKK3 (ab186409, Abcam, UK) and secondary antibody was performed, followed by incubation with conjugated monoclonal rabbit anti-cytokeratin 13 (EPR3671 conjugated to Alexa Fluor 647, ab198585, Abcam, UK) and counterstaining.

xii. ELISA

Primary epithelial cells were grown as monolayers and treated with vehicle or 10 nM 1,25D for 72 h, with treatments refreshed every 24 h. At 48 h, cells were washed and media depleted in bovine pituitary extract was added to prevent detecting exogenous bovine DKK3. Media was collected at 72 h, and cells were counted with a Cellometer Automated Cell Counter (Nexcelom,

MA) for normalization. Protein was quantified using Human Dkk-3 DuoSet Solid Phase Sandwich ELISA (DY1118, R&D Systems, MN), per manufacturer's instructions. Plates were read using Synergy HTX Multi-mode Read (BioTek, VT).

xiii. Lentiviral transduction

Cells were transduced by centrifugation (Xin et al., 2003) with DKK3 siRNA/shRNAi Lentivirus (iV006166) or scrambled siRNA GFP Lentivirus (LVP015-G) (Applied Biological Materials Inc., CA) and selected by passaging at least once into media containing 1–3 µg/mL puromycin until all cells were GFP+ before plating into Matrigel.

xiv. Quantification and statistical analysis

Statistical analyses were performed with GraphPad Prism version 8 (GraphPad Software Inc., CA), Microsoft Excel (Microsoft Windows, WA), Seurat R Package (Butler et al., 2018), and IPA software (QIAGEN Bioinformatics, DK); details can be found in figure legends. A non-parametric, one-sided unpaired, Mann Whitney t-test was used to compare organoid area. We considered $p < 0.1$ as statistically significant. For RT-qPCR and ELISA analyses, standard deviation of replicates is depicted by error bars, calculated with Microsoft Excel, t-test and ANOVA comparisons were made in GraphPad Prism. Differential expression analysis was performed with Seurat, using a non-parametric Wilcoxon rank sum test, and adjusted Bonferroni corrected $p < 0.05$ was considered significant. A cutoff of 1.3 for the $-\log(P\text{-value})$ for pathway analysis in IPA was used.

xv. Data availability

Day 8 and day 14 organoids grown in vehicle or vitamin D are accessible through GEO Series accession number GSE142489. ChIP sequencing for VDR-bound DNA near the *DKK3* promoter was observed in a previously published dataset of 1,25D-treated PrE cells from our lab (Baumann et al., 2019), deposited at NCBI GEO accession number GSE124576.

C. Results

i. Vitamin D supplementation enlarges prostate organoids and alters their epithelial composition

To initially determine the effect of 1,25D on organoid differentiation, organoids derived from a benign region of radical prostatectomy tissue were grown in media supplemented with 10 nM or 50 nM 1,25D or vehicle control (vitamin D-deficient, <0.01% EtOH). Similar to prior reports (Barros-Silva et al., 2018; Wang et al., 2015) organoids showed notable heterogeneity in morphology, with solid, translucent, or acinar/tubule-like structures (**Figure 11A**). Both concentrations of 1,25D produced visibly larger organoid area compared to the vitamin D-deficient control organoids (**Figure 11A**). The 10 nM dosage was selected for usage, as there was robust regulation of response genes *VDR* and *CYP24A1* at that concentration (Chen and DeLuca, 1995; Zierold et al., 1995) (**Figure 11B**). It is equivalent to ~4 ng/mL, which is within the range of circulating levels of active and inactive forms in serum (50 pg/mL and 40 ng/mL, respectively) (Richards et al., 2017). *VDR* was expressed in all patient-derived PrE cells examined (**Figure 11C**). 1,25D-induced phenotypes were further assessed in a diverse group of twelve patients' prostate organoids (**TABLE III**). Phenotypes varied in magnitude, highlighting the model's preservation of patient heterogeneity (**Figure 11D**). Overall, 1,25D significantly increased organoid size across biological and technical replicates (**Figure 11E**).

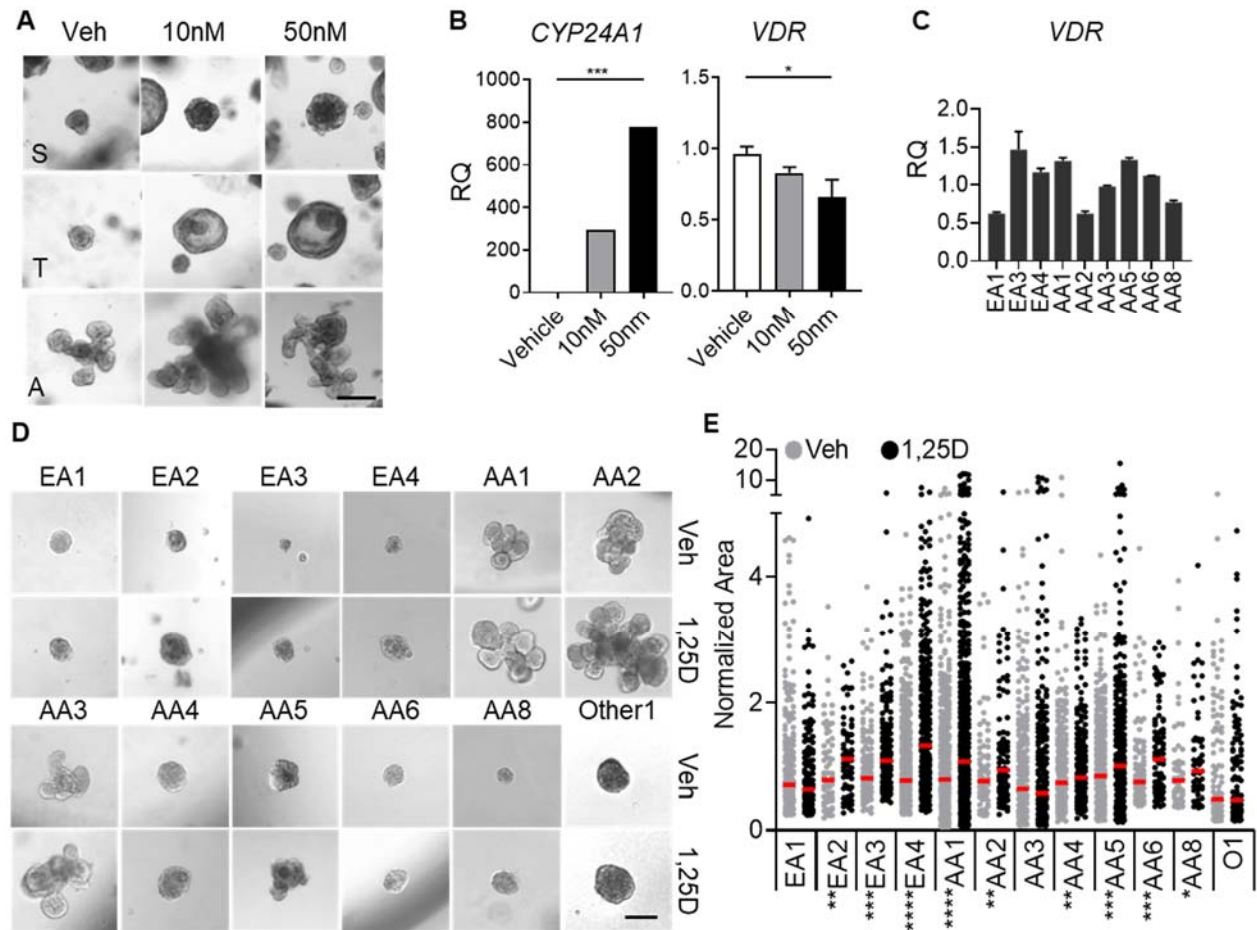


Figure 11. Vitamin D supplementation enlarges prostate organoids and alters their epithelial composition. (A) AA2 organoids grown in vehicle (Veh, <0.01% EtOH), 10 nM or 50 nM 1,25D until day 23. Representative images illustrate the heterogeneity of organoid morphology: solid (S), translucent (T), and acinar (A) structures were seen in each condition. Scale bar = 200 μ m. (B) RT-qPCR of *CYP24A1* and *VDR* expression AA2 organoids treated with veh, 10nM or 50nM 1,25D. RQ shown normalized to *HPRT1*. Error bars represent SD of replicates. (C) RT-qPCR of basal *VDR* expression in patient-derived prostate epithelial cells. (D-E) Day-14 organoids grown in vehicle (Veh) or 10 nM 1,25D (1,25D) from a diverse set of patient samples. (AA, African American; EA, European American; Other, not African or European descent, ancestries were patient self-declared). (D) Representative images and (E) relative area of at least three technical replicates per patient. Area normalized to the mean of the vehicle. Scale bar = 200 μ m (* p < 0.1; ** p < 0.05; *** p < 0.01, **** p < 0.001).

ii. Vitamin D supports normal organoid growth and drives differentiation

To observe epithelial populations in the organoids and determine alterations with 1,25D, AA1 organoids were collected for flow cytometry at day 14 and stained for epithelial markers. Luminal marker CD26 (Henry et al., 2018) and colony-forming, basal-progenitor marker CD49f (Yamamoto et al., 2012) were used. Overlay of flow scatterplots revealed a noticeable shift in CD26^{High}/CD49f^{Low} cells at day 14 with 1,25D as compared to controls (**Figure 12A**), indicating promotion toward a luminal phenotype and implying that 1,25D promotes organoid differentiation.

To further inspect cell populations found during differentiation and understand the influence of 1,25D, AA2 organoids were collected for scRNAseq at an early time point (day 8) and a more differentiated time point (day 14) (**Figure 12B**). Seurat version 3 was used to integrate datasets, align similar cells found in each sample, generate clusters, and perform differential expression analysis (Butler et al., 2018; Satija et al., 2015); the resulting UMAP of the integrated dataset is shown (**Figure 12C**). Organoids contained cells described in **Chapter II**: a resident *KRT13*⁺ stem population (Henry et al., 2018; Hu et al., 2017), a *KRT6A*⁺ progenitors (Schmelz et al., 2005), dividing cells that express basal or luminal markers (Uzgare et al., 2004), and Integrin^{High} polarized cells. The percentage of cells found in each cluster for each sample are shown (**Figure 12C**, right). Culture with 1,25D increased the percentage of dividing cells at day 8 (**Figure 12C**, red text), accounting for the observed increase in organoid area. After differentiation at day 14, culture with 1,25D resulted in a modest increase in the number of polarized cells and decrease number of progenitor cells at day 14 (**Figure 12C**, red asterisks). Taken together, these data indicate that 1,25D supports normal organoid growth and drives differentiation.

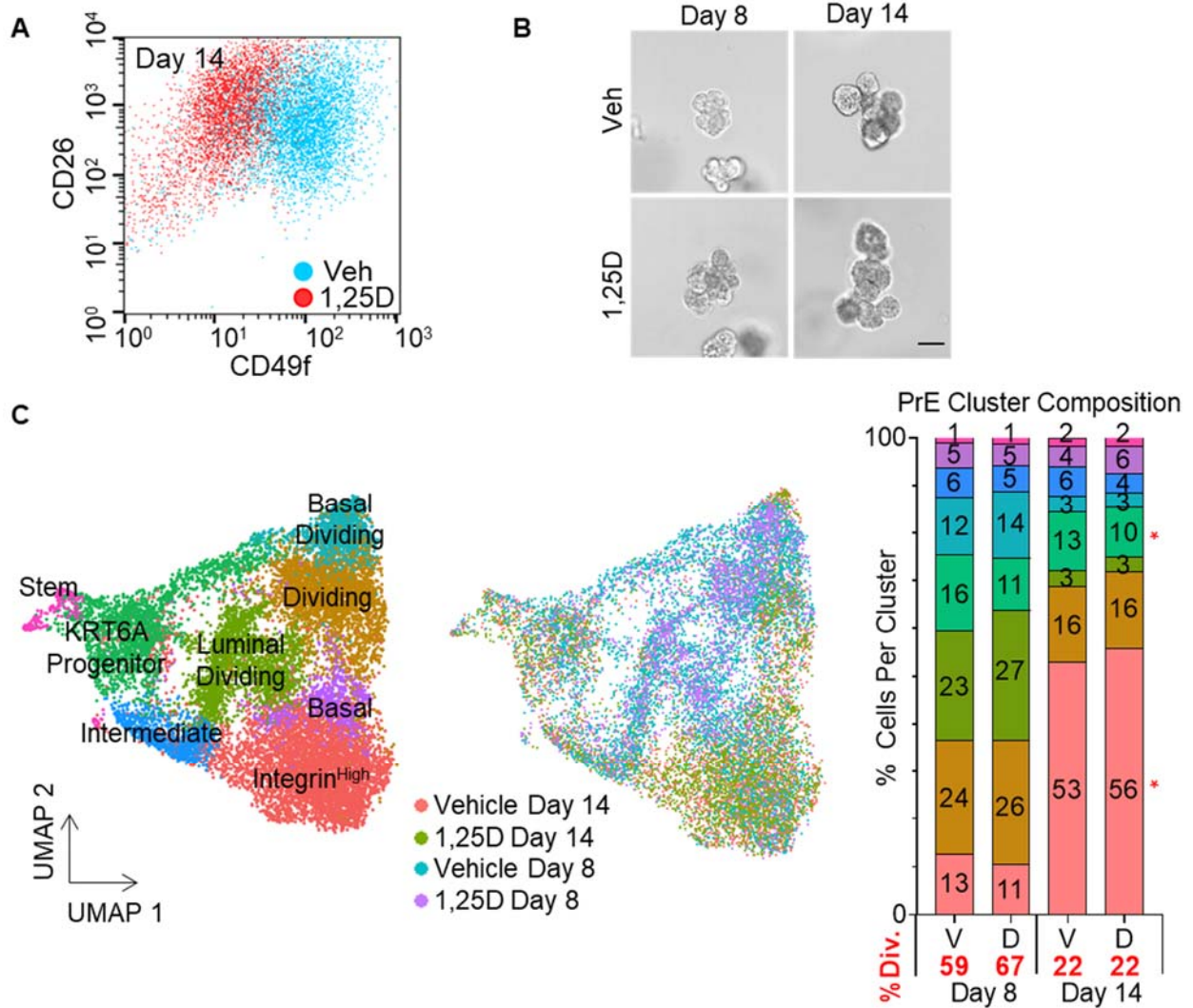


Figure 12. Organoid populations shift with vitamin D. (A) Overlay of flow cytometry scatterplots for luminal CD26 and basal CD49f in AA1 organoids grown until day 14 in vehicle (blue, Veh) or 10 nM 1,25D (red, 1,25D). (B) Representative images of day 8 and day 14 AA2 organoids collected for scRNAseq. Scale bar = 100 μ m. (C) Organoids shown in (B) were collected for scRNAseq and datasets were integrated, the resulting UMAP for clusters and sample distribution is shown (left, middle). The composition of each sample showing the distribution of cells found in each cluster at both time points, vehicle (V) and 1,25D (D) (right), the number of cells per cluster was divided by the sample input. Percent of total dividing (%Div.) cells is shown in red.

iii. Vitamin D modulates the Wnt pathway in organoids

Vitamin D is pleiotropic, like most hormones, and regulates many pathways in prostate cells. To determine the action of 1,25D in organoids, differentially expressed genes (DEGs) after culture with 1,25D were identified for each cluster at each time point. The number of DEGs in each cluster at each time point are shown (**Figure 13A**). Of note, the stem cells had the fewest DEGs with 1,25D, indicating they preserve their stable transcriptional program as was described in **Chapter II**. Next, DEGs were input into IPA software to understand the biological consequence. Enriched Canonical Pathways (**Figure 13B**), Upstream Regulators (**Figure 14**), and their Downstream Effects (**Figure 15**) were probed (Kramer et al., 2014).

As expected, significantly enriched canonical pathways included VDR/RXR activation (**Figure 13B**, top), a result of a high fold-change in the 1,25D-regulated genes *CYP24A1* and *IGFBP3* with vitamin D (**Figure 13B**, upper red box) (Martin and Pattison, 2000; Zierold et al., 1995). To explore genes relevant to organoid growth, enriched pathways related to “Organismal Growth & Development” were examined (**Figure 13B**, bottom). The BMP and Wnt pathways were enriched with culture in 1,25D and are known regulators of prostate development and differentiation (Toivanen and Shen, 2017). Vitamin D DEGs within the Wnt/ β -catenin signaling pathway included upregulation of *DKK1* at day 8 and downregulation of *DKK3* at day 14 (**Figure 13B**, lower red box). Vitamin D has been previously described as upregulating *DKK1* in the gut (Aguilera et al., 2007). Stem cells showed the fewest number of DEGs with 1,25D culture (**Figure 13A**) and this cluster showed no enrichment for pathways related to “Organismal Growth & Development”, indicating that 1,25D mainly regulates lineage-committed cells on the path to differentiation (**Figure 13B**).

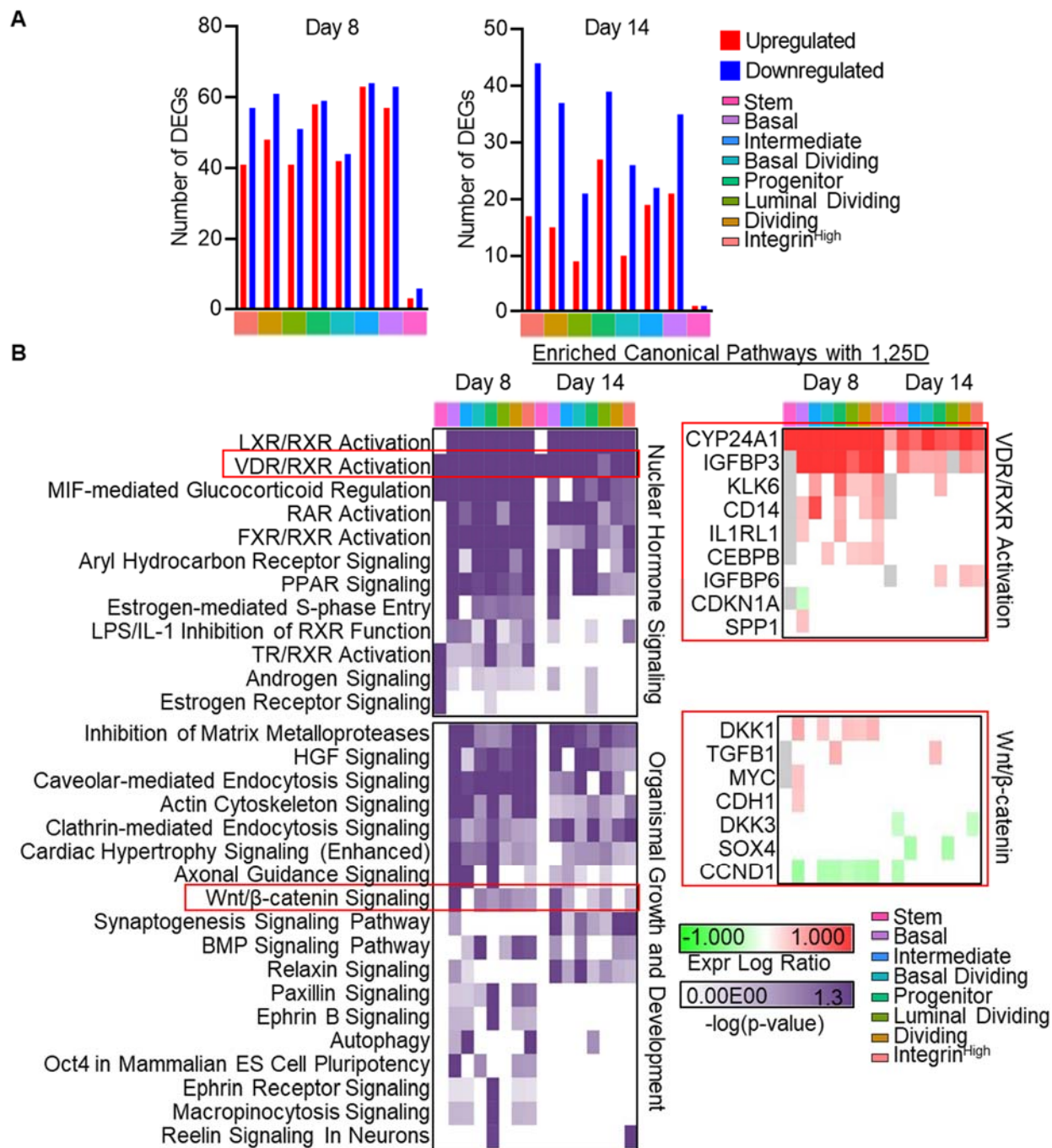


Figure 13. Vitamin D regulates lineage-committed cells. (A) The number of DEGs for organoids grown in 1,25D compared to vehicle, per cluster. (B) DEGs were input into IPA canonical pathway analysis. Significantly enriched pathways related to “Nuclear Hormone Signaling” and “Organismal Growth & Development” are shown. Red boxes show specific DEGs related to VDR/RXR activation and Wnt/ β -catenin signaling. Scale represents $-\log(p\text{-value})$ for enrichment of each pathway (left) and activation z-score for the genes in each pathway (right). P-value cutoff was $<\log_{10}(1.3)$

Upstream Regulator analysis was used to predict active transcription factors which may have influenced the differential gene expression (**Figure 14**). Activation of VitaminD3-VDR-RXR and cell-type-specific regulation of CTNNB1 were the top regulators (**Figure 14, red asterisk**), confirming vitamin D function and further supporting Wnt/B-catenin involvement.

To understand the net effect of the Pathway and Regulator analysis, downstream Disease & Function analysis was performed (**Figure 15**). Consistent with the hypothesis, there was enrichment for “Differentiation of Epithelial Tissue” at both time points with 1,25D (**Figure 15, red box**). The Wnt pathway was selected for additional investigation in the prostate organoids because previous studies in the RWPE1 cells, gut, skin and heart have shown 1,25D inhibition of canonical Wnt signaling (Aguilera et al., 2007; Hlaing et al., 2014; Kovalenko et al., 2010; Larriba et al., 2011; Muralidhar et al., 2019).

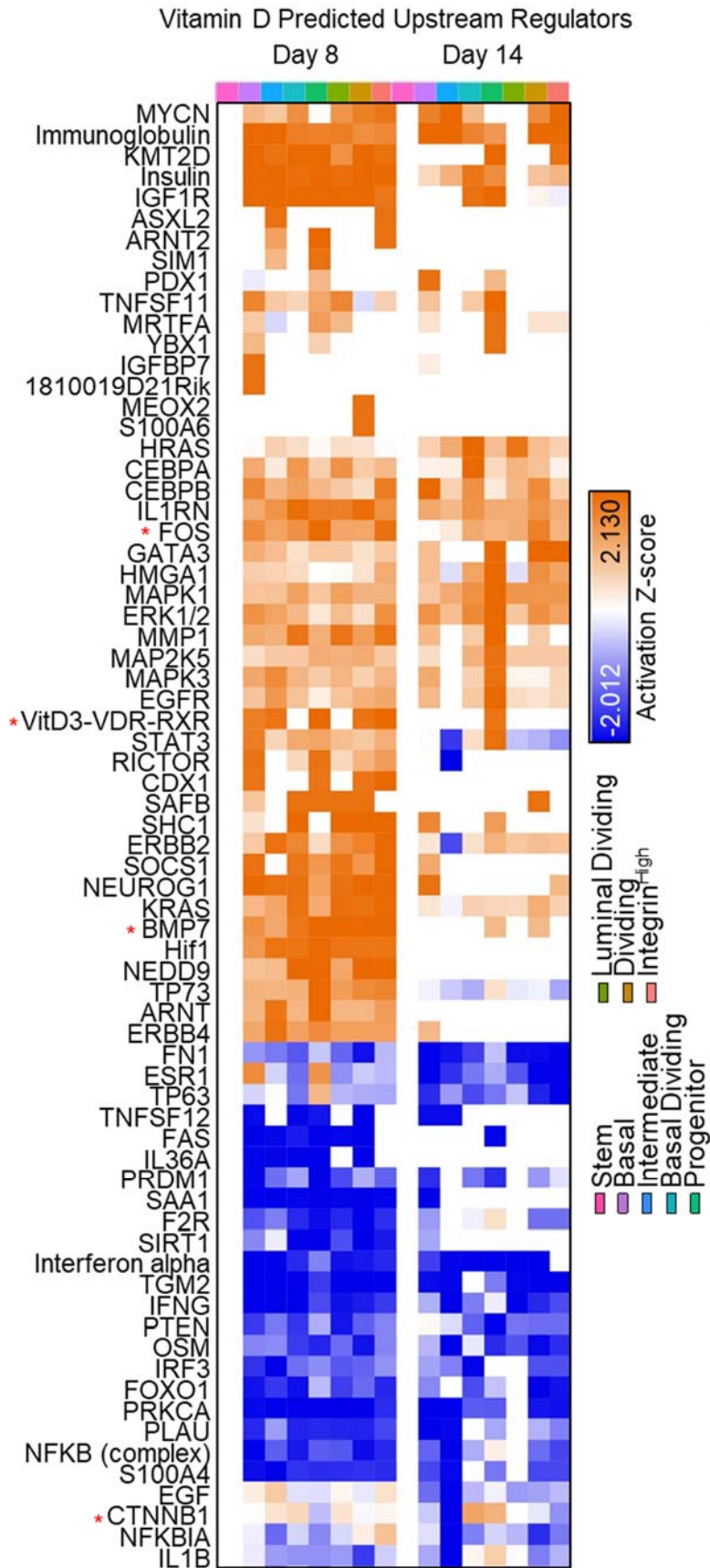


Figure 14. Predicted upstream regulators with vitamin D in each organoid cluster. Upstream regulator analysis for differentially expressed genes with 1,25D treatment per cluster per time point. Top 70 significant regulators from IPA upstream regulator analysis of differentially expressed genes with 1,25D treatment per cluster. Scale represents predicated activation z-score. Z-score cutoff was 2; p-value cutoff was $<\log_{10}(1.3)$.

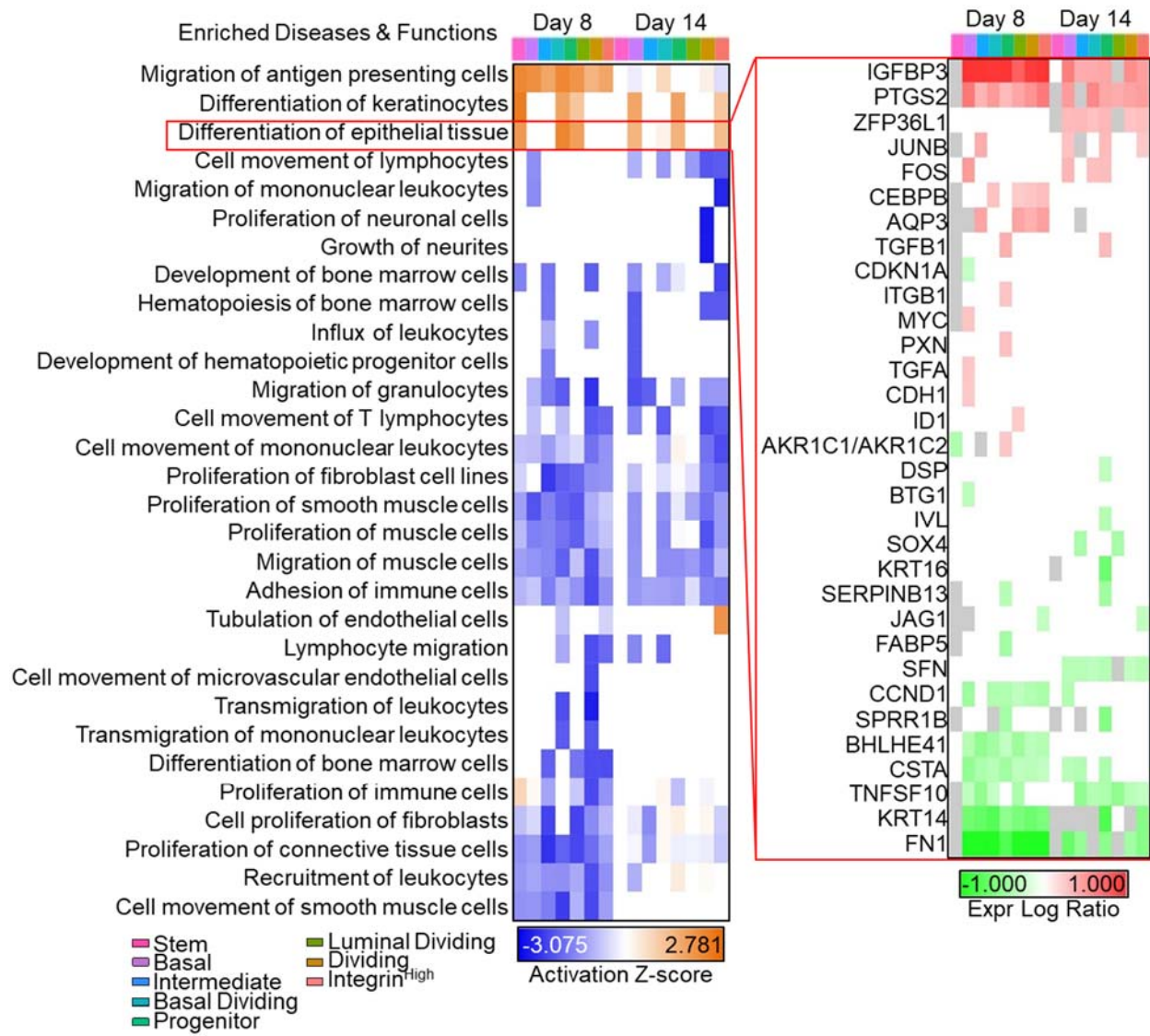


Figure 15. Diseases & Functions Enrichment analysis with vitamin D in each organoid cluster. Differentially expressed genes with 1,25D per cluster per time point were input into IPA Disease and Functions analysis. Resulting significantly enriched Diseases & Functions related to “Molecular and Cellular Function, Physiological System Development and Function” are shown. Red box shows differentially expressed genes related to “Differentiation of Epithelial Tissue”. Scale represents activation z-score for enrichment (left) and expression log ratio with 1,25D compared to control (right). Z-score cutoff was 2; p -value cutoff was $<\log_{10}(1.3)$.

Wnt regulation by 1,25D was validated with a target RT-qPCR array (**Figure 16A**). Prior to RNA isolation, organoids cultured with 10 nM 1,25D or vehicle were separated by FACS. CD49f was used as a basal stem cell marker (Guo et al., 2012; Yamamoto et al., 2012) and cells were separate by high (CD49f^{hi}) or low (CD49f^{lo}) expression to preserve differences in transcription between stem vs lineage-committed cells or basal vs luminal cells. In the array, expression of multiple canonical and non-canonical Wnts were altered by 1,25D, in some cases in a CD49f-cell-type-specific manner, including: *WNT7A*, *WNT9A*, *WNT2B*, *WNT5B*, *WNT7B*, *WNT3*, *WNT5A*, and *WNT4*. Notably, *DKK3* was downregulated with 1,25D treatment in both high (CD49f^{hi}) and low cells (CD49f^{lo}) (**Figure 16A**, red asterisks).

To determine overall directionality of Wnt regulation by 1,25D, β -catenin translocation and *AXIN2* induction were assessed. Inactive Wnt signaling involves cytoplasmic β -catenin, and active Wnt signaling involves nuclear β -catenin with expression of *AXIN2* (**Figure 17**). PrE cells and the benign 957E cell line, grown in vehicle or vitamin D, were treated with the GSK3 β -inhibitor Chiron for β -catenin stabilization and Wnt pathway induction. Cells grown with 1,25D sequestered β -catenin away from the nucleus compared to vehicle controls (**Figure 16B**). As a result of reduced nuclear β -catenin, 1,25D abrogated the Chiron-induced activation of the Wnt response gene *AXIN2* in 957E and PrE cells (**Figure 16C**).

To explore the potential mechanism of 1,25D inhibition of Wnt pathway activity, gene expression of the canonical Wnt inhibitor *DKK1* was assessed. In primary cells derived from 6 separate patients and grown as monolayer, 10nM 1,25D treatment upregulated expression of *DKK1*. Overall, these data support an inhibitory effect of 1,25D on the canonical Wnt pathway.

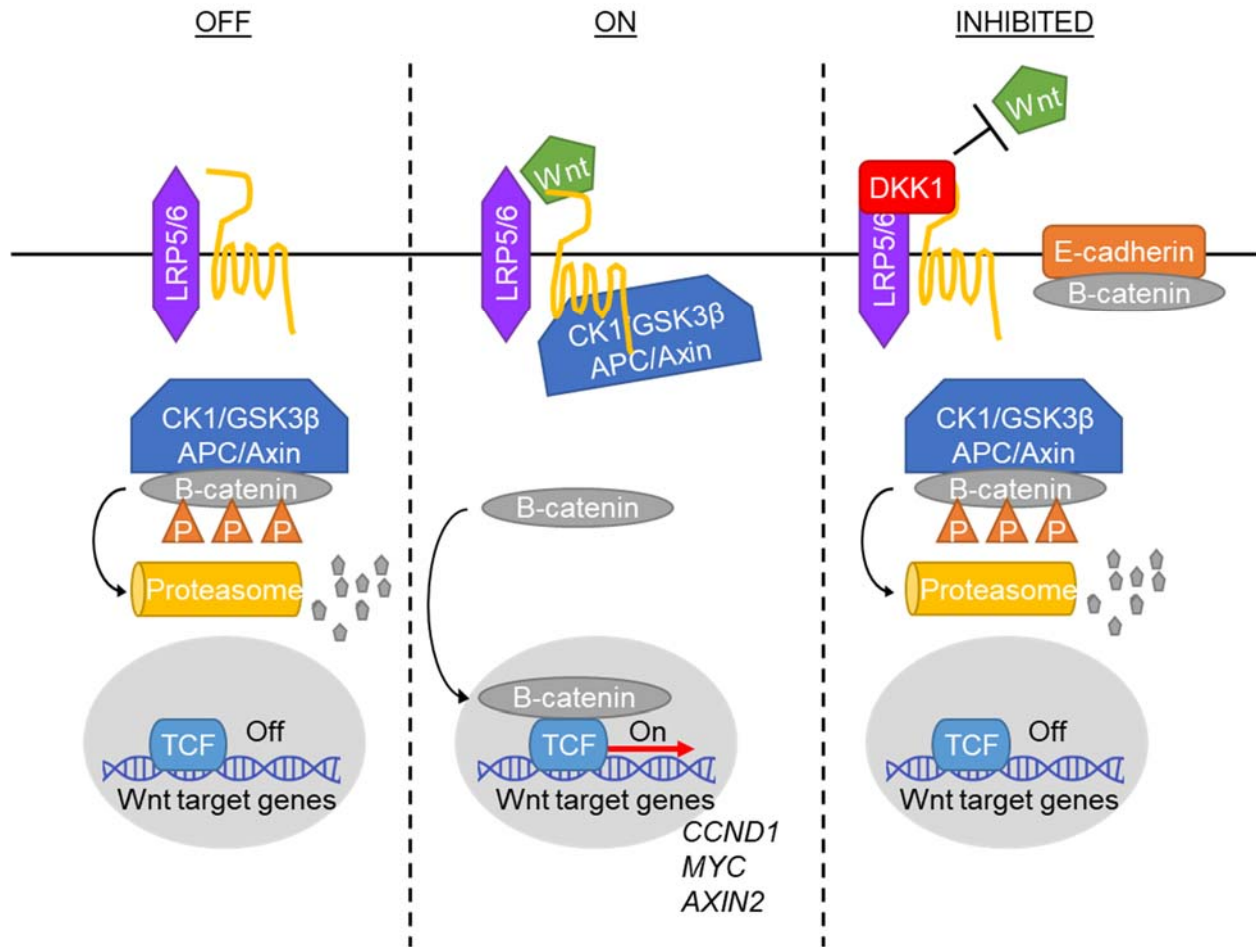


Figure 17. Diagram of the canonical Wnt signaling pathway. When Wnt ligand is not present (“OFF”), β -catenin is cytoplasmic and marked for proteasomal degradation by the APC destruction complex. In the presence of Wnt ligand (“ON”), β -catenin is stabilized and enters the nucleus to associate with transcription factors for induction of Wnt response genes (*CCND1*, *MYC*, *AXIN2*, etc). Inhibition of Wnt signaling (“INHIBITED”) can occur through secreted protein DKK1 out-competing Wnt ligands for the LRP5/6 receptor, or upregulation of E-cadherin sequestering β -catenin at the membrane and preventing nuclear translocation. Adapted from Larriba (Larriba et al., 2013).

iv. Vitamin D inhibits Wnt family member *DKK3*

DKK3 emerged as a 1,25D target in both the scRNAseq dataset and the RT-qPCR array, so its expression was profiled in a panel of prostate cell lines, monolayer PrE cells, and organoids. The LAPC4 PCa cell line had no detectable *DKK3* expression. The PCa cell line PC3, and immortalized lines RWPE1 and 957E, had low expression relative to PrE cells. *DKK3* is also known as “Reduced Expression in Immortalized Cells” (REIC) (Hsieh et al., 2004), thus our findings are consistent with previous reports of limited expression in cell lines. Across all PrE samples grown as monolayers or organoids, 1,25D inhibited *DKK3* expression (**Figure 18A**).

Immunocytochemistry for *DKK3* revealed a vesicular and perinuclear staining pattern (**Figure 18B**, white arrow), similar to other secreted members of the Dickkopf family (Glinka et al., 1998; Inoue et al., 2017). ELISA showed that culture in 1,25D reduced *DKK3* secretion in media (**Figure 18C**), and western blots of cell lysates showed reduced intracellular protein levels in PrE cells compared to vehicle controls (**Figure 18D**). Western blot detected several bands, harmonious with preceding reports describing many variants: a heavy secreted-form (s*DKK3*), a lighter intracellular variant (*DKK3b*), and a 50-kDa secreted form (s*DKK3*) (Abarzua et al., 2005; Hsieh et al., 2004; Kawano et al., 2006; Leonard et al., 2017; Zenzmaier et al., 2008; Zhang K. et al., 2010). The 957E cell line had no detectable expression of s*DKK3* and faint expression of *DKK3b*, uniform with the low RNA expression observed. PrE cells grown as monolayers and organoids showed reductions in all variants of *DKK3* with 1,25D treatment compared to controls (**Figure 18D**). Analysis of our previously published VDR-ChIP-seq dataset (Baumann et al., 2019) in PrE cells showed a peak 20 kb upstream from *DKK3* after 1,25D treatment (**Figure 18E**), supporting potential direct regulation by VDR.

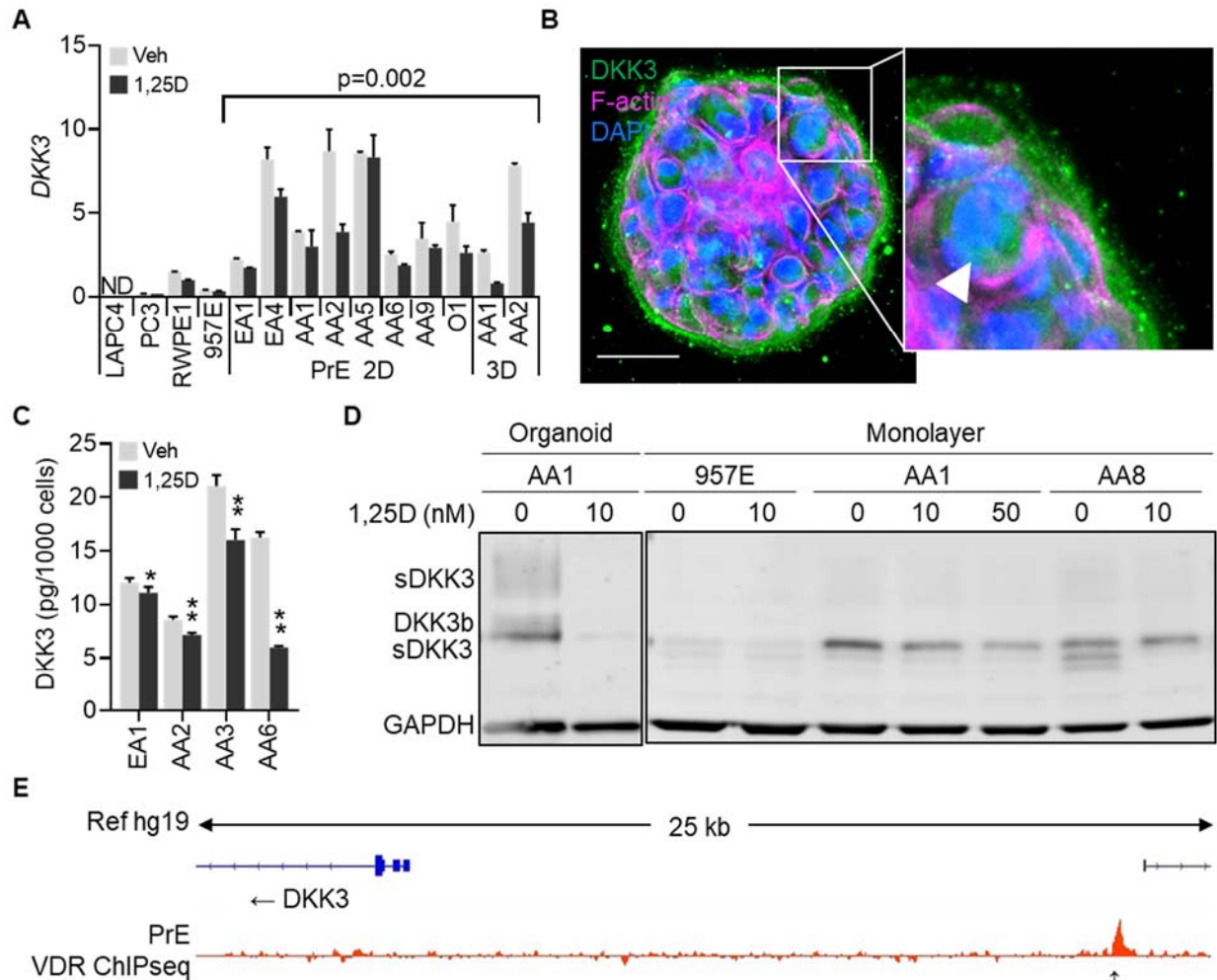


Figure 18. Vitamin D inhibits Wnt family member DKK3. **(A)** RT-qPCR of *DKK3* expression in prostate cell lines (LAPC4, PC3, RWPE1, 957E), monolayer PrE (PrE 2D), and organoid PrE cells (3D) grown in vehicle or 10 nM 1,25D. Monolayer cells were treated for 48–72 h, organoids were treated for 2–3.5 weeks. RQ is normalized to *HPRT1*; error bars represent SD of replicates ($n \geq 2$). P-value represents outcome of paired t-test for vehicle vs. 1,25D. **(B)** Immunostaining for DKK3 (green) in a whole-mounted day-17 AA3 organoid, DAPI (blue) and phalloidin/F-actin (pink). Scale bar = 50 μ m. White arrow highlights perinuclear and vesicular staining of DKK3. **(C)** ELISA quantification of secreted DKK3 in media collected from monolayer PrE cells grown in vehicle or 10 nM 1,25D for 72 h. P value represents outcome of 2 way ANOVA with uncorrected Fisher's comparison by row for vehicle vs 1,25D (* $p < 0.1$; ** $p < 0.01$). Error bars represent the standard error of triplicates. **(D)** Western blot of DKK3 expression in cell lines, monolayer and organoid PrE cells grown in vehicle or 10 nM 1,25D (sDKK3 = secreted DKK3; DKK3b = intracellular DKK3). **(E)** VDR-ChIP sequencing in PrE cells treated with 1,25D for 3 hours, IGV track shown normalized to vehicle (data from NCBI GEO accession number GSE124576).

v. DKK3 inhibition by vitamin D is required to alter organoid growth

To emulate 1,25D actions, PrE cells were transduced with lentivirus containing a siDKK3 sequence and GFP tag (**Figure 19A**) and grown into organoids in the presence of vehicle or 10 nM 1,25D (**Figure 19B**). Knockdown alone did not recapitulate the effect of 1,25D treatment, but combination of siDKK3 with 1,25D significantly enhanced the effect of vitamin D on organoid area (**Figure 19 B & C**).

To mitigate 1,25D inhibition of DKK3, exogenous recombinant DKK3 (rDKK3) was added to culture. PrE organoids from three patients were grown in media supplemented with vehicle, 1,25D, or 1,25D in combination with 50 ng/mL rDKK3 for 2 weeks. rDKK3 blocked the 1,25D-induced increase in organoid area, but did not reduce the organoid size compared to those grown in vehicle (**Figure 19D**).

In sum, these data support that inhibition of DKK3 by 1,25D serves to promote organoid growth.

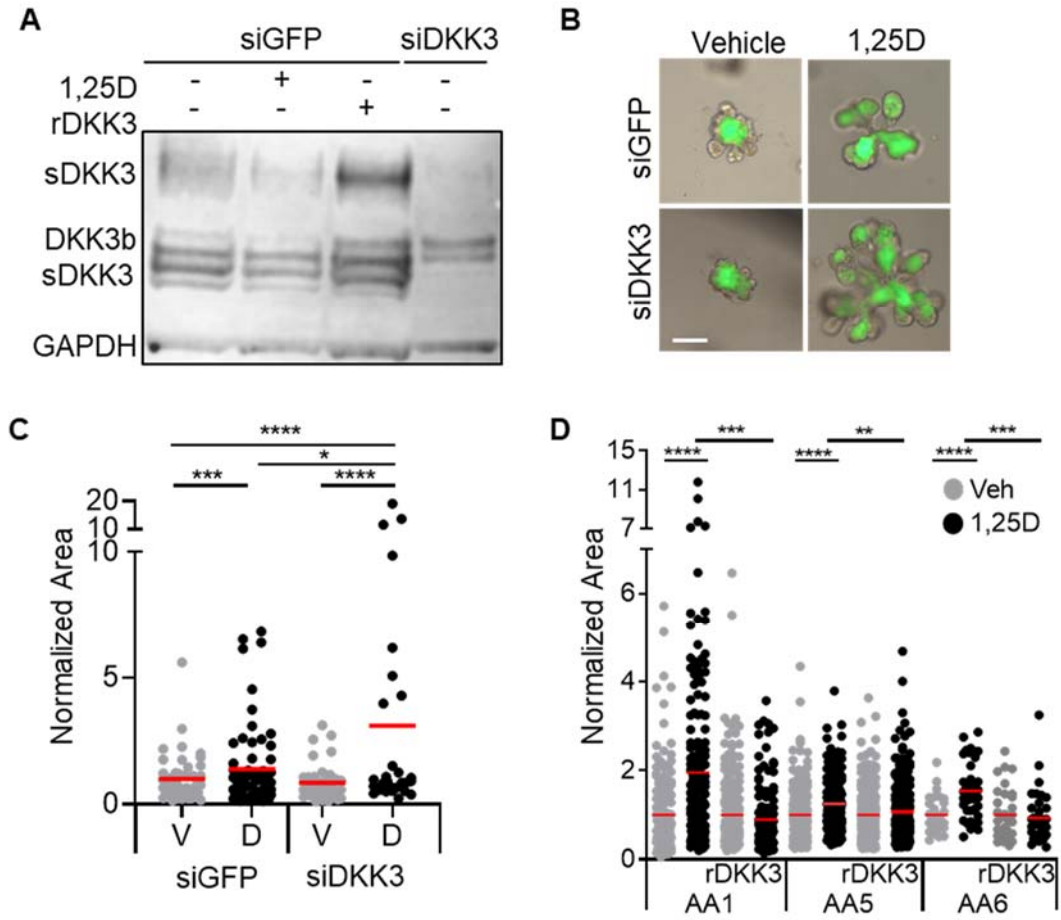


Figure 19. DKK3 inhibition by vitamin D is required to alter organoid growth. (A) Western blot of monolayer AA1 PrE cells transduced with control virus (siGFP) or siDKK3 virus and grown in vehicle, 10 nM 1,25D, or 50 ng/mL rDkk3. **(B)** Representative images of siGFP- or siDKK3-treated AA1 PrE organoids grown in vehicle or 10 nM 1,25D for 2 weeks **(C)** Quantification of relative area, normalized to vehicle (right) (* $p < 0.1$; ** $p < 0.05$, *** $p < 0.01$; **** $p < 0.001$. Scale bar = 200 μ m). **(D)** Relative area of PrE organoids grown in vehicle or 10 nM 1,25D combined with 50 ng/mL rDkk3 treatment for two weeks, normalized to vehicle (* $p < 0.1$, ** $p < 0.05$; *** $p < 0.01$; **** $p < 0.001$).

vi. **DKK3 and DKK1 are expressed by lineage-committed cells**

The function of DKK3 is not well understood, but it has been shown to inhibit proliferation in prostate and breast cancer cell lines (Leonard et al., 2017). To understand which cells may be regulated by DKK3 via 1,25D, its RNA expression was explored in the scRNAseq dataset. Expression of *DKK3* and *KRT13* was mutually exclusive, suggesting that *DKK3* is expressed only in lineage-committed cells (**Figure 20A & B**). Immunofluorescence for KRT13 and DKK3 in organoids confirmed that there was no co-localization (**Figure 20C**).

Similar results were observed for the Wnt pathway inhibitor *DKK1*, which was found to be upregulated by 1,25D earlier in this Chapter (**Figure 20A, right**). This indicates that 1,25D is regulating the expression of Dickkopf family genes in lineage-committed cells as a means to promote differentiation of non-stem cells.

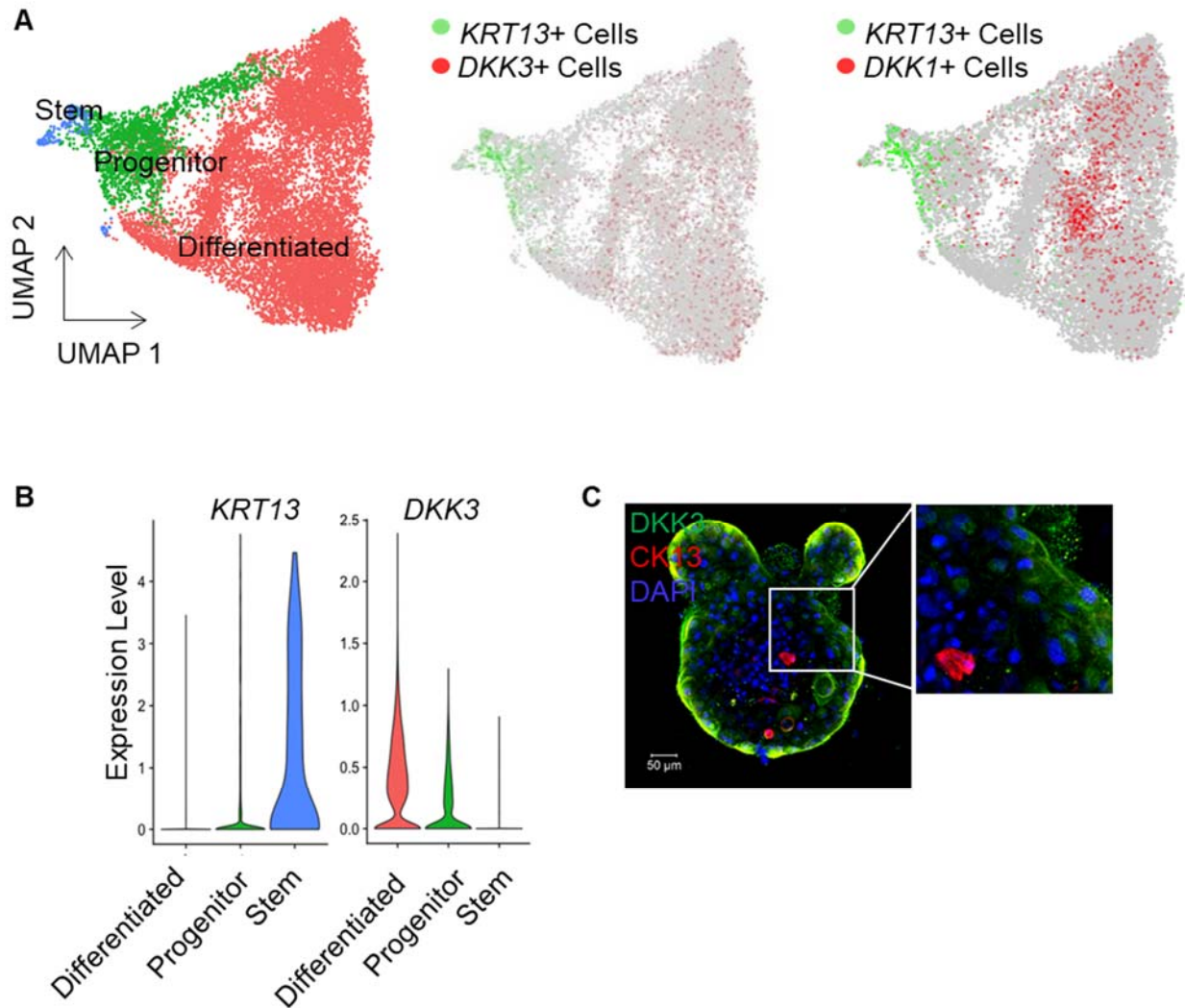


Figure 20. DKK3 and DKK1 are expressed by lineage-committed cells. (A) UMAP of integrated scRNAseq data showing differentiation status (left), blended UMAP of integrated scRNAseq data showing expression of *KRT13* (green) and *DKK3* (red) (middle), blended UMAP of integrated scRNAseq data showing expression of *KRT13* (green) and *DKK1* (red) (right). (B) Violin plots of *KRT13* (left) and *DKK3* expression (right). (C) *DKK3* (green) and *CK13* (red) expression in whole-mounted AA3 organoid counter-stained with DAPI (blue). Scale bar = 50 μ m.

D. Discussion

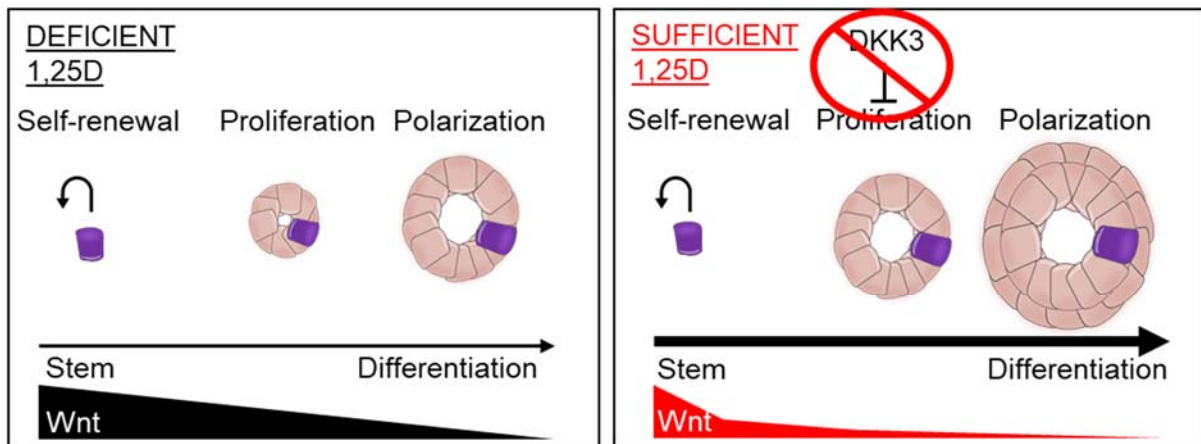
i. Summary

The prostate is a hormonally regulated gland that requires steroids for development, and dysregulation of hormones occurs during carcinogenesis and late-stage PCa. Vitamin D is a steroid hormone that promotes differentiation in many cell types, yet its role had not been fully explored in benign human prostate epithelium. Using patient-derived organoids from twelve patients, we found that continuous culture in physiologically relevant concentrations of 1,25D increased organoid area and differentiation compared to vitamin D-deficient conditions. The dominant mechanisms were inhibition of the canonical Wnt pathway and reduction of DKK3, a Wnt family member, to promote epithelial growth (**Figure 21A**).

ii. The Wnt pathway in prostate epithelium

The Wnt pathway is known to be highly active in prostate stem cells compared to differentiated cells (Blum et al., 2009), and prostate cancer stem cells show increased nuclear β -catenin and TCF/LEF activity (Zhang et al., 2017). This was observed in our organoid model, where the KRT13⁺ stem cell was enriched for Wnt pathway activity (**Figure 8**). In tissue, the Wnt protein Lef-1 identifies an androgen-insensitive population of basal progenitors in mouse prostate maturation (Wu et al., 2011). In kidney organoids and prostate organogenesis, Wnt activity is critical early on to promote progenitor outgrowth but then decreases to allow for differentiation (Prins and Putz, 2008; Simons et al., 2012; Takasato et al., 2016). Similarly, in snake venom gland organoids, Wnt agonists must be removed to allow for differentiation and secretory function (Post et al., 2020). Although Wnt signaling is essential during prostate organogenesis for lineage specification and budding, it is not required, as loss of β -catenin has no consequence for prostate development and tissue homeostasis in knockout mice (Simons et al., 2012). A reduction in Wnt activity is necessary for epithelial differentiation and equipose, as forced stabilization of β -catenin

A



B

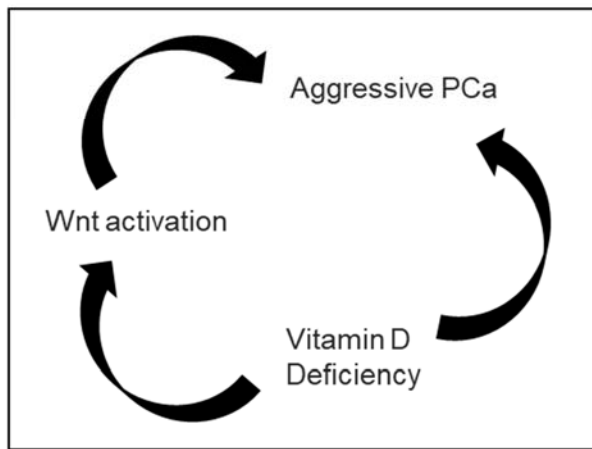


Figure 21. Diagram summarizing the effects of 1,25D on prostate epithelial organoids and the implications for human health. (A) Under vehicle conditions “DEFICIENT 1,25D”, a self-renewing stem cell with high Wnt activity undergoes asymmetric division to produce a progenitor cell that will rapidly expand. As differentiation occurs, cells will switch from highly proliferative to highly regulative of cell polarity via integrin interactions (**Chapter II**), downstream cells will have reduced Wnt activity. Under conditions of replete vitamin D “SUFFICIENT 1,25D”, proliferation is enhanced through inhibition of DKK3, resulting in a larger organoid. Wnt signaling is also inhibited in lineage-committed cells through β -catenin sequestration and DKK1 expression, to promote differentiation away from a stem cell phenotype. **(B)** Patients who are deficient in vitamin D have increased risk of aggressive PCa, these patients will also lose inhibition of Wnt signaling from vitamin D. This will result in activated Wnt signaling that contributes to an aggressive phenotype.

in mouse prostate epithelium results in hyperplasia (Bierie et al., 2003). Our data demonstrate selective Wnt inhibition by 1,25D in lineage-committed cells, but not in stem cells, resulting in enhanced epithelial differentiation in the organoids (**Figure 21**).

iii. Vitamin D activity in Wnt pathway

This report is similar to preceding publications of vitamin D activity. Microarray data from 1,25D treated RWPE1 cells show inhibition of Wnt and promotion of genes “induced during differentiation” from Gene Set Analysis (GSA) (Kovalenko et al., 2010). A dual mechanism has been described in dual colon cancer cell lines, where 1,25D inhibits the Wnt pathway by upregulating E-cadherin to sequester β -catenin outside the nucleus and promotes DKK1 expression to directly inhibit Wnt ligand binding (**Figure 17**) (Aguilera et al., 2007; Larriba et al., 2013). This has also been shown in healthy mouse colon tissue, a high vitamin D diet results in decreased nuclear β -catenin and increased cellular differentiation (Groschel et al., 2016). In benign prostate cells, DKK1 expression was increased with 1,25D and perinuclear β -catenin was observed, not membranous. Direct binding between VDR and β -catenin has been previously reported in colon cancer cells (Palmer et al., 2001) and may occur in the prostate as well. Other hormone pathways have also been shown to be involved in Wnt signaling through interaction with β -catenin, such as retinoic acid and androgen (Shah et al., 2006). Retinoic acid inhibits Wnt activity through activation of the retinoic acid receptor (RAR) and subsequent binding to β -catenin to block interaction with the Wnt TCF family of transcription factors (Easwaran et al., 1999). Ligand activation of the androgen receptor also stimulates AR: β -catenin interaction, which can be inhibited by excess TCF (Song et al., 2003). Taken together, these findings indicate that nuclear hormone receptors can directly inhibit Wnt activity to control self-renewal and development. Lack of membranous β -catenin implies a non-E-cadherin mechanism of inhibition and VDR: β -catenin interaction or 1,25D upregulation of DKK1 in primary prostate cells should be explored.

iv. Wnt pathway in prostate cancer

In prostate cancer, Wnt signaling has been shown to promote resistance to androgen deprivation therapy (Yokoyama et al., 2014). There are a high number of genomic alterations of Wnt signaling in a subset of castration resistant PCa, but localized disease does not frequently show alterations in the Wnt pathway. Specifically, *APC* and *CTNNB1* are mutated in 22% of castration resistant PCa and drive Wnt activity (Murillo-Garzon and Kypta, 2017). In PCa cell lines, disrupted E-cadherin expression led to enhanced Wnt signaling and promoted tumor growth (Davies et al., 2000). It remains unclear whether Wnt-signaling-activation in castration-resistance is a response to a lack of hormonal regulation, or whether Wnt activity is enhanced through spontaneous passenger events acquired during metastasis.

The results of this thesis indicate that vitamin D could inhibit Wnt signaling in PCa to improve patient outcome. They stipulate that patients deficient in vitamin D would have an environment that promotes stemness, bolsters PCa cell outgrowth, and could influence patients' risk of aggressive disease (**Figure 21B**). There are currently no studies that look at vitamin D in aggressive PCa mouse models and explore Wnt pathway activity. There is also no available prostate tissue data for deficient vs. sufficient humans to correlate with β -catenin localization or Wnt activity. But, other Wnt inhibitors block the growth of cells derived from castration resistant PCa patients and xenograft models of castration resistant PCa (Pak et al., 2019), indicating that vitamin D may have a similar effect. Future studies should assess correlations between serum and tissue levels of vitamin D and expression of Wnt pathway genes in patient prostate samples.

v. DKK3

The observed effect of DKK3 in organoids adds to literature that is inconsistent about the function of this protein in prostate cells. In general, the Dickkopf family of proteins inhibits Wnt signaling, such as DKK1 (Glinka et al., 1998; Kruithof-De Julio et al., 2013). However, DKK3 is the most structurally divergent member of the Dickkopf family (Krupnik et al., 1999) and has varied effects on Wnt, ranging from no effect (Krupnik et al., 1999; Pinho Christof Niehrs, 2007; Romero et al., 2013) to promoting (Nakamura and Hackam, 2010) or inhibiting Wnt (Bhattacharyya et al., 2017; Leonard et al., 2017; Sharma Das et al., 2013). DKK3 also functions as both a positive and negative regulator of TGF β signaling, depending on the model (Al Shareef et al., 2018; Busceti et al., 2017; Kardooni et al., 2018; Li et al., 2017; Pinho Christof Niehrs, 2007; Romero et al., 2013; Wang Z et al., 2015).

Despite conflicting reports of DKK3's signaling targets, it has consistently been shown to restrain cell proliferation (Kawano et al., 2006; Leonard et al., 2017). It acts as a cell cycle inhibitor whose expression is reduced in immortalized cells, which have the capacity to divide indefinitely (Kawano et al., 2006), and it is robustly upregulated in senescent PrE cells at passage 10 compared to passage 3 (Untergasser et al., 2002). In developing mouse prostate, during the phase when cell proliferation required, addition of exogenous DKK3 blunted proliferation, preventing luminal differentiation, Nkx3.1 expression and epithelial bud formation (Kruithof-De Julio et al., 2013). DKK3 deficient mice are viable with normal prostate glands, but have increased Ki-67+ proliferating cells (Romero et al., 2013) in agreement with the effect we observed in prostate organoids. By reducing DKK3, 1,25D facilitates an increase in organoid size and promotes differentiation. We observed that DKK3 was not expressed by the stem cells in organoids, similar to patient tissue (Henry et al., 2018), so it likely acts on the downstream cells to regulate growth (**Figure 21**).

vi. Limitations and future directions

Our findings reveal 1,25D as a potent inhibitor of DKK3 during differentiation as a means to control epithelial growth, although downstream targets of DKK3 remain unresolved and are a limitation of the results described in this thesis. Additionally, the mechanism of vitamin D regulation of DKK3 is not yet known, but a VDR-binding site was reported upstream of the DKK3 promoter. DKK3 is commonly silenced via promoter methylation (Bhattacharyya et al., 2017), so this could be the site of administration. Our study is distinct from prior reports in that we examined DKK3 in normal human prostate cells rather than in immortalized cell lines (Al Shareef et al., 2018; Hsieh et al., 2004; Kawano et al., 2006; Leonard et al., 2017; Nakamura and Hackam, 2010; Romero et al., 2016; Zhang K. et al., 2010), where the protein was named for its “reduced expression.” Studies in immortalized cells are dependent on exogenous addition to media or forced overexpression to assess phenotypes. In contrast, there is high endogenous expression and secretion of DKK3 in benign PrE organoid cultures, which is a strength of our study. Notably, DKK3 is also highly expressed in the stroma of the prostate, which further indicates a multifaceted role for this protein (Al Shareef et al., 2018; Henry et al., 2018; Zenzmaier et al., 2013).

In summary, we report two complementary mechanisms by which vitamin D deficiency would disrupt prostate epithelial differentiation—inhibition of canonical Wnt signaling through upregulation of DKK1 and regulation of the protein DKK3 (**Figure 21**). This is the first report, to our knowledge, of the hormone vitamin D regulating DKK3 expression in the prostate. These findings are potentially impactful for patients who are frequently deficient in vitamin D, such as African Americans and adults over the age of 70, who have significantly high rates of PCa (Jacques et al., 1997; Murphy et al., 2014)

CHAPTER IV: CONCLUSIONS

A. Contribution to literature

The body of work described in this thesis addresses relevant gaps in literature surrounding prostate modeling and the role of vitamin D in Wnt pathway regulation in prostate epithelium. Prior to this, there had not been a comparison between monolayer and organoid cells or prostate organoids utilizing the powerful scRNAseq method. In doing so, this work created a deep profile of the two primary prostate epithelial models and cataloged the heterogeneity of epithelial cell types observed during the differentiation of PrE organoids over time. This thesis reported a role of integrin signaling and cell polarity in organoid differentiation, likely in response to the 3D environment and matrix components. The differentiative action of vitamin D had not been assessed in primary prostate organoids and it was not previously known that 1,25D regulated DKK3. This thesis reports two novel mechanisms of vitamin D action in the prostate, inhibition of canonical Wnt and Dickkopf family member 3 in the lineage-committed cells in prostatic epithelium (**Figure 21**).

B. Implication for patient health and prostate cancer

Here, organoids were grown in sufficient or deficient 1,25D conditions to mimic serum levels that are seen in humans. Human studies showed that vitamin D insufficiency results in a more aggressive, less-differentiated prostate cancer (Murphy et al., 2014). To model this, organoids were used to explore the role of vitamin D in epithelial differentiation and found a positive effect. There are many studies that show other potentially chemopreventive mechanisms of vitamin D in prostate tissue and cancer cell lines. For example, 1,25D leads to the suppression of anti-apoptotic gene BCL-2 and increases expression of pro-apoptotic genes BAX, BAK and BAD in cancer cells (Merchan et al., 2017). Vitamin D also increases expression of p21 and p27 to promote cell cycle arrest, and represses HIF1 α and NF-kB signaling to decrease angiogenesis and inflammation (Merchan et al., 2017). Taken together, the data described in this thesis offer

promising support for vitamin D as a chemopreventive agent. Given the prevalence of vitamin D deficiency (Murphy et al., 2014), its requirement for bone health (Feldman et al., 2014), the minimal toxicity of the circulating prehormone 25D (Anderson et al., 2003), and the wide availability of 25D supplements, this thesis would support recommendation to incorporate vitamin D into the diet.

However, despite the convincing in vitro data, prostate cancer clinical trials have had mixed results. One study found that in low-risk patients undergoing active surveillance, vitamin D3 supplementation (4000 IU/day) led to a decrease in the number of positive cores in 55% of patients, but 34% still saw an increase in the number of positive biopsy cores and there was no change in PSA (Marshall et al., 2012). Another trial using a vitamin D analog combined with docetaxel treatment found that vitamin D did not change PSA levels or affect overall survival (Attia et al., 2008). These discrepancies between in vitro data and clinical trials could be due to a variety of considerations: expression of vitamin D pathway members, patient body weight, dosage, differentiation status of tissue, and proliferative capacity of the tissue.

i. Expression of vitamin D pathway proteins

There are mechanisms employed by the cancer cells to resist the anti-proliferative and pro-differentiative effects of vitamin D. Cancer cells show higher levels of the inactivating metabolic enzyme CYP24A1 (Feldman et al., 2014) with low activity of the activating enzyme CYP27B1 (Marco Giammanco et al.). This is demonstrated in vitro, the non-malignant prostate epithelial RWPE-1 cell line responds more to 1,25D than the PC3 cell line that was derived from a metastatic site (Singh et al., 2013). As a result, supplementation in patients may be less effective in late stage disease. For example, delivery of 1,25D in *Nkx3.1;Pten* mice at the precancerous stage of prostate disease progression significantly reduced the number of high-grade PIN lesions with invasion compared to vehicle, but treatment of these mice with existing cancer reduced the ability of vitamin D as an anti-cancer agent (Banach-Petrosky et al., 2006). Organoids in this

thesis were grown in physiological relevant conditions of vitamin D and were from benign regions to determine a role in Wnt signaling. Future studies can utilize samples from patient tissue at different stages of prostate cancer to explore how this mechanism is disrupted in disease, which may help to model the discordant results found in clinical trials.

ii. Patient body weight

Body weight is another factor that could impact patient response to vitamin D in clinical trials. Recently the VITAL trial was conducted nationwide with 2000 IU/day vitamin D3 supplementation and found vitamin to significantly decrease cancer incidence, but only in normal body mass index patients (Manson et al., 2019). Vitamin D is stored in adipose tissue as a possible reserve for times of shortage (Carrelli et al., 2017). However, in obese patients the excess fat storage may absorb extra circulating hormone, resulting in deficiency. Visceral adipose tissue has been shown to be inversely associated with 25D concentrations (Pereira-Santos et al., 2015; Rafiq et al., 2019). Vitamin D levels in fat tissue have been shown to increase after supplementation (Didriksen et al., 2015), which may explain the lack of significant findings in the obese group of the VITAL trial.

iii. Dosage and differentiation status of tissue

The dosage of vitamin D is an important factor to consider when evaluating the work included in the thesis. Vitamin D has been published to inhibit proliferation of prostate cancer lines when used at a high dosage (100nM) (Murthy et al., 2005), yet that is not seen here in benign organoids at 10nM. Vitamin D is known to exert both proliferative and anti-proliferative effects depending on the differentiation status of the tissue and the dosage implemented. In keratinocytes, low concentrations of 1,25D can increase proliferation where high concentrations inhibit proliferation (Hill et al., 2015). This effect has been observed with other steroids such as androgen in LNCaP cells, higher dosage (1nM) inhibits proliferation but lower dosage (0.1nM)

stimulates cell division (Shao et al., 2007). Regarding differentiation status, vitamin D inhibits proliferation and promotes apoptosis of prostate tumor derived endothelial cells, but this effect is not observed in benign endothelial cells (Chung et al., 2006). The action of a low dosage of vitamin D in the benign organoids may induce proliferation and increase organoid area, although utilizing cancer cells or a higher dosage of hormone may result in a different response.

iv. Proliferative capacity of tissue

To extend findings to patients, other contextual considerations should be assessed. Here vitamin D's activity was assayed utilizing a highly proliferative model compared to tissue (**Figure 5A**) and vitamin D's activity is known to be setting specific. In vivo, cells are contact inhibited and show much less turnover, so vitamin D may not promote growth and expansion of those epithelial cells. In patient tissue, a randomized clinical trial of 3 different vitamin D doses (400, 10,000, or 40,000 IU/day) found that prostatic levels of 1,25D inversely associate with Ki67 staining in benign and cancer tissue, indicating inhibition of proliferation (Wagner et al., 2013). This was also shown in mouse tissue, where knocking out VDR in the LPB-Tag model of PCa progression results in tumors that have higher proliferation compared to LPB-Tag wild-type VDR mice (Mordan-McCombs et al., 2010). Similarly, serum 25D has been shown to be inversely associated with the size of the prostate gland in men with benign prostatic hyperplasia, showing that higher vitamin D levels result in less proliferation (Murphy et al., 2017). Overall, vitamin D seems to inhibit proliferation in tissue, yet it increased epithelial proliferation in organoids. Organoids are grown in a permissive environment for expansion, supplemented with androgen to drive cell division. Future studies will utilize the less-proliferative tissue slice culture method in an effort to compliment the organoid work ex vivo. It may be possible that vitamin D regulation of Wnt activity and DKK3 is context dependent and its role in proliferation could fluctuate between development and steady state tissue.

C. Future Directions

Finally, the stromal cells were an important factor omitted from all of the experiments performed in this thesis. Stromal cells play an essential role in prostate development and disease progression (Prins and Putz, 2008). They provide the epithelial cells with secreted factors and androgens to drive differentiation (Toivanen and Shen, 2017). The role of vitamin D in directing the cross-talk of differentiation cues between epithelial and stromal compartments needs to be explored. Work performed by this group, but not included in this thesis, developed a coculture model that incorporates stroma into epithelial organoid growth conditions. This model would be useful to utilize going forward to dissect the activity of vitamin D in stromal and epithelial cells in regulating Wnt activity and DKK3. The stroma has been shown to control Wnt signaling in the prostate in spatially restricted regions. Wnt ligands and Wnt activity differ greatly across the proximal and distal ducts in both the stromal and the epithelial compartments (Wei et al., 2019). Stromal cells surrounding the proximal duct highly express non-canonical Wnt members as a means to suppress epithelial proliferation and preserve stem activity (Wei et al., 2019). As a rich source of Wnt ligands, stromal cells can promote disease progression by enhancing the cancer stem cell Wnt phenotype (Murillo-Garzon and Kypta, 2017). Whether or not vitamin D inhibits Wnt activity in stroma, and if this could be a secondary means of chemoprevention, should be studied in the future. DKK3 is also highly expressed by the stroma (Al Shareef et al., 2018; Henry et al., 2018; Zenzmaier et al., 2013). While DKK3 is downregulated in PCa in epithelial cells (Al Shareef et al., 2018; Zenzmaier et al., 2008), it is overexpressed in BPH in the stroma (Zenzmaier et al., 2013). Stromal DKK3 promotes fibroblast differentiation towards a myofibroblast phenotype, increasing stromal proliferation and remodeling to promote angiogenesis and disease progression. Vitamin D inhibition of DKK3 in epithelial cells would potentially lessen secretion to stroma and could impede progression of BPH. Utilizing the coculture model, or ex vivo tissue slice culture would be worthwhile means to address these questions.

D. Summary

In summary, this thesis has generated an inventory of the epithelial cell populations grown out from radical prostatectomy tissue in monolayer, and in early- and late-stage organoids. The activity of vitamin D as a driver of differentiation was assessed using these models. It was found that physiologically relevant concentrations of 1,25D promoted epithelial growth, yet its function in tissue should be assessed further utilizing ex vivo tissue slice culture. Vitamin D was identified as a regulator of Wnt activity and DKK3 in the epithelium, which are both highly active in stromal cells. Vitamin D regulation of these pathways in stroma should be explored and could have implications for chemoprevention and stromal remodeling in BPH. The work described here identified novel functions of vitamin D and set the stage for future experimentation.

CITED LITERATURE

Aaron, L., Franco, O.E., and Hayward, S.W. (2016). Review of Prostate Anatomy and Embryology and the Etiology of Benign Prostatic Hyperplasia. *Urol Clin North Am* 43, 279-288.

Abarzua, F., Sakaguchi, M., Takaishi, M., Nasu, Y., Kurose, K., Ebara, S., Miyazaki, M., Namba, M., Kumon, H., and Huh, N.-h. (2005). Adenovirus-mediated overexpression of REIC/Dkk-3 selectively induces apoptosis in human prostate cancer cells through activation of c-Jun-NH2-kinase. *Cancer Research* 65, 9617-9622.

Abe, E., Miyaura, C., Sakagami, H., Takeda, M., Konno, K., Yamazaki, T., Yoshiki, S., and Suda, T. (1981). Differentiation of mouse myeloid leukemia cells induced by 1 alpha,25-dihydroxyvitamin D3. *Proc Natl Acad Sci USA* 78, 4990-4994.

Aguilera, O., Pena, C., Garcia, J.M., Larriba, M.J., Ordonez-Moran, P., Navarro, D., Barbachano, A., Lopez de Silanes, I., Ballestar, E., Fraga, M.F., *et al.* (2007). The Wnt antagonist DICKKOPF-1 gene is induced by 1alpha,25-dihydroxyvitamin D3 associated to the differentiation of human colon cancer cells. *Carcinogenesis* 28, 1877-1884.

Al Shareef, Z., Kardooni, H., Murillo-Garzón, V., Domenici, G., Stylianakis, E., Steel, J.H., Rabano, M., Gorroño-Etxebarria, I., Zabalza, I., dM Vivanco, M., *et al.* (2018). Protective effect of stromal Dickkopf-3 in prostate cancer: opposing roles for TGFBI and ECM-1. *Oncogene* 37, 5305-5324.

Anderson, P.H., May, B.K., and Morris, H.A. (2003). Vitamin D metabolism: new concepts and clinical implications. *Clin Biochem Rev* 24, 13-26.

Anselmo da Costa, I., Stenzl, A., and Bedke, J. (2019). Immunotherapy in prostate cancer. *Arch Esp Urol* 72, 211-222.

Arora, K., and Barbieri, C.E. (2018). Molecular Subtypes of Prostate Cancer. *Curr Oncol Rep* 20, 58.

Attia, S., Eickhoff, J., Wilding, G., McNeel, D., Blank, J., Ahuja, H., Jumonville, A., Eastman, M., Shevrin, D., Glode, M., *et al.* (2008). Randomized, double-blinded phase II evaluation of docetaxel with or without doxercalciferol in patients with metastatic, androgen-independent prostate cancer. *Clin Cancer Res* 14, 2437-2443.

Banach-Petrosky, W., Ouyang, X., Gao, H., Nader, K., Ji, Y., Suh, N., DiPaola, R.S., and Abate-Shen, C. (2006). Vitamin D inhibits the formation of prostatic intraepithelial neoplasia in Nkx3.1;Pten mutant mice. *Clin Cancer Res* 12, 5895-5901.

Banjoko, S.O., and Adeseolu, F.O. (2013). Seminal Plasma pH, Inorganic Phosphate, Total and Ionized Calcium Concentrations In The Assessment of Human Spermatozoa Function. *J Clin Diagn Res* 7, 2483-2486.

Banks, M., and Holick, M.F. (2015). Molecular mechanism(s) involved in 25-Hydroxyvitamin D's antiproliferative effects in CYP27B1-transfected LNCaP cells. *Anticancer Res* 35, 3773-3779.

Barker, N., Huch, M., Kujala, P., van de Wetering, M., Snippert, H.J., van Es, J.H., Sato, T., Stange, D.E., Begthel, H., van den Born, M., *et al.* (2010). Lgr5(+ve) stem cells drive self-renewal in the stomach and build long-lived gastric units in vitro. *Cell Stem Cell* 6, 25-36.

Barros-Silva, J.D., Linn, D.E., Steiner, I., Guo, G., Ali, A., Pakula, H., Ashton, G., Peset, I., Brown, M., Clarke, N.W., *et al.* (2018). Single-Cell analysis identifies LY6D as a marker linking castration-resistant prostate luminal cells to prostate progenitors and cancer. *Cell Rep* 25, 3504-3518.

Baumann, B., Lugli, G., Gao, S., Zenner, M., and Nonn, L. (2019). High levels of PIWI-interacting RNAs are present in the small RNA landscape of prostate epithelium from vitamin D clinical trial specimens. *Prostate* 79, 840-855.

Bello-DeOcampo, D., Kleinman, H.K., Deocampo, N.D., and Webber, M.M. (2001). Laminin-1 and alpha6beta1 integrin regulate acinar morphogenesis of normal and malignant human prostate epithelial cells. *Prostate* 46, 142-153.

Bello, D., Webber, M.M., Kleinman, H.K., Wartinger, D.D., and Rhim, J.S. (1997). Androgen responsive adult human prostatic epithelial cell lines immortalized by human papillomavirus 18. *Carcinogenesis* 18, 1215-1223.

Bennett, N.C., Hooper, J.D., Johnson, D.W., and Gobe, G.C. (2014). Expression profiles and functional associations of endogenous androgen receptor and caveolin-1 in prostate cancer cell lines. *Prostate* 74, 478-487.

Bhattacharyya, S., Feferman, L., Tobacman, J.K., Bhattacharyya, S., Feferman, L., and Tobacman, J.K. (2017). Chondroitin sulfatases differentially regulate Wnt signaling in prostate stem cells through effects on SHP2, phospho-ERK1/2, and Dickkopf Wnt signaling pathway inhibitor (DKK3). *Oncotarget* 8, 100242-100260.

Bierie, B., Nozawa, M., Renou, J.P., Shillingford, J.M., Morgan, F., Oka, T., Taketo, M.M., Cardiff, R.D., Miyoshi, K., Wagner, K.U., *et al.* (2003). Activation of beta-catenin in prostate epithelium induces hyperplasias and squamous transdifferentiation. *Oncogene* 22, 3875-3887.

Bikle, D.D. (2004). Vitamin D regulated keratinocyte differentiation. *J Cell Biochem* 92, 436-444.

Blackwood, J.K., Williamson, S.C., Greaves, L.C., Wilson, L., Rigas, A.C., Sandher, R., Pickard, R.S., Robson, C.N., Turnbull, D.M., Taylor, R.W., *et al.* (2011). In situ lineage tracking of human prostatic epithelial stem cell fate reveals a common clonal origin for basal and luminal cells. *J Pathol* 225, 181-188.

Blum, R., Gupta, R., Burger, P.E., Ontiveros, C.S., Salm, S.N., Xiong, X., Kamb, A., Wesche, H., Marshall, L., Cutler, G., *et al.* (2009). Molecular signatures of prostate stem cells reveal novel signaling pathways and provide insights into prostate cancer. *PLoS One* 4, e5722.

Bouillon, R., Carmeliet, G., Verlinden, L., van Etten, E., Verstuyf, A., Luderer, H.F., Lieben, L., Mathieu, C., and Demay, M. (2008). Vitamin D and human health: lessons from vitamin D receptor null mice. *Endocr Rev* 29, 726-776.

Bryant, S.L., Francis, J.C., Lokody, I.B., Wang, H., Risbridger, G.P., Loveland, K.L., and Swain, A. (2014). Sex specific retinoic acid signaling is required for the initiation of urogenital sinus bud development. *Dev Biol* 395, 209-217.

Bühler P, W.P., Katzenwadel A, Schultze-Seemann W, Wetterauer U, Freudenberg N, Elsässer-Beile U. (2010). Primary prostate cancer cultures are models for androgen-independent transit amplifying cells. *Oncol Rep* 23, 465-470.

Busceti, C.L., Marchitti, S., Bianchi, F., Di Pietro, P., Riozzi, B., Stanzione, R., Cannella, M., Battaglia, G., Bruno, V., Volpe, M., *et al.* (2017). Dickkopf-3 upregulates VEGF in cultured human endothelial cells by activating activin receptor-like kinase 1 (ALK1) pathway. *Front Pharmacol* 8, 111.

Butler, A., Hoffman, P., Smibert, P., Papalexi, E., and Satija, R. (2018). Integrating single-cell transcriptomic data across different conditions, technologies, and species. *Nat Biotech* 36, 411.

Campbell, M.J., Elstner, E., Holden, S., Uskokovic, M., and Koeffler, H.P. (1997). Inhibition of proliferation of prostate cancer cells by a 19-nor-hexafluoride vitamin D3 analogue involves the induction of p21waf1, p27kip1 and E-cadherin. *J Mol Endocrinol* 19, 15-27.

Cao, J., Spielmann, M., Qiu, X., Huang, X., Ibrahim, D.M., Hill, A.J., Zhang, F., Mundlos, S., Christiansen, L., Steemers, F.J., *et al.* (2019). The single-cell transcriptional landscape of mammalian organogenesis. *Nature* 566, 496-502.

Carrelli, A., Bucovsky, M., Horst, R., Cremers, S., Zhang, C., Bessler, M., Schrope, B., Evanko, J., Blanco, J., Silverberg, S.J., *et al.* (2017). Vitamin D Storage in Adipose Tissue of Obese and Normal Weight Women. *J Bone Miner Res* 32, 237-242.

Carstens, R.P., Eaton, J.V., Krigman, H.R., Walther, P.J., and Garcia-Blanco, M.A. (1997). Alternative splicing of fibroblast growth factor receptor 2 (FGF-R2) in human prostate cancer. *Oncogene* 15, 3059-3065.

Chen, K.S., and DeLuca, H.F. (1995). Cloning of the human 1 alpha,25-dihydroxyvitamin D-3 24-hydroxylase gene promoter and identification of two vitamin D-responsive elements. *Biochim Biophys Acta* 1263, 1-9.

Chen, L., Wilson, R., Bennett, E., and Zosky, G.R. Identification of vitamin D sensitive pathways during lung development.

Chen, M., Hsu, I., Wolfe, A., Radovick, S., Huang, K., Yu, S., Chang, C., Messing, E.M., and Yeh, S. (2009). Defects of prostate development and reproductive system in the estrogen receptor-alpha null male mice. *Endocrinology* 150, 251-259.

Chua, C.W., Shibata, M., Lei, M., Toivanen, R., Barlow, L.J., Bergren, S.K., Badani, K.K., McKiernan, J.M., Benson, M.C., Hibshoosh, H., *et al.* (2014). Single luminal epithelial progenitors can generate prostate organoids in culture. *Nat Cell Biol* 16, 951-961, 951-954.

Chung, I., Wong, M.K., Flynn, G., Yu, W.D., Johnson, C.S., and Trump, D.L. (2006). Differential antiproliferative effects of calcitriol on tumor-derived and matrigel-derived endothelial cells. *Cancer Res* 66, 8565-8573.

- Clevers, H. (2016). Modeling Development and Disease with Organoids. *Cell* 165, 1586-1597.
- Co, J.Y., Margalef-Catala, M., Li, X., Mah, A.T., Kuo, C.J., Monack, D.M., and Amieva, M.R. (2019). Controlling Epithelial Polarity: A Human Enteroid Model for Host-Pathogen Interactions. *Cell Rep* 26, 2509-2520 e2504.
- Davies, G., Jiang, W.G., and Mason, M.D. (2000). Cell-cell adhesion molecules and signaling intermediates and their role in the invasive potential of prostate cancer cells. *J Urol* 163, 985-992.
- Descotes, J.L. (2019). Diagnosis of prostate cancer. *Asian J Urol* 6, 129-136.
- Didriksen, A., Burild, A., Jakobsen, J., Fuskevåg, O.M., and Jorde, R. (2015). Vitamin D3 increases in abdominal subcutaneous fat tissue after supplementation with vitamin D3. *Eur J Endocrinol* 172, 235-241.
- Drost, J., Karthaus, W.R., Gao, D., Driehuis, E., Sawyers, C.L., Chen, Y., and Clevers, H. (2016). Organoid culture systems for prostate epithelial and cancer tissue. *Nat Protoc* 11, 347-358.
- Easwaran, V., Pishvaian, M., Salimuddin, and Byers, S. (1999). Cross-regulation of beta-catenin-LEF/TCF and retinoid signaling pathways. *Curr Biol* 9, 1415-1418.
- Elshazly, M.A., Sultan, M.F., Aboutaleb, H.A., Salem, S.M., Aziz, M.S., Abd Elbaky, T.M., Elsharif, E.A., Gawish, M.M., Alajrawi, F.T., Elgadi, F.A.A., *et al.* (2017). Vitamin D deficiency and lower urinary tract symptoms in males above 50 years of age. *Urol Ann* 9, 170-173.
- Fang, F., Kasperzyk, J.L., Shui, I., Hendrickson, W., Hollis, B.W., Fall, K., Ma, J., Gaziano, J.M., Stampfer, M.J., Mucci, L.A., *et al.* (2011). Prediagnostic plasma vitamin D metabolites and mortality among patients with prostate cancer. *PLoS One* 6, e18625.
- Fatehullah, A., Tan, S.H., and Barker, N. (2016). Organoids as an in vitro model of human development and disease. *Nature Cell Biology* 18, 246-254.
- Feldman, D., Krishnan, A.V., Swami, S., Giovannucci, E., and Feldman, B.J. (2014). The role of vitamin D in reducing cancer risk and progression. *Nature Reviews Cancer* 14, 342-357.
- Fleet, J.C., Kovalenko, P.L., Li, Y., Smolinski, J., Spees, C., Yu, J.G., Thomas-Ahner, J.M., Cui, M., Neme, A., Carlberg, C., *et al.* (2019). Vitamin D Signaling Suppresses Early Prostate Carcinogenesis in TgAPT121 Mice. *Cancer Prev Res (Phila)* 12, 343-356.
- Frank, S.B., and Miranti, C.K. (2013). Disruption of prostate epithelial differentiation pathways and prostate cancer development. *Front Oncol* 3, 273.
- Gaisa, N.T., Graham, T.A., McDonald, S.A., Poulosom, R., Heidenreich, A., Jakse, G., Knuechel, R., and Wright, N.A. (2011). Clonal architecture of human prostatic epithelium in benign and malignant conditions. *J Pathol* 225, 172-180.
- Gandhi, J., Afridi, A., Vatsia, S., Joshi, G., Joshi, G., Kaplan, S.A., Smith, N.L., and Khan, S.A. (2018). The molecular biology of prostate cancer: current understanding and clinical implications. *Prostate Cancer Prostatic Dis* 21, 22-36.

Genevet, A., and Tapon, N. (2011). The Hippo pathway and apico-basal cell polarity. *Biochem J* 436, 213-224.

Giancotti, F.G., and Ruoslahti, E. (1999). Integrin signaling. *Science* 285, 1028-1032.

Gilbert, R., Metcalfe, C., Oliver, S.E., Whiteman, D.C., Bain, C., Ness, A., Donovan, J., Hamdy, F., Neal, D.E., Lane, J.A., *et al.* (2009). Life course sun exposure and risk of prostate cancer: Population-based nested case-control study and meta-analysis. *International Journal of Cancer* 125, 1414-1423.

Giovannucci, E., Liu, Y., Rimm, E.B., Hollis, B.W., Fuchs, C.S., Stampfer, M.J., and Willett, W.C. (2006). Prospective study of predictors of vitamin D status and cancer incidence and mortality in men. *J Natl Cancer Inst* 98, 451-459.

Glinka, A., Wu, W., Delius, H., Monaghan, A.P., Blumenstock, C., and Niehrs, C. (1998). Dickkopf-1 is a member of a new family of secreted proteins and functions in head induction. *Nature* 391, 357-362.

Gocek, E., and Studzinski, G.P. (2009). Vitamin D and differentiation in cancer. *Critical reviews in clinical laboratory sciences* 46, 190-209.

Goel, H.L., Alam, N., Johnson, I.N., and Languino, L.R. (2009). Integrin signaling aberrations in prostate cancer. *Am J Transl Res* 1, 211-220.

Grabowska, M.M., DeGraff, D.J., Yu, X., Jin, R.J., Chen, Z., Borowsky, A.D., and Matusik, R.J. (2014). Mouse models of prostate cancer: picking the best model for the question. *Cancer Metastasis Rev* 33, 377-397.

Groschel, C., Aggarwal, A., Tennakoon, S., Hobaus, J., Prinz-Wohlgenannt, M., Marian, B., Heffeter, P., Berger, W., and Kallay, E. (2016). Effect of 1,25-dihydroxyvitamin D3 on the Wnt pathway in non-malignant colonic cells. *J Steroid Biochem Mol Biol* 155, 224-230.

Guo, C., Liu, H., Zhang, B.H., Cadaneanu, R.M., Mayle, A.M., and Garraway, I.P. (2012). Epcam, cd44, and cd49f distinguish sphere-forming human prostate basal cells from a subpopulation with predominant tubule initiation capability. *PLoS ONE* 7.

Hainline, K.M., Gu, F., Handley, J.F., Tian, Y.F., Wu, Y., de Wet, L., Vander Griend, D.J., and Collier, J.H. (2018). Self-Assembling Peptide Gels for 3D Prostate Cancer Spheroid Culture. *Macromolecular Bioscience*, 1800249.

Hall, C.L., Dubyk, C.W., Riesenberger, T.A., Shein, D., Keller, E.T., and van Golen, K.L. (2008). Type I collagen receptor (alpha2beta1) signaling promotes prostate cancer invasion through RhoC GTPase. *Neoplasia* 10, 797-803.

Hanchette, C.L., and Schwartz, G.G. (1992). Geographic patterns of prostate cancer mortality. Evidence for a protective effect of ultraviolet radiation. *Cancer* 70, 2861-2869.

Hendrickson, W.K., Flavin, R., Kasperzyk, J.L., Fiorentino, M., Fang, F., Lis, R., Fiore, C., Penney, K.L., Ma, J., Kantoff, P.W., *et al.* (2011). Vitamin D receptor protein expression in tumor tissue and prostate cancer progression. *J Clin Oncol* 29, 2378-2385.

- Henry, G.H., Malewska, A., Joseph, D.B., Malladi, V.S., Lee, J., Torrealba, J., Mauck, R.J., Gahan, J.C., Raj, G.V., Roehrborn, C.G., *et al.* (2018). A cellular anatomy of the normal adult human prostate and prostatic urethra. *Cell Rep* 25, 3530-3542.
- Hepburn, A.C., Sims, C.H.C., Buskin, A., and Heer, R. (2020). Engineering Prostate Cancer from Induced Pluripotent Stem Cells-New Opportunities to Develop Preclinical Tools in Prostate and Prostate Cancer Studies. *Int J Mol Sci* 21.
- Hill, N.T., Zhang, J., Leonard, M.K., Lee, M., Shamma, H.N., and Kadakia, M. (2015). 1 α , 25-Dihydroxyvitamin D(3) and the vitamin D receptor regulates DeltaNp63 α levels and keratinocyte proliferation. *Cell Death Dis* 6, e1781.
- Hlaing, S.M., Garcia, L.A., Contreras, J.R., Norris, K.C., Ferrini, M.G., and Artaza, J.N. (2014). 1,25-Vitamin D3 promotes cardiac differentiation through modulation of the WNT signaling pathway. *J Mol Endocrinol* 53, 303-317.
- Hoffman, P., Satija, R., Papalexi, E., Smibert, P., and Butler, A. (2018). Integrating single-cell transcriptomic data across different conditions, technologies, and species. *Nature Biotechnology* 36.
- Holick, C.N., Stanford, J.L., Kwon, E.M., Ostrander, E.A., Nejentsev, S., and Peters, U. (2007). Comprehensive association analysis of the vitamin D pathway genes, VDR, CYP27B1, and CYP24A1, in prostate cancer. *Cancer Epidemiol Biomarkers Prev* 16, 1990-1999.
- Hsieh, S.-Y., Hsieh, P.-S., Chiu, C.-T., and Chen, W.-Y. (2004). Dickkopf-3/REIC functions as a suppressor gene of tumor growth. *Oncogene* 23, 9183-9189.
- Hu, H., Gehart, H., Artegiani, B., C, L.O.-I., Dekkers, F., Basak, O., van Es, J., Chuva de Sousa Lopes, S.M., Begthel, H., Korving, J., *et al.* (2018). Long-Term Expansion of Functional Mouse and Human Hepatocytes as 3D Organoids. *Cell* 175, 1591-1606 e1519.
- Hu, W.-Y., Hu, D.-P., Xie, L., Li, Y., Majumdar, S., Nonn, L., Hu, H., Shioda, T., and Prins, G.S. (2017). Isolation and functional interrogation of adult human prostate epithelial stem cells at single cell resolution. *Stem Cell Res* 23, 1-12.
- Hughes, C.S., Postovit, L.M., and Lajoie, G.A. (2010). Matrigel: a complex protein mixture required for optimal growth of cell culture. *Proteomics* 10, 1886-1890.
- Humphries, J.D., Byron, A., and Humphries, M.J. (2006). Integrin ligands at a glance. *J Cell Sci* 119, 3901-3903.
- Hutabarat, M., Wibowo, N., Obermayer-Pietsch, B., and Huppertz, B. (2018). Impact of vitamin D and vitamin D receptor on the trophoblast survival capacity in preeclampsia. *PLoS One* 13, e0206725.
- Hyuga, T., Alcantara, M., Kajioka, D., Haraguchi, R., Suzuki, K., Miyagawa, S., Kojima, Y., Hayashi, Y., and Yamada, G. (2019). Hedgehog Signaling for Urogenital Organogenesis and Prostate Cancer: An Implication for the Epithelial-Mesenchyme Interaction (EMI). *Int J Mol Sci* 21.

- Inoue, J., Fujita, H., Bando, T., Kondo, Y., Kumon, H., and Ohuchi, H. (2017). Expression analysis of Dickkopf-related protein 3 (Dkk3) suggests its pleiotropic roles for a secretory glycoprotein in adult mouse. *J Mol Histol* 48, 29-39.
- Ivan V. Litvinov, D.J.V.G., Yi Xu, Lizamma Antony, Susan L. Dalrymple, and John T. Isaacs (2006). Low-Calcium Serum-Free Defined Medium Selects for Growth of Normal Prostatic Epithelial Stem Cells. *Cancer Res* 66, 1-27.
- Jacques, P.F., Felson, D.T., Tucker, K.L., Mahnken, B., Wilson, P.W., Rosenberg, I.H., and Rush, D. (1997). Plasma 25-hydroxyvitamin D and its determinants in an elderly population sample. *Am J Clin Nutr* 66, 929-936.
- James, S.Y., Williams, M.A., Kelsey, S.M., Newland, A.C., and Colston, K.W. (1997). Interaction of vitamin D derivatives and granulocyte-macrophage colony-stimulating factor in leukaemic cell differentiation. *Leukemia* 11, 1017-1025.
- Kalinska, M., Meyer-Hoffert, U., Kantyka, T., and Potempa, J. (2016). Kallikreins - The melting pot of activity and function. *Biochimie* 122, 270-282.
- Karantanos, T., Corn, P.G., and Thompson, T.C. (2013). Prostate cancer progression after androgen deprivation therapy: mechanisms of castrate resistance and novel therapeutic approaches. *Oncogene* 32, 5501-5511.
- Kardooni, H., Gonzalez-Gualda, E., Stylianakis, E., Saffaran, S., Waxman, J., and Kypta, R.M. (2018). CRISPR-mediated reactivation of DKK3 expression attenuates TGF- β signaling in prostate cancer. *Cancers* 10, 1-19.
- Karthaus, W.R., Iaquinia, P.J., Drost, J., Gracanin, A., Van Boxtel, R., Wongvipat, J., Dowling, C.M., Gao, D., Begthel, H., Sachs, N., *et al.* (2014). Identification of multipotent luminal progenitor cells in human prostate organoid cultures. *Cell* 159, 163-175.
- Kawano, Y., Kitaoka, M., Hamada, Y., Walker, M., Waxman, J., and Kypta, R. (2006). Regulation of prostate cell growth and morphogenesis by Dickkopf-3. *Oncogene* 25, 6528-6537.
- Kesby, J.P., Eyles, D.W., Burne, T.H., and McGrath, J.J. (2011). The effects of vitamin D on brain development and adult brain function. *Mol Cell Endocrinol* 347, 121-127.
- Khan, F.U., Ihsan, A.U., Khan, H.U., Jana, R., Wazir, J., Khongorzul, P., Waqar, M., and Zhou, X. (2017). Comprehensive overview of prostatitis. *Biomed Pharmacother* 94, 1064-1076.
- Kovalenko, P.L., Zhang, Z., Cui, M., Clinton, S.K., and Fleet, J.C. (2010). 1,25 dihydroxyvitamin D-mediated orchestration of anticancer, transcript-level effects in the immortalized, non-transformed prostate epithelial cell line, RWPE1. *BMC Genomics* 11, 26.
- Kramer, A., Green, J., Pollard, J., Jr., and Tugendreich, S. (2014). Causal analysis approaches in Ingenuity Pathway Analysis. *Bioinformatics* 30, 523-530.
- Kretschmar, K., and Clevers, H. (2016). Organoids: Modeling Development and the Stem Cell Niche in a Dish. *Developmental Cell* 38, 590-600.

Kruithof-De Julio, M., Shibata, M., Desai, N., Reynon, M., Halili, M.V., Hu, Y.-P., Price, S.M., Abate-Shen, C., and Shen, M.M. (2013). Canonical Wnt signaling regulates Nkx3.1 expression and luminal epithelial differentiation during prostate organogenesis. *Dev Dyn* 242, 1160-1171.

Krupnik, V.E., Sharp, J.D., Jiang, C., Robison, K., Chickering, T.W., Amaravadi, L., Brown, D.E., Guyot, D., Mays, G., Leiby, K., *et al.* (1999). Functional and structural diversity of the human Dickkopf gene family. *Gene* 238, 301-313.

Kwon, O.J., Zhang, Y., Li, Y., Wei, X., Zhang, L., Chen, R., Creighton, C.J., and Xin, L. (2019). Functional Heterogeneity of Mouse Prostate Stromal Cells Revealed by Single-Cell RNA-Seq. *iScience* 13, 328-338.

Larriba, M.J., González-Sancho, J.M., Barbáchano, A., Niell, N., Ferrer-Mayorga, G., and Muñoz, A. (2013). Vitamin D is a multilevel repressor of Wnt/ β -catenin signaling in cancer cells. *Cancers (Basel)* 5, 1242-1260.

Larriba, M.J., Ordonez-Moran, P., Chicote, I., Martin-Fernandez, G., Puig, I., Munoz, A., and Palmer, H.G. (2011). Vitamin D receptor deficiency enhances Wnt/beta-catenin signaling and tumor burden in colon cancer. *PLoS One* 6, e23524.

Lee, J.L., and Streuli, C.H. (2014). Integrins and epithelial cell polarity. *J Cell Sci* 127, 3217-3225.

Leonard, J.L., Leonard, D.M., Wolfe, S.A., Liu, J., Rivera, J., Yang, M., Leonard, R.T., Johnson, J.P.S., Kumar, P., Liebmann, K.L., *et al.* (2017). The Dkk3 gene encodes a vital intracellular regulator of cell proliferation. *PLoS One* 12, e0181724.

Li, Y., Liu, H., Liang, Y., Peng, P., Ma, X., and Zhang, X. (2017). DKK3 regulates cell proliferation, apoptosis and collagen synthesis in keloid fibroblasts via TGF- β 1/Smad signaling pathway. *Biomed Pharmacother* 91, 174-180.

Livak, K.J., and Schmittgen, T.D. (2001). Analysis of relative gene expression data using real-time quantitative PCR and the 2(-Delta Delta C(T)) Method. *Methods* 25, 402-408.

Long, R.M., Morrissey, C., Fitzpatrick, J.M., William, R., and Watson, G. (2005). Prostate epithelial cell differentiation and its relevance to the understanding of prostate cancer therapies. *Clinical Science* 108, 1-11.

MacLaughlin, J.A., Cantley, L.C., and Holick, M.F. (1990). 1,25(OH)₂D₃ increases calcium and phosphatidylinositol metabolism in differentiating cultured human keratinocytes. *J Nutr Biochem* 1, 81-87.

Macosko, E.Z., Basu, A., Regev, A., Mccarroll Correspondence, S.A., Satija, R., Nemesh, J., Shekhar, K., Goldman, M., Tirosh, I., Bialas, A.R., *et al.* (2015). Highly Parallel Genome-wide Expression Profiling of Individual Cells Using Nanoliter Droplets. *Cell* 161, 1202-1214.

Manson, J.E., Cook, N.R., Lee, I.-M., Christen, W., Bassuk, S.S., Mora, S., Gibson, H., Gordon, D., Copeland, T., D'Agostino, D., *et al.* (2019). Vitamin D Supplements and Prevention of Cancer and Cardiovascular Disease. *N Engl J Med* 380, 33-44.

Marco Giammanco, D.D.M., Maurizio La Guardia, Stefania Aiello, Marilena Crescimannno, C.F., Francesca M. Tumminello &, and Leto, G. Vitamin D in cancer chemoprevention.

Marina, S., and Bissell, M.J. (2017). Organoids: a historical perspective of thinkin in three dimensions. *J Cell Biol* 216, 1-10.

Marshall, D.T., Savage, S.J., Garrett-Mayer, E., Keane, T.E., Hollis, B.W., Horst, R.L., Ambrose, L.H., Kindy, M.S., and Gattoni-Celli, S. (2012). Vitamin D3 supplementation at 4000 international units per day for one year results in a decrease of positive cores at repeat biopsy in subjects with low-risk prostate cancer under active surveillance. *J Clin Endocrinol Metab* 97, 2315-2324.

Martin, J.L., and Pattison, S.L. (2000). Insulin-like growth factor binding protein-3 is regulated by dihydrotestosterone and stimulates deoxyribonucleic acid synthesis and cell proliferation in LNCaP prostate carcinoma cells. *Endocrinology* 141, 2401-2409.

McCray, T., Moline, D., Baumann, B., Vander Griend, D.J., and Nonn, L. (2019a). Single-cell RNA-Seq analysis identifies a putative epithelial stem cell population in human primary prostate cells in monolayer and organoid culture conditions. *Am J Clin Exp Urol* 7, 123-138.

McCray, T., Richards, Z., Marsili, J., Prins, G.S., and Nonn, L. (2019b). Handling and assessment of human primary prostate organoid culture. *J Vis Exp*, 1-4.

Merchan, B.B., Morcillo, S., Martin-Nuñez, G., Tinahones, F.J., and Macías-González, M. (2017). The role of vitamin D and VDR in carcinogenesis: Through epidemiology and basic sciences. *J Steroid Biochem Mol Biol* 167, 203-218.

Moad, M., Hannezo, E., Buczacki, S.J., Robson, C.N., Simons, B.D., Correspondence, R.H., Wilson, L., El-Sherif, A., Sims, D., Pickard, R., *et al.* (2017). Multipotent Basal Stem Cells, Maintained in Localized Proximal Niches, Support Directed Long- Ranging Epithelial Flows in Human Prostates Multipotent Basal Stem Cells, Maintained in Localized Proximal Niches, Support Directed Long-Ranging Epithelial Flows. *Cell Reports* 20.

Moran-Jones, K., Ledger, A., and Naylor, M.J. (2012). beta1 integrin deletion enhances progression of prostate cancer in the TRAMP mouse model. *Sci Rep* 2, 526.

Mordan-McCombs, S., Brown, T., Wang, W.L., Gaupel, A.C., Welsh, J., and Tenniswood, M. (2010). Tumor progression in the LPB-Tag transgenic model of prostate cancer is altered by vitamin D receptor and serum testosterone status. *J Steroid Biochem Mol Biol* 121, 368-371.

Mucuk, G., Sepet, E., Erguven, M., Ekmekci, O., and Bilir, A. (2017). 1,25-Dihydroxyvitamin D3 stimulates odontoblastic differentiation of human dental pulp-stem cells in vitro. *Connect Tissue Res* 58, 531-541.

Muralidhar, S., Filia, A., Nsengimana, J., Pozniak, J., O'Shea, S.J., Diaz, J.M., Harland, M., Randerson-Moor, J.A., Reichrath, J., Laye, J.P., *et al.* (2019). Vitamin D-VDR Signaling Inhibits Wnt/beta-Catenin-Mediated Melanoma Progression and Promotes Antitumor Immunity. *Cancer Res* 79, 5986-5998.

Murillo-Garzon, V., and Kypta, R. (2017). WNT signalling in prostate cancer. *Nat Rev Urol* 14, 683-696.

- Murphy, A.B., Nyame, Y., Martin, I.K., Catalona, W.J., Hollowell, C.M., Nadler, R.B., Kozlowski, J.M., Perry, K.T., Kajdacsy-Balla, A., and Kittles, R. (2014). Vitamin D deficiency predicts prostate biopsy outcomes. *Clin Cancer Res* 20, 2289-2299.
- Murphy, A.B., Nyame, Y.A., Batai, K., Kalu, R., Khan, A., Gogana, P., Dixon, M., Macias, V., Kajdacsy-Balla, A., Hollowell, C.M., *et al.* (2017). Does prostate volume correlate with vitamin D deficiency among men undergoing prostate biopsy? *Prostate Cancer Prostatic Dis* 20, 55-60.
- Murthy, S., Agoulnik, I.U., and Weigel, N.L. (2005). Androgen receptor signaling and vitamin D receptor action in prostate cancer cells. *Prostate* 64, 362-372.
- Nakamura, R.E.I., and Hackam, A.S. (2010). Analysis of Dickkopf3 interactions with Wnt signaling receptors. *Growth Factors* 28, 232-242.
- Naylor, M.J., Li, N., Cheung, J., Lowe, E.T., Lambert, E., Marlow, R., Wang, P., Schatzmann, F., Wintermantel, T., Schuetz, G., *et al.* (2005). Ablation of beta1 integrin in mammary epithelium reveals a key role for integrin in glandular morphogenesis and differentiation. *J Cell Biol* 171, 717-728.
- Niranjan, B., Lawrence, M.G., Papargiris, M.M., Richards, M.G., Hussain, S., Frydenberg, M., Pedersen, J., Taylor, R.A., and Risbridger, G.P. (2013). Primary culture and propagation of human prostate epithelial cells. *Methods Mol Biol* 945, 365-382.
- Odero-Marah, V., Hawsawi, O., Henderson, V., and Sweeney, J. (2018). Epithelial-Mesenchymal Transition (EMT) and Prostate Cancer. *Adv Exp Med Biol* 1095, 101-110.
- Orkin, R.W., Gehron, P., McGoodwin, E.B., Martin, G.R., Valentine, T., and Swarm, R. (1977). A murine tumor producing a matrix of basement membrane. *J Exp Med* 145, 204-220.
- Ousset, M., Van Keymeulen, A., Bouvencourt, G., Sharma, N., Achouri, Y., Simons, B.D., and Blanpain, C. (2012). Multipotent and unipotent progenitors contribute to prostate postnatal development. *Nat Cell Biol* 14, 1131-1138.
- Pak, S., Park, S., Kim, Y., Park, J.H., Park, C.H., Lee, K.J., Kim, C.S., and Ahn, H. (2019). The small molecule WNT/beta-catenin inhibitor CWP232291 blocks the growth of castration-resistant prostate cancer by activating the endoplasmic reticulum stress pathway. *J Exp Clin Cancer Res* 38, 342.
- Palmer, H.G., Gonzalez-Sancho, J.M., Espada, J., Berciano, M.T., Puig, I., Baulida, J., Quintanilla, M., Cano, A., de Herreros, A.G., Lafarga, M., *et al.* (2001). Vitamin D(3) promotes the differentiation of colon carcinoma cells by the induction of E-cadherin and the inhibition of beta-catenin signaling. *J Cell Biol* 154, 369-387.
- Peehl, D.M. (2002). Human Prostatic Epithelial Cells. *Cultures* 8, 171-194.
- Peehl, D.M. (2003). Growth of prostatic epithelial and stromal cells in vitro. *Methods in Molecular Medicine* 81, 41-57.
- Peehl, D.M. (2004). Are primary cultures realistic models of prostate cancer? *J Cell Biochem* 91, 185-195.

- Peehl, D.M., Shinghal, R., Nonn, L., Seto, E., Krishnan, A.V., Brooks, J.D., and Feldman, D. (2004). Molecular activity of 1,25-dihydroxyvitamin D₃ in primary cultures of human prostatic epithelial cells revealed by cDNA microarray analysis. *J Steroid Biochem Mol Biol* 92, 131-141.
- Peehl, D.M., and Stamey, T.A. (1986). Serum-Free Growth of Adult Human Prostatic Epithelial Cells. 22.
- Peehl, D.M., Wong, S.T., and Stamey, T.A. (1988). Clonal growth characteristics of adult human prostatic epithelial cells. *In Vitro Cellular and Developmental Biology - Animal* 24, 530-536.
- Peregrina, K., Houston, M., Daroqui, C., Dhima, E., Sellers, R.S., and Augenlicht, L.H. (2015). Vitamin D is a determinant of mouse intestinal Lgr5 stem cell functions. *Carcinogenesis* 36, 25-31.
- Pereira-Santos, M., Costa, P.R., Assis, A.M., Santos, C.A., and Santos, D.B. (2015). Obesity and vitamin D deficiency: a systematic review and meta-analysis. *Obes Rev* 16, 341-349.
- Philippe, C.L. (2016). Therapeutic Value of an Integrin Antagonist in Prostate Cancer. *Curr Drug Targets* 17, 321-327.
- Pinho Christof Niehrs, S. (2007). Dkk3 is required for TGF- β signaling during *Xenopus* mesoderm induction. *Differentiation* 75, 957-967.
- Post, Y., Puschhof, J., Beumer, J., Kerckamp, H.M., de Bakker, M.A.G., Slagboom, J., de Barbanson, B., Wevers, N.R., Spijkers, X.M., Olivier, T., *et al.* (2020). Snake Venom Gland Organoids. *Cell* 180, 233-247 e221.
- Prins, G.S., and Lindgren, M. (2015). Accessory Sex Glands in the Male. In Knobil and Neill's *Physiology of Reproduction*, 4th ed, T.M. Plant, and A.J. Zeleznik, eds. (Elsevier), pp. 773-797.
- Prins, G.S., and Putz, O. (2008). Molecular signaling pathways that regulate prostate gland development. *Differentiation* 76, 641-659.
- Qiu, X., Mao, Q., Tang, Y., Wang, L., Chawla, R., Pliner, H.A., and Trapnell, C. (2017). Reversed graph embedding resolves complex single-cell trajectories. *Nat Methods* 14, 979-982.
- Rafiq, R., Walschot, F., Lips, P., Lamb, H.J., de Roos, A., Rosendaal, F.R., Heijer, M.D., de Jongh, R.T., and de Mutsert, R. (2019). Associations of different body fat deposits with serum 25-hydroxyvitamin D concentrations. *Clin Nutr* 38, 2851-2857.
- Rawla, P. (2019). Epidemiology of Prostate Cancer. *World J Oncol* 10, 63-89.
- Richards, Z., Batai, K., Farhat, R., Shah, E., Makowski, A., Gann, P.H., Kittles, R., and Nonn, L. (2017). Prostatic compensation of the vitamin D axis in African American men. *JCI Insight* 2, e91054.
- Richards, Z., McCray, T., Marsili, J., Zenner, M.L., Garcia, J., Manlucu, J.T., Voisine, C., Murphy, A.B., Prins, G.S., Murray, M., *et al.* (2019). Prostate stroma increases the viability and maintains the branching phenotype of human prostate organoids. *iScience* 12, 304-317.

- Robsahm, T.E., Tretli, S., Dahlback, A., and Moan, J. (2004). Vitamin D3 from sunlight may improve the prognosis of breast-, colon- and prostate cancer (Norway). *Cancer causes & control* : CCC 15, 149-158.
- Romagnoli, M., Cagnet, S., Chiche, A., Bresson, L., Baulande, S., de la Grange, P., De Arcangelis, A., Kreft, M., Georges-Labouesse, E., Sonnenberg, A., *et al.* (2019). Deciphering the Mammary Stem Cell Niche: A Role for Laminin-Binding Integrins. *Stem Cell Reports* 12, 831-844.
- Romero, D., Al-Shareef, Z., Gorroño-Etxebarria, I., Atkins, S., Turrell, F., Chhetri, J., Bengoa-Vergniory, N., Zenzmaier, C., Berger, P., Waxman, J., *et al.* (2016). Dickkopf-3 regulates prostate epithelial cell acinar morphogenesis and prostate cancer cell invasion by limiting TGF- β -dependent activation of matrix metalloproteases. *Carcinogenesis* 37, 18-29.
- Romero, D., Kawano, Y., Bengoa, N., Walker, M.M., Maltry, N., Niehrs, C., Waxman, J., and Kypta, R. (2013). Downregulation of Dickkopf-3 disrupts prostate acinar morphogenesis through TGF- β /Smad signalling. *J Cell Sci* 126, 1858-1867.
- Russell, P.J., and Kingsley, E.A. (2003). Human prostate cancer cell lines. *Methods Mol Med* 81, 21-39.
- Satija, R., Farrell, J.A., Gennert, D., Schier, A.F., and Regev, A. (2015). Spatial reconstruction of single-cell gene expression data. *Nat Biotechnol* 33, 495-502.
- Sato, T., Vries, R.G., Snippert, H.J., van de Wetering, M., Barker, N., Stange, D.E., van Es, J.H., Abo, A., Kujala, P., Peters, P.J., *et al.* (2009). Single Lgr5 stem cells build crypt-villus structures in vitro without a mesenchymal niche. *Nature* 459, 262-265.
- Scardino, P.T. (1989). Early detection of prostate cancer. *Urol Clin North Am* 16, 635-655.
- Schmelz, M., Moll, R., Hesse, U., Prasad, A.R., Gandolfi, J.A., Hasan, S.R., Bartholdi, M., and Cress, A.E. (2005). Identification of a stem cell candidate in the normal human prostate gland. *Eur J Cell Biol* 84, 341-354.
- Schutgens, F., Rookmaaker, M.B., Margaritis, T., Rios, A., Ammerlaan, C., Jansen, J., Gijzen, L., Vormann, M., Vonk, A., Viveen, M., *et al.* (2019). Tubuloids derived from human adult kidney and urine for personalized disease modeling. *Nat Biotechnol* 37, 303-313.
- Shah, S., Islam, M.N., Dakshanamurthy, S., Rizvi, I., Rao, M., Herrell, R., Zinser, G., Valrance, M., Aranda, A., Moras, D., *et al.* (2006). The molecular basis of vitamin D receptor and beta-catenin crossregulation. *Mol Cell* 21, 799-809.
- Shao, C., Wang, Y., Yue, H.H., Zhang, Y.T., Shi, C.H., Liu, F., Bao, T.Y., Yang, Z.Y., Yuan, J.L., and Shao, G.X. (2007). Biphasic effect of androgens on prostate cancer cells and its correlation with androgen receptor coactivator dopa decarboxylase. *J Androl* 28, 804-812.
- Sharma Das, D., Wadhwa, N., Kunj, N., Sarda, K., Shankar Pradhan, B., and Majumdar, S.S. (2013). Dickkopf homolog 3 (DKK3) plays a crucial role upstream of WNT/ β -CATENIN signaling for sertoli cell mediated regulation of spermatogenesis. *PLoS One* 8, e63603.

- Siegel, R.L., Miller, K.D., and Jemal, A. (2020). Cancer statistics, 2020. *CA Cancer J Clin* 70, 7-30.
- Simons, B.W., Hurley, P.J., Huang, Z., Ross, A.E., Miller, R., Marchionni, L., Berman, D.M., and Schaeffer, E.M. (2012). Wnt signaling through beta-catenin is required for prostate lineage specification. *Dev Biol* 371, 246-255.
- Singh, P.K., Doig, C.L., Dhiman, V.K., Turner, B.M., Smiraglia, D.J., and Campbell, M.J. (2013). Epigenetic distortion to VDR transcriptional regulation in prostate cancer cells. *J Steroid Biochem Mol Biol* 136, 258-263.
- Sobel, R.E., and Sadar, M.D. (2005a). Cell lines used in prostate cancer research: a compendium of old and new lines--part 1. *The Journal of Urology* 173, 342-359.
- Sobel, R.E., and Sadar, M.D. (2005b). Cell lines used in prostate cancer research: a compendium of old and new lines--part 2. *The Journal of Urology* 173, 360-372.
- Song, L.N., Herrell, R., Byers, S., Shah, S., Wilson, E.M., and Gelmann, E.P. (2003). Beta-catenin binds to the activation function 2 region of the androgen receptor and modulates the effects of the N-terminal domain and TIF2 on ligand-dependent transcription. *Mol Cell Biol* 23, 1674-1687.
- Spielvogel, A.M., Farley, R.D., and Norman, A.W. (1972). Studies on the mechanism of action of calciferol. V. Turnover time of chick intestinal epithelial cells in relation to the intestinal action of vitamin D. *Exp Cell Res* 74, 359-366.
- Streuli, C.H., Edwards, G.M., Delcommenne, M., Whitelaw, C.B., Burdon, T.G., Schindler, C., and Watson, C.J. (1995). Stat5 as a target for regulation by extracellular matrix. *J Biol Chem* 270, 21639-21644.
- Studzinski, G.P., and Moore, D.C. (1995). Sunlight--can it prevent as well as cause cancer? *Cancer Res* 55, 4014-4022.
- Suyin, P.C., Dickinson, J.L., and Holloway, A.F. (2013). *Advances in Prostate Cancer In.*
- Takasato, M., Er, P.X., Chiu, H.S., and Little, M.H. (2016). Generation of kidney organoids from human pluripotent stem cells. *Nat Protoc* 11, 1681-1692.
- Tavera-Mendoza, L.E., Westerling, T., Libby, E., Marusyk, A., Cato, L., Cassani, R., Cameron, L.A., Ficarro, S.B., Marto, J.A., Klawitter, J., *et al.* (2017). Vitamin D receptor regulates autophagy in the normal mammary gland and in luminal breast cancer cells. *Proc Natl Acad Sci USA* 114, E2186-E2194.
- Toivanen, R., and Shen, M.M. (2017). Prostate organogenesis: tissue induction, hormonal regulation and cell type specification. *Development* 144, 1382-1398.
- Trapnell, C., Cacchiarelli, D., Grimsby, J., Pokharel, P., Li, S., Morse, M., Lennon, N.J., Livak, K.J., Mikkelsen, T.S., and Rinn, J.L. (2014). The dynamics and regulators of cell fate decisions are revealed by pseudotemporal ordering of single cells. *Nat Biotechnol* 32, 381-386.

Tu, C., Fiandalo, M.V., Pop, E., Stocking, J.J., Azabdaftari, G., Li, J., Wei, H., Ma, D., Qu, J., Mohler, J.L., *et al.* (2018). Proteomic Analysis of Charcoal-Stripped Fetal Bovine Serum Reveals Changes in the Insulin-like Growth Factor Signaling Pathway. *J Proteome Res* 17, 2963-2977.

Untergasser, G., Koch, H.B., Menssen, A., and Hermeking, H. (2002). Characterization of epithelial senescence by serial analysis of gene expression: identification of genes potentially involved in prostate cancer. *Cancer Res* 62, 6255-6262.

Uzgare, A.R., Xu, Y., and Isaacs, J.T. (2004). In vitro culturing and characteristics of transit amplifying epithelial cells from human prostate tissue. *J Cell Biochem* 91, 196-205.

Varzavand, A., Hacker, W., Ma, D., Gibson-Corley, K., Hawayek, M., Tayh, O.J., Brown, J.A., Henry, M.D., and Stipp, C.S. (2016). alpha3beta1 Integrin Suppresses Prostate Cancer Metastasis via Regulation of the Hippo Pathway. *Cancer Res* 76, 6577-6587.

Vežina, C.M., Allgeier, S.H., Fritz, W.A., Moore, R.W., Strerath, M., Bushman, W., and Peterson, R.E. (2008). Retinoic acid induces prostatic bud formation. *Developmental Dynamics* 237, 1321-1333.

Wagner, D., Trudel, D., Van der Kwast, T., Nonn, L., Giangreco, A.A., Li, D., Dias, A., Cardoza, M., Laszlo, S., Hersey, K., *et al.* (2013). Randomized Clinical Trial of Vitamin D ³ Doses on Prostatic Vitamin D Metabolite Levels and Ki67 Labeling in Prostate Cancer Patients. *The Journal of Clinical Endocrinology & Metabolism* 98, 1498-1507.

Wang, C., Liu, Z., Ke, Y., and Wang, F. (2019). Intrinsic FGFR2 and Ectopic FGFR1 Signaling in the Prostate and Prostate Cancer. *Front Genet* 10, 12.

Wang, G., Zhao, D., Spring, D.J., and DePinho, R.A. (2018). Genetics and biology of prostate cancer. *Genes Dev* 32, 1105-1140.

Wang, H.H., Wang, L., Jerde, T.J., Chan, B.D., Savran, C.A., Burcham, G.N., Crist, S., and Ratliff, T.L. (2015). Characterization of autoimmune inflammation induced prostate stem cell expansion. *Prostate* 75, 1620-1631.

Wang, Y., Hayward, S.W., Thayer, K., Cunha, G.R., W, Y.W.S., Cao, H.M., Thayer, K.A., and Cunha, G.R. (2001). Cell differentiation lineage in the prostate.

Wang Z, Lin L., Thomas D. G. , Nadal E., Chang A. C., Beer D. G., and J., L. (2015). The Role of Dickkopf-3 Overexpression in Esophageal Adenocarcinoma. *J Thorac Cardiovasc Surg* 25, 368-379.

Wei, X., Zhang, L., Zhou, Z., Kwon, O.J., Zhang, Y., Nguyen, H., Dumpit, R., True, L., Nelson, P., Dong, B., *et al.* (2019). Spatially Restricted Stromal Wnt Signaling Restrains Prostate Epithelial Progenitor Growth through Direct and Indirect Mechanisms. *Cell Stem Cell* 24, 753-768 e756.

Wise, C. (2002). Epithelial cell culture protocols - primary culture and propagation of human prostate epithelial cells (pg 365-382). 188, 365-382.

- Woo, T.C., Choo, R., Jamieson, M., Chander, S., and Vieth, R. (2005). Pilot study: potential role of vitamin D (Cholecalciferol) in patients with PSA relapse after definitive therapy. *Nutr Cancer* 51, 32-36.
- Wright, A.S., Thomas, L.N., Douglas, R.C., Lazier, C.B., and Rittmaster, R.S. (1996). Relative potency of testosterone and dihydrotestosterone in preventing atrophy and apoptosis in the prostate of the castrated rat. *J Clin Invest* 98, 2558-2563.
- Wu, X., Daniels, G., Shapiro, E., Xu, K., Huang, H., Li, Y., Logan, S., Greco, M.A., Peng, Y., Monaco, M.E., *et al.* (2011). LEF1 identifies androgen-independent epithelium in the developing prostate. *Mol Endocrinol* 25, 1018-1026.
- Xin, L., Ide, H., Kim, Y., Dubey, P., and Witte, O.N. (2003). In vivo regeneration of murine prostate from dissociated cell populations of postnatal epithelia and urogenital sinus mesenchyme. *Proc Natl Acad Sci USA* 100 Suppl 1, 11896-11903.
- Yamamoto, H., Masters, J.R., Dasgupta, P., Chandra, A., Popert, R., Freeman, A., and Ahmed, A. (2012). CD49f Is an Efficient Marker of Monolayer- and Spheroid Colony-Forming Cells of the Benign and Malignant Human Prostate. *PLoS ONE* 7, 1-11.
- Yang, J., Zhu, S., Lin, G., Song, C., and He, Z. (2017). Vitamin D enhances omega-3 polyunsaturated fatty acids-induced apoptosis in breast cancer cells. *Cell Biol Int* 41, 890-897.
- Yasunaga, Y., Nakamura, K., Ewing, C.M., Isaacs, W.B., Hukku, B., and Rhim, J.S. (2001). A novel human cell culture model for the study of familial prostate cancer. *Cancer Res* 61, 5969-5973.
- Yokoyama, N.N., Shao, S., Hoang, B.H., Mercola, D., and Zi, X. (2014). Wnt signaling in castration-resistant prostate cancer: implications for therapy. *Am J Clin Exp Urol* 2, 27-44.
- Yu, W., Datta, A., Leroy, P., O'Brien, L.E., Mak, G., Jou, T.S., Matlin, K.S., Mostov, K.E., and Zegers, M.M. (2005). Beta1-integrin orients epithelial polarity via Rac1 and laminin. *Mol Biol Cell* 16, 433-445.
- Zent, R., Bush, K.T., Pohl, M.L., Quaranta, V., Koshikawa, N., Wang, Z., Kreidberg, J.A., Sakurai, H., Stuart, R.O., and Nigam, S.K. (2001). Involvement of laminin binding integrins and laminin-5 in branching morphogenesis of the ureteric bud during kidney development. *Dev Biol* 238, 289-302.
- Zenzmaier, C., Sampson, N., Plas, E., and Berger, P. (2013). Dickkopf-related protein 3 promotes pathogenic stromal remodeling in benign prostatic hyperplasia and prostate cancer. *Prostate* 73, 1441-1452.
- Zenzmaier, C., Untergasser, G., Hermann, M., Dirnhofer, S., Sampson, N., and Berger, P. (2008). Dysregulation of Dkk-3 expression in benign and malignant prostatic tissue. *Prostate* 68, 540-547.
- Zhang, D., Park, D., Zhong, Y., Lu, Y., Rycaj, K., Gong, S., Chen, X., Liu, X., Chao, H.-P., Whitney, P., *et al.* (2016). Stem cell and neurogenic gene-expression profiles link prostate basal cells to aggressive prostate cancer. *Nature communications* 7, 10798.

Zhang, K., Guo, Y., Wang, X., Zhao, H., Ji, Z., Cheng, C., Li, L., Fang, Y., Xu, D., Zhu, H.H., *et al.* (2017). WNT/beta-Catenin Directs Self-Renewal Symmetric Cell Division of hTERT(high) Prostate Cancer Stem Cells. *Cancer Res* 77, 2534-2547.

Zhang K., Watanabe M., Kashiwakura Y., Li S. A. , Edamura K., Huang P. , Yamaguchi K., Nasu Y., Kobayashi Y., Sakaguchi M., *et al.* (2010). Expression pattern of REIC/Dkk-3 in various cell types and the implications of the soluble form in prostatic acinar development. *Int J Oncol* 151, 414-420.

Zhang, X., Fournier, M.V., Ware, J.L., Bissell, M.J., Yacoub, A., and Zehner, Z.E. (2009a). Inhibition of vimentin or beta1 integrin reverts morphology of prostate tumor cells grown in laminin-rich extracellular matrix gels and reduces tumor growth in vivo. *Mol Cancer Ther* 8, 499-508.

Zhang, X., Mernaugh, G., Yang, D.H., Gewin, L., Srichai, M.B., Harris, R.C., Iturregui, J.M., Nelson, R.D., Kohan, D.E., Abrahamson, D., *et al.* (2009b). beta1 integrin is necessary for ureteric bud branching morphogenesis and maintenance of collecting duct structural integrity. *Development* 136, 3357-3366.

Zierold, C., Darwish, H.M., and DeLuca, H.F. (1995). Two vitamin D response elements function in the rat 1,25-dihydroxyvitamin D 24-hydroxylase promoter. *J Biol Chem* 270, 1675-1678.

APPENDICES

UNIVERSITY OF ILLINOIS AT CHICAGO

Office for the Protection of Research Subjects (OPRS)
Office of the Vice Chancellor for Research (MC 672)
203 Administrative Office Building
1737 West Polk Street
Chicago, Illinois 60612-7227

Notice of Determination of Human Subject Research

October 29, 2012

***20120935-
71032-1***

20120935-71032-1

Larisa Nonn, PhD
Pathology
840 S. Wood Street, Rm. 130 CSN
M/C 847
Chicago, IL 60612
Phone: (312) 355-3726 / Fax: (312) 996-4812

RE: Protocol # 2012-0935
Vitamin D reverses global repression of microRNAs in prostate cancer

Sponsor:	American Cancer Society
PAF#:	2012-04897
Grant/Contract No:	124264-RSG-13-012-01-CNE
Grant/Contract Title:	Vitamin D reverses global repression of microRNAs in prostate cancer

Dear Dr. Nonn:

The UIC Office for the Protection of Research Subjects received your "Determination of Whether an Activity Represents Human Subjects Research" application, and has determined that this activity **DOES NOT** meet the definition of human subject research as defined by 45 CFR 46.102(f).

You may conduct your activity without further submission to the IRB.

If this activity is used in conjunction with any other research involving human subjects or if it is modified in any way, it must be re-reviewed by OPRS staff.

Phone: 312-996-1711

<http://www.uic.edu/depts/ovcr/oprs/>

Fax: 312-413-2929

APPENDICES

Home Help Email Support Sign in Create Account

Prostate Stroma Increases the Viability and Maintains the Branching Phenotype of Human Prostate Organoids



Author:
Zachary Richards, Tara McCray, Joseph Marsili, Morgan L. Zenner, Jacob T. Manlucu, Jason Garcia, Andre Kajdacsy-Balla, Marcus Murray, Cindy Voisine, Adam B. Murphy, Sarki A. Abdulkadir, Gail S. Prins, Larisa Nonn

Publication: iScience
Publisher: Elsevier
Date: 22 February 2019

© 2019 The Author(s).

Please note that, as the author of this Elsevier article, you retain the right to include it in a thesis or dissertation, provided it is not published commercially. Permission is not required, but please ensure that you reference the journal as the original source. For more information on this and on your other retained rights, please visit: <https://www.elsevier.com/about/our-business/policies/copyright#Author-rights>

[BACK](#) [CLOSE WINDOW](#)

About Elsevier Products & Solutions Services Shop & Discover

[Journal author rights](#) [Government employees](#) [Elsevier's rights](#) [Protecting author rights](#) [Open access](#)

Personal use

Authors can use their articles, in full or in part, for a wide range of scholarly, non-commercial purposes as outlined below:

- Use by an author in the author's classroom teaching (including distribution of copies, paper or electronic)
- Distribution of copies (including through e-mail) to known research colleagues for their personal use (but not for Commercial Use)
- **Inclusion in a thesis or dissertation (provided that this is not to be published commercially)**
- Use in a subsequent compilation of the author's works
- Extending the Article to book-length form
- Preparation of other derivative works (but not for Commercial Use)
- Otherwise using or re-using portions or excerpts in other works

These rights apply for all Elsevier authors who publish their article as either a subscription article or an open access article. In all cases we require that all Elsevier authors always include a full acknowledgement and, if appropriate, a link to the final published version hosted on Science Direct.

APPENDICES

AJCEU

American Journal of
Clinical and Experimental Urology

[Am J Clin Exp Urol](#). 2019; 7(3): 123–138. PMCID: PMC6627543
Published online 2019 Jun 15. PMID: [31317052](#)

Single-cell RNA-Seq analysis identifies a putative epithelial stem cell population in human primary prostate cells in monolayer and organoid culture conditions

[Tara McCray](#),^{1,*} [Daniel Moline](#),^{2,*} [Bethany Baumann](#),¹ [Donald J Vander Griend](#),^{1,3} and [Larisa Nonn](#)^{1,3}

AJCEU

American Journal of
Clinical and Experimental Urology

[Home](#), [Editorial Board](#), [Table of Contents](#), [Information for Authors](#), [Manuscript Submission](#), [Forthcoming](#), [Journal Information](#)

Information for Authors

Copyright Policy

By submitting a manuscript to any of [e-Century Publishing Corporation](#) journal, all authors agree that all copyrights of all materials included in the submitted manuscript will be exclusively transferred to the publisher, e-Century Publishing Corporation once the manuscript is accepted.

Once the paper is published, the copyright will be released by the publisher under the “Creative Commons Attribution Noncommercial License”, enabling the unrestricted non-commercial use, distribution, and reproduction of the published article in any medium, provided that the original work is properly cited. **If the manuscript contains a figure or table reproduced from a book or another journal article, the authors should obtain permission from the copyright holder before submitting the manuscript**, and be fully responsible for any legal and/or financial consequences if such permissions are not obtained.

All PDF, XML and html files for all articles published in this journal are the property of the publisher, e-Century Publishing Corporation ([www.e-Century.org](#)). Authors and readers are granted the right to freely use these files for all academic purposes. In addition, **the author has the right to reuse any materials in his/her own paper for any purpose without getting the permission from the publisher** provided that the original work is properly cited. By publishing paper in this journal, the authors grant the permanent right to the publisher to use any articles published in this journal without any restriction including, but not limited to academic and/or commercial purposes.

If you are interested in using PDF, html, XML files or any art works published in this journal for **any commercial purposes**, please contact the publisher at business@e-century.org.

Use of Human Tissue and/or Animal Policy

Experiments involving human subjects should be in accord with the ethical standards established by the institution or in accord with the [Helsinki Declaration](#), or the guidelines of Office for [Human Research Protections \(OHRP\)](#) Human Subject Protections. For studies involved human subjects, when [informed consent](#) has been obtained it should be indicated in the manuscript.

Experiments involving animals should follow the institution or [the National Research Council guide](#) for the care and use of laboratory animals.

APPENDICES

JoVE Search 11,783 video articles Advanced LOG IN

BIOPHARMA **NEW** ABOUT JoVE FOR LIBRARIANS PUBLISH VIDEO JOURNAL SCIENCE EDUCATION

ABSTRACT INTRODUCTION PROTOCOL RESULTS DISCUSSION MATERIALS REFERENCES DOWNL

BIOENGINEERING

Handling and Assessment of Human Primary Prostate Organoid Culture

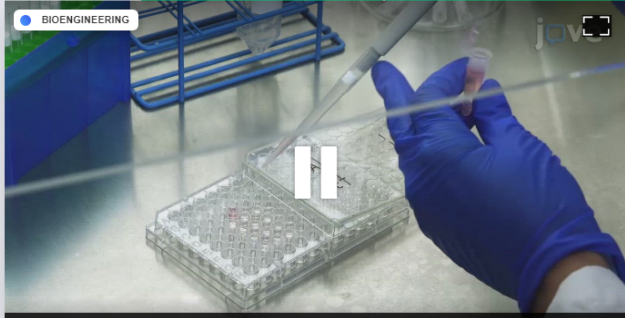
Tara McCray¹, Zachary Richards^{*1}, Joseph Marsili¹, Gail S. Prins^{1,2,3}, Larisa Nonn^{1,3}

¹Department of Pathology, **University of Illinois at Chicago**, ²Departments of Urology, Physiology, and Biophysics, **University of Illinois at Chicago**, ³University of Illinois Cancer Center

* These authors contributed equally

VIEWED 4,774 **CITE THIS** **SHARE**

BIOENGINEERING



THIS CONTENT IS OPEN ACCESS

CHAPTERS

- 0:04 Title
- 1:04 Collection of Organoids from Matrix Gel
- 2:09 Formalin Fixation and Paraffin Embedding of Organoids for Histological Endpoints
- 4:00 Sectioning the Formalin Fixed Paraffin Embedded (FFPE) Histology Gel Blocks
- 5:04 Whole-mounting of Organoids for Immunofluorescent Staining
- 6:35 Results: Analysis of Human Primary Prostate Organoids

JoVE

Hi Tara,

Thank you for publishing your article Handling and Assessment of Human Primary Prostate Organoid Culture with JoVE.

You have permission to reuse the following material from it in your thesis or dissertation, pursuant to your Author License Agreement:

Figure(s):
2

Please ensure that JoVE is properly cited in the legends as well as the References: "This is adapted from McCray, T., Richards, Z., Marsili, J., Prins, G. S., Nonn, L. Handling and Assessment of Human Primary Prostate Organoid Culture. *J. Vis. Exp.* (143), e59051, doi:10.3791/59051 (2019)."

Best regards,

Review
JoVE
617.674.1888
Follow us: [Facebook](#) | [Twitter](#) | [LinkedIn](#)
[About JoVE](#)

This message was sent to you by JoVE, the [Journal of Visualized Experiments](#).
JoVE, One Alewife Center, Suite 200, Cambridge, MA 02140 | tel: 617.945.9051 | fax: 866.381.2236

APPENDICES

The Differentiation of Patient-derived Prostate Organoids and the Influence of Vitamin D

ORIGINALITY REPORT

0%

SIMILARITY INDEX

PRIMARY SOURCES

- | | | |
|---|---|-----------------|
| 1 | Sonja Soininen, Aino-Maija Eloranta, Anna Viitasalo, Geneviève Dion et al. "Serum 25-hydroxyvitamin D, Plasma Lipids, and Associated Gene Variants in Prepubertal Children", <i>The Journal of Clinical Endocrinology & Metabolism</i> , 2018
<small>Crossref</small> | 20 words — < 1% |
| 2 | journals.plos.org
<small>Internet</small> | 17 words — < 1% |
| 3 | Vandanajay Bhatia, Ramanjaneya V. Mula, Miriam Falzon. "1,25-Dihydroxyvitamin D3 regulates PTHrP expression via transcriptional, post-transcriptional and post-translational pathways", <i>Molecular and Cellular Endocrinology</i> , 2011
<small>Crossref</small> | 16 words — < 1% |
| 4 | www.jbc.org
<small>Internet</small> | 15 words — < 1% |
| 5 | Lihui Duan, Xiao-Di Zhang, Wan-Ying Miao, Yun-Jun Sun et al. "PDGFRβ Cells Rapidly Relay Inflammatory Signal from the Circulatory System to Neurons via Chemokine CCL2", <i>Neuron</i> , 2018
<small>Crossref</small> | 15 words — < 1% |
| 6 | Wang, X.. "Expression of human kinase suppressor of Ras 2 (hKSR-2) gene in HL60 leukemia cells is directly upregulated by 1,25-dihydroxyvitamin D ³ and is required for optimal cell differentiation", <i>Experimental Cell Research</i> , 20070815
<small>Crossref</small> | 15 words — < 1% |
| 7 | dx.doi.org
<small>Internet</small> | 15 words — < 1% |

EXCLUDE QUOTES
EXCLUDE
BIBLIOGRAPHY

ON
ON

EXCLUDE MATCHES OFF

VITA

RESEARCH EXPERIENCE

The University of Illinois Chicago, *PhD Candidate*, Dr. Nonn's Lab March 2016 - present
Dissertation: The Differentiation of Patient-derived Prostate Organoids and the Influence of Vitamin D

Molecular and Cellular Biology

- Established patient primary prostate epithelial and stromal cell lines and ex vivo patient tissue culture
- Developed a novel human epithelial organoid model that incorporates primary stromal support
- Identified vitamin D target genes and validated using RNA- and protein-based methods: RT-qPCR, western blotting, ELISA, lentiviral knockdown, immunostaining, MTS assay, Edu assay, flow cytometry

Bioinformatics

- Characterized organoid differentiation by single cell RNA sequencing with 10x genomics technology and analysis using Seurat and Monocle in R
- Selected to participate in the Big Data Training for Translational Omics Research Workshop, funded by the NIH BD2K Initiative (2017) – learned analysis methods for microarray, RNA-sequencing, DNA-sequencing, and Genome-Wide Association Studies in R and Python

In vivo Modeling

- Collected fetal rat urogenital sinus (UGS) and isolated UGS mesenchyme and epithelium
- Generated recombination grafts of human prostate organoids with rat UGSM
- Performed surgery on mice to implant recombination grafts in renal capsule

Verbal & Written Communication

- Co-authored 3 publications in peer reviewed journals and 1 methods paper
- Delivered 2 oral and 14 poster presentations at conferences in 6 U.S. cities
- Managed 2 graduate rotation students and 3 lab volunteers of high school through Masters level training

The University of Illinois Chicago, *Rotation Student*, Dr. Merrill's Lab January– March 2016

- Generated a TCF/LEF knockdown mouse ES cell line in naïve conditions using CRISPR/Cas9

SNBL USA, Everett WA, *Research Associate*

2013 – 2015

- Handled nonhuman primates, mice rats, canines, rabbits and swine
- Performed in-life procedures (dose administration, animal health and behavior observations, sedation, socialization, and sample collection (blood, cerebrospinal fluid, urine, etc.))
- Performed end-of-life procedures (necropsy, organ weighing, tissue trimming, and bone marrow smears)
- Obtained Laboratory Animal Technician certification from the American Association for Laboratory Animal Science

The University of North Carolina Greensboro, *Undergrad Assistant*, Dr. Rueppell's Lab 2011

- Studied the effect of queen and brood presence on honey bee mortality and behavior

VITA

PUBLICATIONS

- **McCray T. et al. (2020).** “Patient-derived Prostate Organoids Reveal Vitamin D as a Vital Regulator of Epithelial Differentiation”, **Submitted, Cell Reports**
- **McCray T. et al. (2019).** “Single-Cell RNA-Seq Analysis Identifies a Putative Epithelial Stem Cell Population in Human Primary Prostate Cells in Monolayer and Organoid Culture Conditions”, Am J Clin Exp Urol., June 15 2019, 7(3):123-138
- **Richards Z*, McCray T*, et al. (2019).** “Prostate stroma increases the viability and maintains the branching phenotype of human prostate organoids”, iScience, February 22 2019, 12:304-317
- **McCray T. et al. (2019)** “Handling and Assessment of Human Primary Prostate Organoid Culture”, J. Vis. Exp., Jan 17 2019, (143)
- **Dambal S (2017).** “The miR-183 family cluster alters zinc homeostasis in benign prostate cells, organoids and prostate cancer xenografts”. Scientific Reports. August 9 2017, 7(1):7704

EDUCATION

University of Illinois Chicago, IL Expected Mar 2020

PhD Candidate in Pathology, Larisa Nonn Laboratory, Pathology

- Graduate Education in Medical Sciences Program
- CCTS Pre-doctoral Education for Clinical and Translational Scientists (PECTS) Fellowship

University of North Carolina Greensboro, NC 2009 - 2013

Bachelor of Science; Biology

- βββ Biology Honors Society

PRESENTATIONS

Talk , Graduate Education in Medical Sciences Annual Symposium, Chicago IL	2019
Talk , 10x User Group Meeting, Chicago IL	2019
Talk , GEMS Program Recruitment, Chicago IL	2019, 2018
Poster , Society for Basic Urological Research Annual Meeting	2019, 2018, 2017, 2016
Poster , Cell Symposia Engineering Organoids and Organs Meeting, CA	2019
Poster , Cellular Plasticity, Keystone Meeting, CO	2019
Poster , Gary Kruh Cancer Research Symposium, Chicago IL	2019, 2018
Poster , College of Medicine Research Symposium, Chicago IL	2019, 2017
Poster , American Association for Cancer Research Annual Meeting, Chicago IL	2018
Poster , Graduate Education in Medical Sciences Symposium, Chicago IL	2018, 2017, 2016

AWARDS

Travel Award , Graduate Student Council, University of Illinois Chicago	2019
Travel Award , Society for Basic Urological Research Annual Meeting	2018
2nd Place Winner , Image of Research Competition at University of Illinois, Chicago	2018
Honorable Mention , Poster at GEMS Symposium, Chicago	2018
Chancellor’s Student Service Award , University of Illinois Chicago	2018
Honorable Mention , Poster at College of Medicine Research Symposium, Chicago	2017

VITA

LEADERSHIP EXPERIENCE

SBUR Trainee Affairs Committee, *Trainee Representative* 2019

- Organized the trainee affairs symposium for the 2019 SBUR annual meeting
- Corresponded with faculty to strategize opportunities for the development of in-training members of SBUR

GEMS Student Association, *Executive Board Member* 2016-2019

- Acted as President, Vice President and Treasurer for the GEMS student association
- Represented graduate students to the College of Medicine and Dean to maintain a competitive stipend, enact a TA program, and re-organize the program's departmental and educational structure
- Executed meeting agendas and implemented social, volunteer and fundraising opportunities for students
- Established and maintained a program-wide calendar of seminars, journal clubs and events

GEMS Symposium Planning Committee, *Member* 2016-2018

- Organized a student-run initiative to showcase GEMS students' research
- Coordinated abstract submission and event advertising
- Arranged faculty involvement in abstract selection and presentation judging
- Invited and corresponded with keynote speakers
- Supervised day-of-event scheduling logistics

Graduate Student Council, *Pathology Student Representative* 2017